Binding Bamboo

The Effect of Chemical Treatments & Manufacturing Process on Bamboo Fibre Reinforced Bio-Based Polycarbonate Composites

Prajwal Jayaraman

Delft University of Technology

TU Delft

Binding Bamboo

The Effect of Chemical Treatments & Manufacturing Process on Bamboo Fibre Reinforced Bio-Based Polycarbonate Composites

by

Prajwal Jayaraman

to obtain the degree of Master of Science
at the Delft University of Technology,
to be defended publicly on Thursday July 10, 2025 at 10:30 AM.

Student number:	5901324	
Faculty:	Faculty of Aerospace Engineering, Delft	
Project duration:	December 2024 – July 2025	
Thesis committee:	D. Apostolidis,	TU Delft, Daily Supervisor
	Dr. B. Kumru,	TU Delft, Supervisor
	Dr. ir. J. J. E. Teuwen,	TU Delft, Chair
	Dr. ir. O. K. Bergsma,	TU Delft, External Examiner

Cover:	©Dimitris Apostolidis - Bamboo plantation in Sao Paulo, Brazil
Style:	TU Delft Report Style, with modifications by Daan Zwaneveld

An electronic version of this thesis is available at http://repository.tudelft.nl/.

TU Delft

“I alone cannot change the world, but I can cast a stone across the waters to create many ripples.”

- Mother Teresa

TU Delft Delft University of Technology

Delft University of Technology
Faculty of Aerospace Engineering
Department of Aerospace Structures and Materials

GRADUATION COMMITTEE

Date of Graduation: July 10, 2025

Chair Holder:

Dr. ir. J.J.E. Teuwen

Supervisors:

Dr. B. Kumru

D. Apostolidis

External Member:

Dr. ir. O.K. Bergsma

Preface

Working in the field of sustainable composites often feels like an uphill journey with few accolades. It is a path laden with challenges, where the impact is rarely immediate or widely acknowledged. Nevertheless, we must remain committed—if we can help push us even 1% closer to a more sustainable materials future, that will be enough.

This work would not have taken shape without several remarkable individuals' unwavering support and guidance. I am deeply grateful to Dr. Baris Kumru, my supervisor, for his technical expertise, sharp insights, and patient guidance throughout this project. His critical feedback always helped sharpen my direction while leaving room for creative freedom.

I also want to thank Dimitris Apostolidis profoundly—a mentor, daily supervisor and a friend from my first day in the master's program. Dimitris, your constant support in the lab, your belief in me during difficult phases, and your moments of encouragement and humour made this experience both productive and memorable. I would also like to thank Dr. Niklas Lorenz for his repeated support in understanding different equipment in the lab.

I extend my appreciation to the DASML team: Roy Awater, Chantal de Zeeuw, Alexander Uithol, Dave Ruijtenbeek, Caitlin van den Houndel, Christiaan Snaathorst, and Victor Horboweic. Your assistance in the labs and open-door approach to helping students made this journey much smoother. I would also like to take this opportunity to thank Cristina Panez and the Department of Geosciences for allowing me to use their lab.

A sincere thank-you also goes to the PhDs and PostDocs in the ASM department for their assistance and stimulating conversations. I would also like to acknowledge my committee chair, Dr. Julie Teuwen, and the external member, Dr. Otto Bergsma, for generously agreeing to be part of this evaluation process.

To my friends—thank you for being my sounding boards, distractions, and lifelines.

Most of all, I thank my parents. Their sacrifices, love, and daily encouragement are the foundation of everything I do. I owe more to them than words can capture. I also wish to honour the memory of my late grandparents, whose values, love, and quiet strength continue to guide me. Their influence remains a source of inspiration in all that I pursue.

This work marks not an end but a beginning. I am committed to continuing the journey in bio-based composites—one that bridges experimental rigour with sustainable aspirations—long after submitting this document.

Prajwal Jayaraman
Delft, June 2025

Abstract

Binding Bamboo: The Effect of Chemical Treatments & Manufacturing Process on Bamboo Fibre Reinforced Bio-Based Polycarbonate Composites

This research investigates the feasibility of bamboo fibre-reinforced bio-derived polycarbonate composites for secondary aerospace applications. Motivated by the need for sustainable alternatives to synthetic composites, the study focuses on the effects of chemical fibre treatments on mechanical, thermal, and interfacial performance. Bamboo fibres were treated using alkali (2–8% w/v), silane (2-8 g/L), and acetylation methods. Acetylated fibres were excluded early due to structural degradation.

Comprehensive fibre characterisation included density, water absorption, Fourier-transform infrared spectroscopy, scanning electron microscopy, thermogravimetric analysis, and single fibre tensile testing. Notably, 2% NaOH-treated fibres exhibited a tensile strength of 249 MPa, and 5 g/L silane-treated fibres reached 194 MPa, compared to 110 MPa for untreated fibres. TGA showed improved thermal stability with onset degradation temperatures of 277°C for 5 g/L silane compared to 267°C for untreated fibres.

Treated fibres were used to fabricate unidirectional laminates via solvent-based prepreg processing with Durabio, followed by compression moulding. Composite testing included tensile, flexural, and microscopic cross-sectional analysis. The highest tensile strength of 162 MPa and flexural strength of 184 MPa were recorded for composites with 2 g/L silane-treated fibres, with 5 and 8 g/L silane laminates being only slightly lower than that. Untreated composites recorded 121 MPa and 154 MPa, respectively. Void content decreased from 21% for untreated to 18% for silane-treated, accompanied by a bonding efficiency of 95% for the 5 g/L silane laminate, indicating significantly improved fibre-matrix bonding efficiency. This was supported by optical microscopy, which showed more cohesive interfaces and reduced delamination in silane-treated laminates. Alkali-treated fibres, however, consistently showed worsening properties and quality on the composite level due to fibre degradation and poor bonding.

The study concludes that silane treatment, particularly at 2 g/L, enhances fibre-matrix compatibility, leading to superior composite performance. Future work is recommended in areas including environmental durability, manufacturing optimisation, and closed-loop recycling, with potential expansion to other bio-based matrices.

Keywords: Bamboo fibre, durabio, alkali, silane, acetylation, pre-impregnation, compression moulding, lignin, hemicellulose, cellulose, interface, voids, tetrahydrofuran, fibrils.

Contents

List of Figures

List of Tables

Nomenclature

Abbreviations

Abbreviation	Definition
4PB	4 Point Bending
ACARE	Advisory Council for Aviation Research and Innovation in Europe
APTES	Amino-Propyl-Tri-Ethoxy-Silane
ASTM	American Society for Testing and Materials
BE	Bonding Efficiency
BF	Bamboo Fibre
BFRTPC	Bamboo Fibre Reinforced Thermo-Plastic Composite
BPA	Bisphenol-A
CFRP	Carbon Fibre Reinforced Polymer
CNT	Carbon Nanotubes
DI	De-Ionised
DTG	Derivative of Thermo-Gravimetry
ECO-COMPASS	Ecological and Multifunctional Composites for Application in Aircraft Interior and Secondary Structures
FTIR	Fourier Transform Infra-Red
GFRP	Glass Fibre Reinforced Polymer
IR	Infra-Red
PA	Polyamide
PAEK	Polyaryletherketone
PC	Poly-Carbonate
PEEK	Polyether Ether Ketone
PHA	Polyhydroxyalkanoates
PLA	Poly-Lactic-Acid
PPS	Polyphenylene Sulfide
ROM	Rule Of Mixtures
SEM	Scanning Electron Microscopy
TGA	Thermo-Gravimetric Analysis
THF	Tetrahydrofuran
TP	Thermo-Plastic
TS	Thermo-Set
UTM	Universal Testing Machine

Symbols

Symbol	Definition	Unit
A	Weight of specimen in air	[g]
B	Weight of specimen in auxiliary liquid	[g]
E_{1a}	Actual longitudinal elastic modulus of composite	[MPa]
E_{1t}	Theoretic longitudinal elastic modulus of composite	[MPa]
E_f	Longitudinal elastic modulus of fibre	[MPa]
E_m	Longitudinal elastic modulus of matrix	[MPa]

Symbol	Definition	Unit
L	Span Length	[mm]
P	Load	[N]
T_g	Glass Transition Temperature	[$^\circ$C]
b	Specimen width	[mm]
h	Specimen thickness	[mm]
k	Fibre-matrix bonding efficiency	[-]
w_f	Weight fraction of fibre	[%]
w_f	Weight fraction of matrix	[%]
δ	Displacement at mid-point	[mm]
$\delta_{nominal}$	Displacement at loading span	[mm]
ϵ	Strain	[-]
ρ_0	Density of auxiliary liquid	[g/cm^3]
ρ_L	Density of air	[g/cm^3]
ρ_a	Measured density of composite	[g/cm^3]
ρ_c	Calculated density of composite	[g/cm^3]
ρ_f	Density of fibre	[g/cm^3]
ρ_m	Density of matrix	[g/cm^3]
σ	Stress	[MPa]

Part I
Project Background

1

Introduction

The aviation industry has been instrumental in connecting the world, enabling rapid transportation of people and goods. However, this growth comes at a significant environmental cost. The sector contributes approximately 2-3% of global carbon dioxide emissions, a figure expected to rise with increasing air traffic (Internation Energy Agency, 2023). Addressing this challenge requires urgent and innovative solutions that focus on sustainability. The role of aerospace-related material science in reducing emissions cannot be overstated, as lightweight structures directly correlate to reduced fuel consumption and emissions.

Polymers and polymer-based composites have become essential to this goal. Their high strength-to-weight ratio, corrosion resistance, and design flexibility have enabled the aerospace sector to reduce component mass drastically. In modern aircraft such as the Boeing 787 and Airbus A350, composites account for over 50% of the structural weight (Kesarwani, 2017). Beyond primary structures, interior design has emerged as a significant area for reducing weight. Cabin elements such as seats, panels, and overhead compartments are being redesigned using composite materials to lower aircraft weight without compromising safety or comfort. For instance, studies show that replacing traditional materials in seat structures with advanced composites can reduce weight by 10–15 kg per seat. Additional research also shows that a 1% reduction in aircraft weight can lead to up to 0.75% fuel savings over an aircraft's lifespan, significantly cutting CO_2 emissions (Babikian et al., 2002; Tsai et al., 2014).

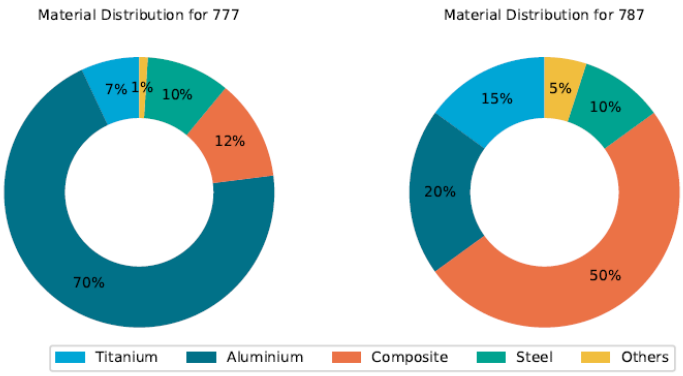

Figure 1.1: Material distribution in modern aircraft (Kaushik, 2024)

Despite these advances, conventional aerospace composites rely heavily on synthetic fibres like carbon and glass paired with thermosetting resins. These materials, while mechanically robust, raise sustainability concerns due to their energy-intensive production, limited recyclability, and dependence on petroleum-derived feedstocks. As the aerospace sector commits to net-zero emissions by 2050, there is growing interest in bio-derived, renewable, and recyclable alternatives that can support circular

material flows and reduce life-cycle environmental impact (Bachmann et al., 2018).

Natural fibres, such as jute, hemp, flax, and bamboo, present a promising alternative to synthetic fibres. They are abundant, renewable, biodegradable, and exhibit comparable mechanical properties for many engineering applications (Kabir et al., 2012). Bamboo fibre, in particular, stands out due to its rapid growth rate, low water requirements, and high tensile strength. As a perennial grass, bamboo can be harvested sustainably without damaging ecosystems, making it an attractive option for environmentally conscious engineering applications (Khalil et al., 2012).

The matrix material in composites plays an equally vital role in determining their mechanical performance and sustainability. Bio-derived thermoplastics, such as polylactic acid and polyhydroxyalkanoates, offer renewable and biodegradable alternatives to petroleum-based polymers. These can be synthesised from agricultural waste, corn, sugarcane, or other biomass, reducing reliance on fossil fuels and supporting circular economy principles. Alongside TPs, bio-based thermosets are also being developed, further expanding the material landscape. Recent advancements have improved the thermal stability, impact resistance, and mechanical performance of both categories, making them increasingly viable for high-performance sectors such as aerospace (Dyer & Kumru, 2023; Hottle et al., 2017).

Despite their benefits, natural fibres still face limitations that must be addressed to meet aerospace-grade standards. These include high moisture absorption, weak interfacial bonding with matrices, and variability in mechanical properties. Surface modification treatments—such as alkali, silane coupling, or grafting techniques—are commonly employed to enhance compatibility with polymer matrices. These treatments alter the fibre surface, improving adhesion and reducing water uptake (Faruk et al., 2012). By optimising these treatments, natural fibre composites' mechanical performance and durability can be significantly enhanced, making them suitable for demanding aerospace applications.

The manufacturing processes for natural fibre composites must balance performance, scalability, and sustainability. Compression moulding, resin transfer moulding, and additive manufacturing have been adapted to accommodate natural fibres. These processes emphasise low energy consumption, minimal waste, and use bio-based resins to achieve a greener composite manufacturing pipeline. Furthermore, hybrid composites that combine natural and synthetic fibres have shown potential for meeting specific performance requirements while reducing environmental impact (Andrew & Dhakal, 2022). Continued research and development in this field will enable the widespread adoption of natural fibre composites in aerospace structures.

This thesis explores the development and application of bamboo fibre-reinforced bio-derived thermoplastics for interior aerospace structures. The research focuses on optimising fibre treatment and manufacturing processes and evaluating the mechanical performance of bamboo-reinforced bio-based polycarbonate composites. By addressing these aspects, the study aims to contribute to the growing body of knowledge on sustainable materials and support the aviation industry's transition toward a greener future.

Research Objective

Demonstrate the **feasibility** of **bamboo-fibre** reinforced **bio-based polycarbonate** composites for secondary aviation applications by analysing the impact of **fibre treatments** and **manufacturing conditions** on the **interfacial properties** of the composite.

This thesis has three main parts: Part I: Project Background, Part II: Research Activities, and Part III: Conclusions and Recommendations. The first part includes Chapter 1, which provides an overview of the project and outlines the research objectives. Chapters 2 and 3 offer essential background information, identify gaps in the existing literature, and formulate the research questions. The second part encompasses Chapters 4 and 5, which detail the methodologies employed and present the results related to fibre, matrix, and composite characterisation. Finally, the third part, comprising Chapters 6 and 7, summarises the key findings, draws conclusions, and proposes directions for future research.

2

Literature Analysis

This chapter provides a concise overview of the literature reviewed during the early stages of the research, offering readers the necessary background and conceptual foundation. This literature analysis presents a cohesive narrative: the evolution of composite materials in the aviation industry, the growing imperative for sustainability, and the emerging potential of bio-based composites for secondary structural applications in aerospace. The chapter also explores various strategies to enhance the fibre-matrix interface, including chemical modification techniques and manufacturing process optimisations, thereby addressing one of the key challenges in developing natural fibre composites with high strength-to-weight ratios.

2.1. Polymer Matrix Composite Materials

Composite materials are engineered materials composed of two or more constituent materials with distinct physical or chemical properties. These constituents remain separate within the finished structure but combine to create superior performance characteristics not achievable by individual components. The primary components of composite materials are the reinforcement and the matrix, each serving specific roles to enhance the composite's overall functionality as seen in Figure 2.1 (Mallick, 2017).

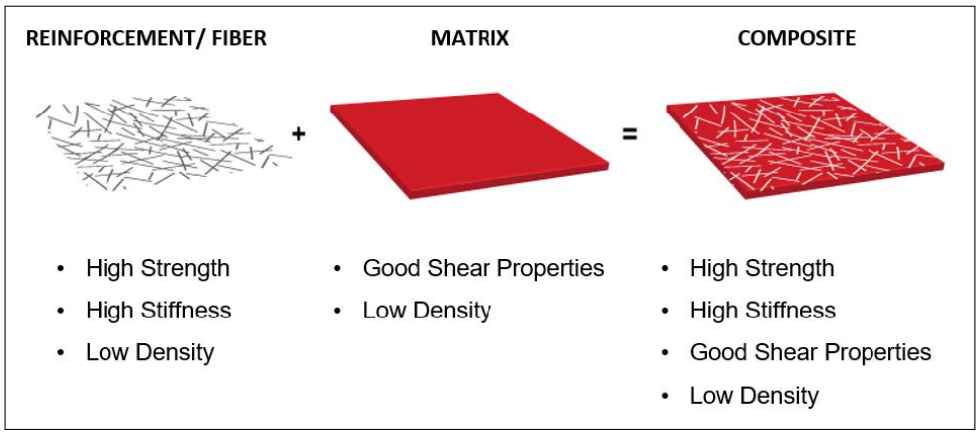

Figure 2.1: Constituents of composite materials (Kesarwani, 2017)

2.1.1. Reinforcements

Reinforcements are the main load-bearing elements within composite materials and occupy a large volume fraction. Reinforcements can range from nano-scale powder like CNT to short strands, long unidirectional tapes, and woven fabrics. In the aerospace industry, fibres are used as the primary reinforcement owing to their capability to provide high strengths in the longitudinal direction.

Moduli, strength, thermal stability, density and cost primarily dictate the selection of fibres. However, the fibre architecture, including direction, weave, and sizing, also influences the mechanical properties and suitability for specific applications. Reinforcements typically consist of high-strength synthetic fibres, such as glass, carbon, and aramid fibres (Figure 2.2a), which have unique mechanical and chemical properties (Mallick, 2007).

2.1.2. Matrices

The matrix acts as the binding agent, holding the reinforcement in place, distributing loads among the fibres, and protecting them from environmental damage. Matrices contribute majorly to the composite's compressive strength and control the composite's processing requirements, such as temperature, method, and pressure. Matrices are broadly categorised as ceramic, metal and polymer matrices (Figure 2.2b). However, aviation composites primarily use polymer matrices - thermosets and thermoplastics (Kaushik, 2024).

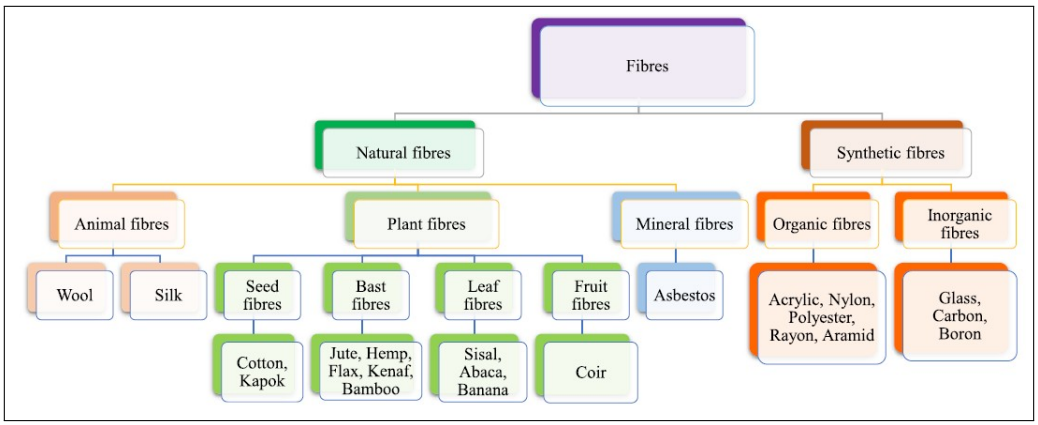

(a) Classification of fibres in composites (Awais et al., 2021)

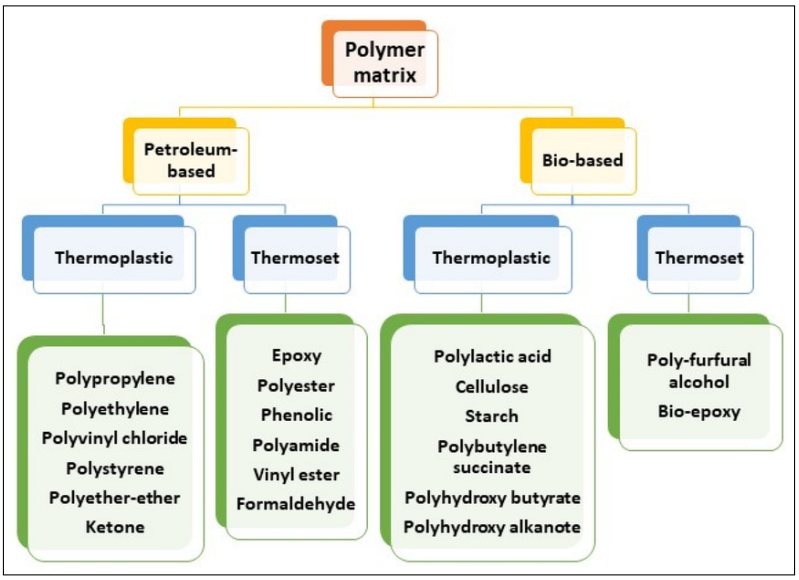

(b) Categorisation of matrices (Islam et al., 2025)

Figure 2.2: Classification of composite constituents

Thermoset and thermoplastic polymers are both integral to high-performance composites, each offering distinct advantages. Thermosets, such as epoxies, unsaturated polyesters, and vinyl esters, begin as low-viscosity liquids that cure irreversibly into rigid, cross-linked structures. This cross-linking yields high stiffness, thermal stability, and chemical resistance, making thermosets ideal for structural applications (Mallick, 2007). In contrast, thermoplastics like polyether ether ketone (PEEK), polyaryletherketone (PAEK), polyamides, and polyphenylene sulfide (PPS) feature linear or branched

chains without permanent bonds, allowing them to be remelted and reshaped. Their recyclability, ductility, and rapid processing make them attractive for aerospace and automotive uses, where toughness, chemical resistance, and thermal performance are critical (Biron, 2018). However, the synthesis of high-performance petroleum-derived thermoplastics is energy-intensive and chemically complex, often involving toxic intermediates and multiple high-temperature steps, which significantly inflate their environmental footprint when full life cycle impacts are considered (Yaghoubi & Kumru, 2024).

Processing also differs significantly between these matrix types. Thermosets are processed at relatively low viscosities and temperatures, followed by irreversible curing. In contrast, thermoplastics require melt processing at elevated temperatures. Within thermoplastics, amorphous polymers soften gradually above their glass transition temperature (T_g), making them easier to process and better suited for thermoforming and welding. In contrast, semi-crystalline polymers exhibit a sharp melting point and require precise control of heating and cooling cycles to manage crystallisation and avoid defects such as warping or voids (Biron, 2018).

2.2. Secondary Aviation Applications

Secondary aviation applications refer to non-critical structural components of an aircraft where mechanical loading and certification requirements are less severe than primary structures. These include cabin ceiling and sidewall panels, luggage compartments, tray tables, and door linings. While these parts are not directly involved in maintaining flight safety, they are vital in passenger comfort, aircraft functionality, and operational efficiency. Thus, apart from the standard aviation material requirements of lightweight properties, acoustic insulation, fire resistance, low cost and ease of processing, factors such as visual appeal, comfort and increasingly—sustainability are valuable (Bachmann et al., 2018).

2.2.1. Current Practices

Traditional secondary and interior aircraft structures primarily rely on synthetic composites, particularly GFRP systems for sandwich panels and CFRP for components demanding higher mechanical strength due to their excellent performance-to-weight ratio and thermal stability. Common thermosets such as epoxy/glass fibre laminates and phenolic-based panels are widely used for flooring, sidewalls, ceilings, and lavatory modules, offering good fire resistance and structural integrity (Dyer & Kumru, 2023). However, their manufacturing is resource-intensive, relies heavily on non-renewable petroleum-based feedstocks, and poses significant end-of-life challenges due to the crosslinked nature of thermosets and the heterogeneity of composite structures. Closed-loop recycling remains elusive, often resulting in downcycled products of reduced utility and value. In contrast, high-performance petroleum-based thermoplastics such as PEEK, PAEK, and PPS are increasingly used in interior applications like seat frames, tray tables, cable conduits, and cladding panels owing to their recyclability, impact resistance, and compatibility with rapid processing techniques (Ozturk et al., 2024). However, due to the aesthetic and customer satisfaction demands in the aviation industry, interior components are frequently replaced, contributing to higher emissions—thus calling for more sustainable materials and design approaches.

2.2.2. Potential Alternatives

The growing need for environmentally conscious materials in aviation has sparked significant interest in eco-composites—materials made from renewable, recyclable, or multifunctional constituents. As demonstrated by the ECO-COMPASS project, using bio-based thermoset resins and natural fibres such as flax, ramie, and hemp offers promising alternatives for secondary structures and interior components. These fibres are lightweight, biodegradable, and offer unique mechanical, acoustic, and damping characteristics due to their hollow, lumen-rich microstructure (Dong et al., 2018).

2.2.3. Environmental Benefits and Challenges

The adoption of eco-composites in aviation is driven by global sustainability goals, such as those outlined by ACARE's Flightpath 2050, which targets a 75% reduction in CO_2 emissions and a 90% reduction in NO_x emissions per passenger-kilometre. Lightweight materials play a central role in achieving these targets due to their significant influence on fuel consumption during an aircraft's lifetime. According to life cycle assessments conducted in the ECO-COMPASS project, eco-composites can reduce

global warming potential, fossil depletion, and photochemical oxidation relative to traditional composites. However, inevitable trade-offs were observed, including potential increases in eutrophication[1] and ozone depletion linked to bio-fibre cultivation and processing (Bachmann et al., 2021).

2.2.4. Future Outlook

While current eco-composites are not yet suitable for primary structures due to their limited mechanical strength and certification barriers, they are highly promising for less demanding secondary structures. Further work is needed to enhance fire resistance, ageing durability, and compatibility with existing certification protocols. Hybrid solutions combining natural fibres with conventional reinforcements or nano-modified matrices may bridge the performance gap. With continued international collaboration and iterative improvements, eco-composites could become integral to sustainable aerospace design, supporting circular economy principles without compromising performance or safety (Bachmann et al., 2021).

2.3. The Bio-Factor

2.3.1. Bio-Based Matrices

Bio-based thermosets are synthesised from renewable sources such as lignin, vanillin, furfuryl alcohol, and phloroglucinol, offering potential substitutes for petroleum-based resins in structural applications. Vanillin, derived from lignin, can be functionalised into vanillyl alcohol diglycidyl ether, forming resins that demonstrate high flexural strength and stiffness, even surpassing traditional BADGE-based epoxies in some metrics. Similarly, phloroglucinol triglycidyl ether exhibits high thermal resistance and mechanical integrity, with a bio-based carbon content above 60%, making it suitable for aerospace-grade applications. These formulations exhibit reduced toxicity and good crosslinking potential, indicating their viability for high-performance composites (Apostolidis, 2023; Kaushik, 2024).

Bio-based thermoplastics, including PLA, PHAs, PCs, and cellulose derivatives, are increasingly used for sustainable composite matrices. PLA and PHA are produced from fermentation processes using biomass like sugarcane or corn starch, offering complete biodegradability and a reduced carbon footprint (Mustafa & Talha, 2025). Despite drawbacks like low thermal stability and brittleness, their performance is being enhanced via blending, plasticisation, and the development of multiphase systems. For instance, combining PLA with jute and sisal fibres under optimised compression moulding conditions results in improved tensile and flexural strengths (Mustafa & Talha, 2025).

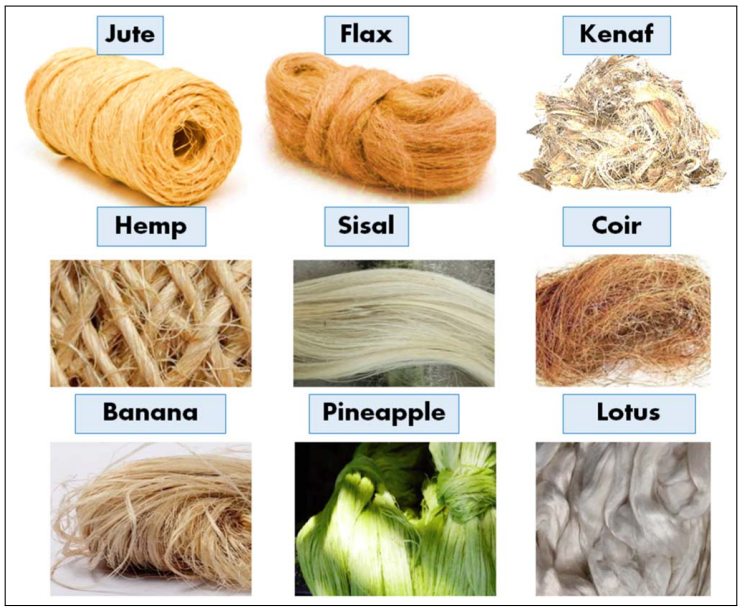

Figure 2.3: Types of natural fibres (Jayaraman et al., 2024)

[1] A process in which nutrients accumulate in a body of water

2.3.2. Natural Fibres

Natural fibres like bamboo, flax, hemp, jute, and ramie are extensively researched for their renewability, low density, and good specific mechanical properties. Bamboo, in particular, offers a high tensile modulus and is being studied in epoxy, polypropylene, and polyamide-11 matrices with promising results (Beaumann, 2024). However, these fibres present challenges, including moisture absorption and poor compatibility with hydrophobic matrices, leading to weak interfacial bonding (Syduzzaman et al., 2020).

2.4. Durabio - A Bio-Derived Polycarbonate

2.4.1. Production

Durabio is a bio-based polycarbonate developed by Mitsubishi Chemical Corporation. Durabio with a T_g of 125°C is synthesised using isosorbide derived from plant-based glucose as a sustainable alternative to fossil-based bisphenol-A. Isosorbide is obtained through catalytic hydrogenation of glucose into sorbitol, followed by a dehydration step. The polymerisation of isosorbide results in a thermoplastic polycarbonate network known as isosorbide-based PC or bio-PC (Figure 2.4). This approach eliminates toxic intermediates like BPA and reduces the dependency on petrochemical feedstocks (Bonnin et al., 2020; Lee et al., 2015).

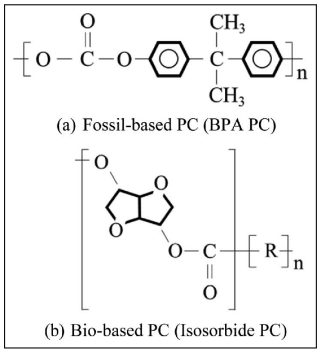

(a) Difference in chemical structures of bio-based and fossil-based PCs (Choi & Lyu, 2020)

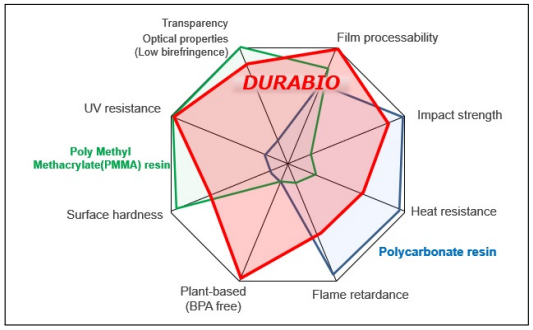

(b) Comparitive assessment of Durabio with other matrices (Mitsubishi Chemical Group, 2024)

Figure 2.4: Comparision of Durabio with fossile=based PC and other matrices

2.4.2. Properties

Choi et al. (Choi & Lyu, 2020) conducted a comprehensive study comparing bio-based polycarbonate's rheological and mechanical behaviour. They used a variety of bio-PCs, including but not limited to Durabio. Their findings highlight key performance and processing behaviour differences between the two materials and have been tabulated in Table 2.1.

Table 2.1: Comparative assessment of properties of fossil-based and bio-based PCs (Adapted from (Choi & Lyu, 2020))

Property	Fossil-Based PC	Bio-Based PC
Tensile Strength & Moduli	60 MPa & 1670 MPa	72 MPa & 2400 MPa
Impact Resistance	100 kg_fcm/cm	15 kg_fcm/cm
Shear Viscosity	Higher (better melt elasticity and processability)	Lower and variable across temperat--ures
Storage & Loss Moduli	Higher (better melt strength). Standard processing conditi--ons sufficient	Lower (reduced melt strength during processing) Requires adjusted conditions due to lower toughness and viscosity

2.4.3. Applications

Durabio is used in various optical and structural applications, including automotive grilles, dashboards, interior panels, and consumer electronics such as touchscreen displays. In experimental studies involving injection moulding of bamboo fibre composites, Durabio was shown to maintain structural integrity under flexural testing, indicating the potential for use in hybrid natural fibre composites (Takeuchi et al., 2024). Its combination of transparency, rigidity, and bio-based origin positions Durabio as a promising material for eco-conscious product design in industries ranging from transportation to electronics.

2.5. Bamboo Fibre

2.5.1. Structure and Composition of Bamboo Fibres

Bamboo fibres exhibit a hierarchical, anisotropic structure, with their strength dictated mainly by the distribution of vascular bundles within the culm[2]. Cellular studies have shown that bundle density increases from the inner to the outer culm, imparting superior mechanical strength to the outer layers (Grosser & Liese, 1971). Microstructurally, bamboo fibres possess a low microfibrillar angle (2°–10°), contributing to high tensile strength and stiffness. Chemically, they are rich in cellulose (up to 75%), with low lignin (approx. 10%) and hemicellulose contents, enhancing both biodegradability and mechanical properties (Beaumann, 2024).

The fibres follow a poly-lamellate pattern with cellulose fibrils structured for directional strength transmission (Figure 2.5). Their structure makes them highly effective reinforcements for thermoplastic and thermoset composite matrices.

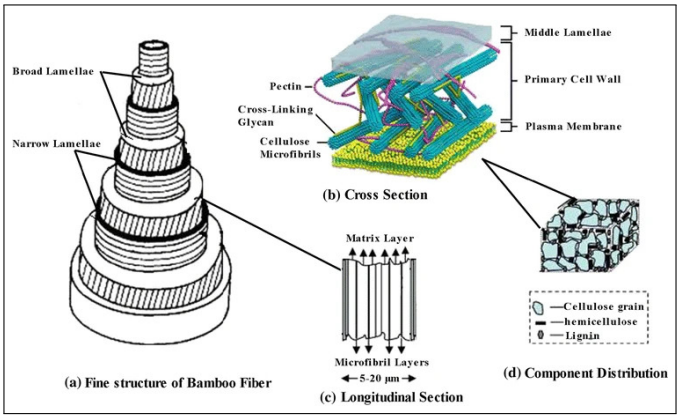

Figure 2.5: Schematic representation of the structure of bamboo fibre (Beaumann, 2024)

2.5.2. Growth and Availability of Bamboo

Bamboo is a perennial grass with exceptional growth rates—nearly 1m per day—and maximises its growth in an average of 4 years, making it one of the fastest renewable natural resources (Liese & Weiner, 1996). It grows widely in tropical and subtropical regions across Asia, Africa, and Latin America, with global distribution enabling region-specific applications. Its rapid growth also supports high biomass yields, carbon sequestration, and sustainability goals, contributing significantly to environmental mitigation strategies (Beaumann, 2024).

2.5.3. Properties of Bamboo Fibre

Bamboo fibres demonstrate tensile strength of 430 $\pm$ 170 MPa and an average elastic modulus of 26.5 GPa, influenced by extraction method and microstructure (Liu et al., 2012). The outer culm layers show superior performance due to dense vascular bundles. Fracture toughness, an essential metric for impact resistance, is around 3 MPa$\cdot m^{1/2}$, enabled by crack deflection mechanisms (Amada & Untao, 2001). These characteristics make bamboo suitable for load-bearing and energy-absorbing applications.

[2] the hollow stem of a grass or cereal plant

Bamboo fibres have densities between 1.2–1.5 g/cm^3, lower than glass fibres (Beaumann, 2024). This low density facilitates lightweight composites.

Thermal degradation of bamboo occurs in two phases: moisture loss up to 150 ^{o}C and decomposition of hemicellulose and cellulose up to 450^{o}C, with peak degradation near 350^{o}C and a processing window of under 215°C taking into consideration the processing duration (Beaumann, 2024). Moisture sensitivity is significant; 100g of untreated fibres can absorb up to 15g of their weight in water, reducing tensile strength to nearly 70% of its original value (Kushwaha & Kumar, 2011).

2.5.4. Processing and Impact of Bamboo Fibres

Extraction Methods

Mechanical extraction (e.g., combing and refining) preserves structural integrity and leads to tensile strengths and moduli higher than the average but introduces fibre dimension variability. Chemical methods improve uniformity but reduce strength due to degradation of the fibre's native structure (Buson et al., 2018).

Fibre Alignment, Scatter and Volume Fraction

Fibre alignment drastically impacts mechanical performance. Random fibres are shown to have up to 30% lesser strength than well-arranged fibres (Senthil Muthu Kumar et al., 2021). However, achieving consistent alignment at scale remains challenging. Natural variability in species, harvesting, and processing leads to scatter in fibre dimensions and properties.

An optimal volume fraction of 40% maximises tensile and flexural strength without compromising matrix wetting. Beyond this, fibre agglomeration and voids may reduce composite quality (Beaumann, 2024).

Environmental Impact

Mechanical extraction uses 60% less energy and results in lower CO_2 emissions compared to chemical methods. Bamboo's embodied energy is about 40% lower than that of glass fibres, and its CO_2 emission is less than 50% of glass . Lifecycle assessments reveal that bamboo fibre composites can reduce environmental impacts by up to 60% compared to GFRPs (Das et al., 2022).

Applications

Bamboo fibre composites are suited for automotive interiors, lightweight construction panels, sports goods, and hybrid bio-composites. Their high specific strength, damping capacity, and eco-friendliness enable multifunctional design, particularly in green manufacturing sectors. Challenges remain in scaling up processing, maintaining fibre consistency, and ensuring long-term durability under cyclic environmental loads (Beaumann, 2024).

2.6. Interfacial Engineering

2.6.1. Importance of Fibre-Matrix Adhesion

Effective stress transfer in fibre-reinforced polymer composites depends critically on the adhesion quality at the fibre-matrix interface. Natural fibres like bamboo possess hydrophilic surfaces, waxes, and surface extractives that hinder compatibility with typically hydrophobic polymer matrices. This results in weak interfacial bonding, fibre pull-out, and reduced mechanical performance of composites (Huang et al., 2021) as illustrated in Figure 2.6.

2.6.2. Bonding Mechanisms at the Fibre-Matrix Interface

The interface facilitates stress transfer and is governed by multiple mechanisms (Mohit & Arul Mozhi Selvan, 2018) (Figure 2.7):

- **Mechanical Interlocking:** Occurs when matrix resin penetrates surface asperities or microfibrils on roughened fibre surfaces, especially after alkali or plasma treatments.
- **Chemical Bonding:** Involves covalent, ionic, or hydrogen bonds between functional groups (e.g., hydroxyls, carbonyls, silanols) on the fibre and polymer matrix. Silane coupling agents enhance this mechanism.

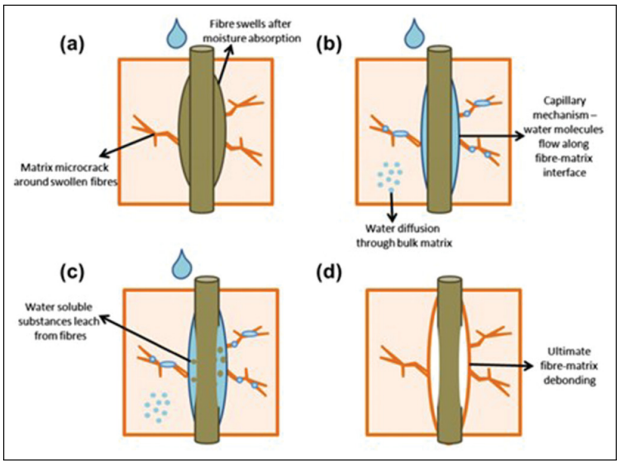

Figure 2.6: Debonding of natural fibre composites due to hydrophilicity (Azwa et al., 2013)

- **Electrostatic Interactions:** Arise due to attraction between oppositely charged fibre and matrix surfaces, although this is less common in polymer composites.
- **Molecular Diffusion:** Relies on interdiffusion of polymer chains at the interface, requiring sufficient mobility and affinity between phases.

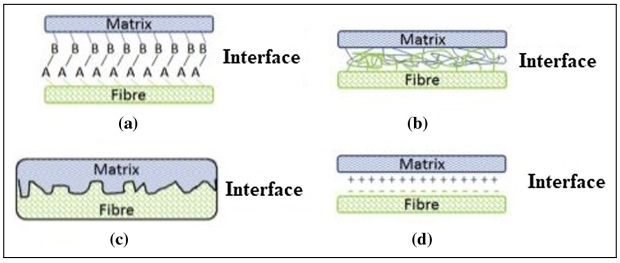

Figure 2.7: Fibre-matrix bonding mechanisms (a) Chemical, (b) Diffusion, (c) Mechanical and (d) Electrostatic (Mohit & Arul Mozhi Selvan, 2018)

2.6.3. Effects of Fibre Treatments on Lignocellulosic Fibres

Surface treatments chemically modify lignocellulosic fibres, increasing surface roughness, removing amorphous constituents, and introducing functional groups (Figure 2.8). These changes enhance fibre wettability, reduce moisture absorption, and improve interfacial adhesion and mechanical integrity of composites (Ramachandran et al., 2022).

Alkali (NaOH) Treatment

Also known as mercerisation, this treatment removes lignin, hemicellulose, waxes, and oils. SEM analysis shows a cleaner surface with microfibrillar exposure, promoting mechanical interlocking (Kabir et al., 2012). It also converts crystalline cellulose I to more amorphous cellulose II, improving matrix infiltration. Tensile tests on treated bamboo show enhanced strength (234.7 MPa) and Young's modulus (12.2 GPa) despite a slight reduction in failure strain (Costa et al., 2017). Over-treatment, however, can degrade cellulose and weaken fibres (Kabir et al., 2012).

$$\text{Fibre} - \text{O} - \text{H} + \text{NaOH} \longrightarrow \text{Fibre} - \text{O}^{-}\,\text{Na}^{+} + \text{H}_2\text{O}$$

Silane Treatment

Silane coupling agents (e.g., APS, MPS) hydrolyse in aqueous ethanol to form silanols, which condense with hydroxyls on the fibre and matrix to form stable Si–O–Si bonds. This bridge reduces moisture

sensitivity and improves adhesion via covalent bonding (Ramachandran et al., 2022; Verma et al., 2022). Studies on bamboo and other fibres show silane treatment improves tensile and flexural strength by up to 40% and interfacial shear strength by 55% (Kabir et al., 2012; Ramachandran et al., 2022). Water contact angle and thermal stability also improve.

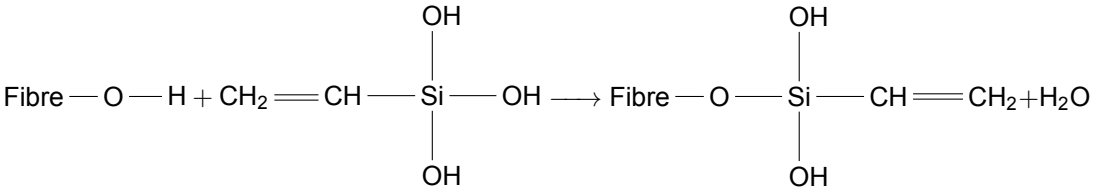

Acetylation

This treatment introduces acetyl groups (CH_3CO) via reaction with acetic anhydride, replacing hydrophilic –OH groups on cellulose. This reduces hygroscopicity and improves dimensional and thermal stability (Kabir et al., 2012). Acetylated fibres show rougher surfaces with fewer voids, enhancing interlocking and mechanical strength. Treated flax and bamboo fibres show increased degradation temperature (up to 360°C) and improved compatibility with polyolefin matrices (Verma et al., 2022).

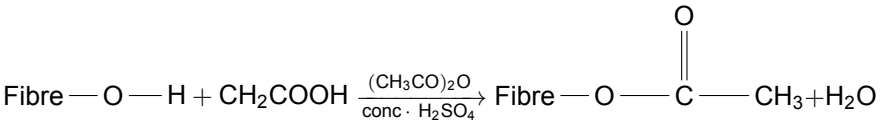

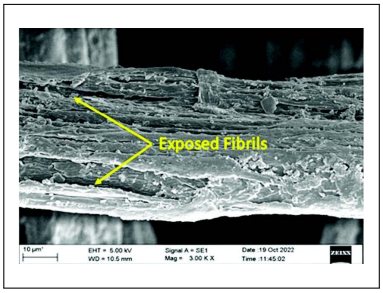

(a) Alkali-treated fibre showing rough texture and fibril exposure (Kudva et al., 2024)

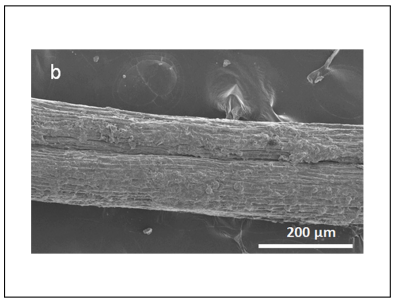

(b) Silane-treated fibre with cleaner surface texture (Sabarinathan et al., 2020)

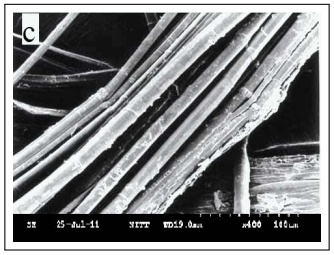

(c) Acetylation-treated fibre showing wax removal with a smoother surface (Sampathkumar et al., 2012)

Figure 2.8: SEM images of natural fibres under different treatments

2.6.4. Potential Compatibility of Hemicellulose and Polycarbonate

The chemical compatibility between hemicellulosic fibres and PC matrices has been demonstrated through multiple studies that reveal the potential of surface modification techniques and interfacial reactions to enhance adhesion. Lignocellulosic fibres, which include hemicellulose, possess abundant hydroxyl groups, making them inherently hydrophilic and thus poorly compatible with the non-polar PC matrix. However, chemical modifications can bridge this polarity gap. For example, in situ, esterification between hydroxyl groups of lignocellulose and carbonate groups of PC during melt extrusion has

improved interfacial bonding and mechanical performance (Zhang et al., 2020).

Additional research involving the coating of natural fibres like tamarind with PC confirmed that surface treatments improved fibre-matrix interaction and thermal stability (Maheswari et al., 2012). Furthermore, hemicellulose derivatives such as xylans have been successfully used in biopolymer films, where incorporation with cellulose derivatives improved barrier and mechanical properties, indicating potential compatibility in thermoplastic matrices (Hussain et al., 2024). These findings collectively support the idea that through targeted surface functionalisation or reactive processing, hemicellulosic fibres can be rendered chemically compatible with polycarbonate matrices, offering a viable route to bio-based composite development.

2.7. Composite Fabrication Techniques

2.7.1. Challenges in Fabrication of Natural Fibre Composites

Natural fibre composites face numerous fabrication challenges arising from the intrinsic variability of natural fibres and their interaction with polymer matrices. Fibre length, diameter, chemical composition, and moisture content variations can result in inconsistent mechanical performance across batches. Additionally, natural fibres are hydrophilic and typically incompatible with hydrophobic polymer matrices, leading to poor interfacial adhesion, fibre pull-out, and void formation (Salit et al., 2014).

Another critical limitation is the low thermal degradation temperature of most natural fibres, typically between 200–250^{o}C (Salit et al., 2014). This restricts the processing temperature window, particularly with thermoplastics like polypropylene and polyamides that require higher melt temperatures. Exceeding this threshold can result in thermal degradation, fibre embrittlement, discolouration, and emission of volatile compounds (Alonso-Montemayor et al., 2022). Hence, strict control over processing parameters such as temperature, pressure, and dwell time is crucial.

Moreover, achieving uniform fibre alignment and dispersion within the matrix is difficult, especially in complex geometries or when using short fibres. Maintaining an optimal fibre volume fraction is essential but challenging, as excessive fibre content can lead to agglomeration and hinder proper wetting by the matrix, ultimately compromising composite strength and stiffness (Beaumann, 2024).

2.7.2. Prepreg Processing Techniques

Prepreg processing involves impregnating fibres with a matrix prior to moulding, allowing precise control over fibre alignment, resin content, and part quality. While thermoset prepregs are widely used, thermoplastic prepregs are gaining attention due to their recyclability, damage tolerance, and rapid processing capabilities. However, processing thermoplastic matrices presents significant challenges. Above their melting temperature—or glass transition temperature for amorphous polymers—thermoplastics exhibit high melt viscosity, which severely limits their ability to infiltrate fibre bundles effectively. This difficulty is especially pronounced when working with natural fibres, which are susceptible to thermal degradation at the elevated temperatures required for thermoplastic melt processing (Beaumann, 2024). To overcome these limitations, alternative impregnation strategies such as powder impregnation (using polymer particles) or solvent-based processing are employed. These methods aim to reduce the thermal load on fibres and improve resin flow into the fibre network, enabling more uniform distribution and reducing void content in the final composite (Vaidya & Chawla, 2008).

The **solvent bath method** is a practical approach to address this issue. This technique involves dissolving a thermoplastic polymer in a suitable solvent to create a low-viscosity solution. Fibre tows are passed through this solution, allowing the polymer to coat the fibres uniformly (Figure 2.9). The solvent evaporates under controlled conditions, leaving behind a dry, pre-impregnated tow (Miller & Gibson, 1996). This process allows excellent fibre wetting at ambient or moderately elevated temperatures, mitigating thermal degradation risk during impregnation. It also improves interfacial bonding by enabling polymer infiltration into microvoids and fibre surface irregularities.

Commonly used solvents include (Salit et al., 2014):

- **Tetrahydrofuran (THF)** – a strong, moderately volatile solvent suitable for dissolving PLA, PC,

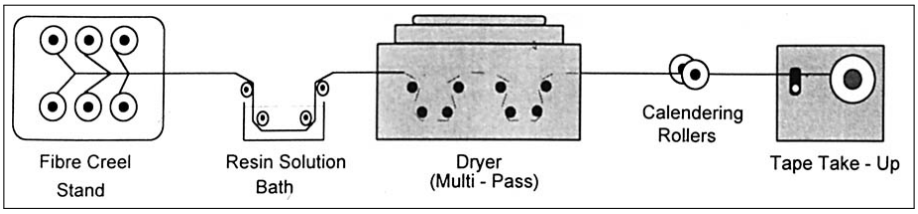

Figure 2.9: Solvent bath impregnation of unidirectional tapes (Miller & Gibson, 1996)

and other biodegradable thermoplastics; offers good fibre wetting and fast drying characteristics (Shawon & Sung, 2004).

- **Dimethylformamide (DMF)** and **dimethyl sulfoxide (DMSO)** – used for dissolving engineering thermoplastics like PA11; they have high boiling points, which may slow evaporation (Li et al., 2025).
- **Acetone** and **ethyl acetate** – fast-evaporating, lower toxicity alternatives suitable for some bio-based polymers (Bosworth & Downes, 2012).

The selection is guided by polymer compatibility, volatility, toxicity, and environmental safety. Improper solvent removal can lead to trapped volatiles that compromise composite quality during consolidation. When optimised, the solvent bath method can produce thermoplastic prepregs with high fibre volume fractions, low void content, and uniform polymer distribution. These prepregs are suitable for subsequent consolidation by compression moulding or thermoforming, enabling high-performance natural fibre-reinforced composites with controlled structure and reproducible properties.

2.7.3. Compression Moulding

Compression moulding is a widely used technique for fabricating thermoplastic natural fibre composites. It involves placing a fibre and matrix material mixture into a heated mould cavity and applying pressure to form and consolidate the composite. The process typically operates at 14–20 MPa and 150–190°C for thermoplastics. Compression moulding is beneficial for its low cycle time, dimensional precision, and minimal fibre damage, making it ideal for producing high-strength biocomposites (Salit et al., 2014). Bamboo fibre-reinforced polypropylene and polyamide 11 composites, for instance, have been successfully fabricated using this method, achieving consistent thickness and mechanical performance when processing parameters were tightly controlled (Beaumann, 2024).

3

Research Gaps & Questions

This chapter outlines key gaps in the literature on natural fibre composites, focusing on interfacial engineering and processing challenges. Based on these gaps, it formulates targeted and feasible research questions to address the unresolved issues through systematic experimental and modelling approaches.

3.1. Literature Gaps

While the development of bio-based fibre composites has gained momentum, several targeted gaps remain in the literature. These gaps are particularly relevant to the experimental investigation of the fibre morphology and interphase in bamboo fibre composites and can be addressed within the scope of this research:

1. **Insufficient Interfacial Characterisation of Bamboo Fibre-Polycarbonate Composites**
   Despite increasing research on bamboo fibre-reinforced polycarbonate polymers, the fibre–matrix interphase remains poorly understood. Most existing studies focus on bulk composite properties, while the role of interfacial adhesion and interphase morphology is underexplored. Quantitative characterisation through mechanical testing is limited and necessary to evaluate the influence of surface treatments and matrix chemistry.
2. **Uncertainty in the Effectiveness of Surface Modification Techniques**
   Common fibre treatments such as alkali, silane, and acetylation are frequently reported to enhance compatibility with polymer matrices. However, systematic and uniform comparative analyses on how they affect the interfacial properties—especially in bio-based thermoplastics and thermosets—are lacking. There is a need to link surface chemistry, morphological changes, and resulting interfacial shear strength to validate and optimise these treatments.
3. **Limited Understanding of Bio-Fibre Compatibility with Polycarbonate Matrices**
   While bio-based polycarbonate offers attractive mechanical and sustainability properties, its interaction with hydrophilic natural fibres such as bamboo is not yet fully understood. Evidence suggests poor adhesion due to polarity mismatch. However, there is little work exploring whether functionalisation or reactive processing can bridge this compatibility gap at the interphase level.
4. **Lack of Processing–Structure–Property Correlations for Thermoplastic Bio-Composites**
   Fabrication techniques like compression moulding and solvent-based prepreg processing are promising for natural fibre composites. However, their influence on interfacial development is not fully mapped. Processing parameters such as temperature, pressure, and solvent drying influence wetting and fibre dispersion, affecting interfacial adhesion. A systematic study that correlates process conditions with interphase quality and composite performance is needed.

3.2. Research Questions

Research Question

How do fibre treatments and manufacturing processes affect the feasibility of Bamboo Fibre Reinforced Bio-Derived Polycarbonate Composites (BFRTPC) in secondary aerospace applications?

Table 3.1: Research Sub-Questions

	Questions	
SQ 1	What effect do different chemical treatments have on the composition, morphology & properties of bamboo fibres?	
	SQ 1.1	What is the effect of varying concentrations of Alkali treatment?
	SQ 1.2	What is the effect of varying concentrations of Silane treatment?
	SQ 1.3	What is the effect of varying concentrations of Acetylation treatment?
SQ 2	What effect do different chemical treatments have on the interfacial properties of BFRTPC?	
	SQ 2.1	What is the effect of varying concentrations of Alkali treatment?
	SQ 2.2	What is the effect of varying concentrations of Silane treatment?
	SQ 2.3	What is the effect of varying concentrations of Acetylation treatment?
SQ 3	What role do fibre prepreg processing and manufacturing conditions play on quality and strength of BFRTPC?	
	SQ 3.1	What is the quality of prepreg produced through solvent-based processing?
	SQ 3.2	What is the quality of composite obtained using produced prepreg?

Part II
Research Activities

4

Methodology

This chapter details the systematic approach undertaken to investigate the interfacial properties of BF-PC composites. The methodology encompasses the preparation of materials, including fibres, matrix, and relevant chemicals, followed by chemical treatments. Characterisation of both fibre and matrix materials was conducted to evaluate physical, chemical, and mechanical properties such as density, thermal degradation behaviour, morphology, and rheological characteristics. Subsequent to characterisation, the manufacturing process of the composites involved careful material preparation, pre-impregnation, and moulding techniques. Prepared specimens were then subjected to various mechanical and microstructural characterisation techniques, including tensile and flexural testing, as well as microscopy-based assessments to evaluate fibre-matrix bonding efficiency and laminate quality. This integrated methodology ensures a comprehensive understanding of how treatment and processing influence the final composite performance.

4.1. Materials

4.1.1. Fibres

Bambooder provided the fibres in this study's experimental work and composite production. A purely mechanical method created and patented by Bambooder was used to extract the fibres.

Full-length bamboo stems are transported from the cultivation site to the manufacturing facility to start the mechanical extraction process. The stems are then divided into smaller portions known as slats after being segmented according to internodal length. After that, these slats are put on an automated manufacturing line. They go through a combing procedure that mechanically removes the fibres if they meet the dimensional requirements (Beumann, 2024).

The length of the resultant fibres typically ranges between 12 and 15 cm. The fibres are bundled in their raw state and differ slightly in length, number of fibres per bundle, and homogeneity. The fibres appear tangled, with some individual fibres detached and not yet in a state suitable for manufacture, as seen in Figure 4.1a.

4.1.2. Matrix

The matrix material used in this study was Durabio, obtained in pellet form (Figure 4.1b) from Mitsubishi Chemicals. The density of Durabio as per the datasheet provided by Mitsubishi Chemicals is 1.34 g/cm^3. Additional properties of Durabio have been summarised in Table 4.1.

4.1.3. Chemicals

The following chemicals were used as received without any further purification. Acetic anhydride (99%), perchloric acid (60%), 3-aminopropyltriethoxysilane (99%), sodium hydroxide (98%, pellets), and tetrahydrofuran (99%) were procured from Merck Sigma. From Central Warehouse L&M, acetic acid (99.8%) and denatured ethanol (96%) were obtained. Toluene (99.85%) was supplied by Thermo

(a) Bamboo Fibre

(b) Durabio Pellets

Figure 4.1: Materials used for this project

Table 4.1: Summary of Durabio properties (Mitsubishi Chemical Group, 2024)

Property	Value
Density (g/cm^3)	1.34
Glass Transition Temperature (°C)*	120
Melt Temperature (°C)	230-250
Tensile Modulus (MPa)	2200
Tensile Strength (MPa)	70
Flexural Modulus (MPa)	2500
Flexural Strength (MPa)	95
Melt Flow Index (g/10min)	12

* (Baltscheit et al., 2020)

Fisher Scientific. All chemicals were in liquid form except for sodium hydroxide, which was in pellet form.

4.2. Chemical Treatments

This section describes the chemical modification procedures applied to the bamboo fibres to enhance their surface properties and interfacial compatibility with the polymer matrix. All fibres were subjected to an identical pre-treatment and post-treatment protocol to ensure consistency in moisture content and chemical residue removal. The three chemical treatments explored—alkali, silane, and acetylation—were performed independently. Each method was selected for its potential to tailor specific surface characteristics and improve fibre–matrix interaction. Additionally, consistency was maintained in selected concentrations of the treatments, treatment durations and amount of fibres used. The preparation protocols for each treatment are detailed in the following subsections and summarised in Table 4.2.

Table 4.2: Summary of chemical treatment protocols

Specimen ID	Chemical Treatment	Primary Chemicals	Additional Chemicals	Concentration	Additional Comments
Untreated	N/A				
2-NaBF	Alkali	Sodium Hydroxide	DI Water	2%	
5-NaBF				5%	
8-NaBF				8%	
2-SiBF	Silane	3-Aminopropyl triethoxysilane	Ethanol DI Water (80:20) Acetic Acid	2 g/L	Acetic acid added to maintain a pH of 5
5-SiBF				5 g/L	
8-SiBF				8 g/L	
2-AcBF	Acetylation	Toluene Acetic Acid	Acetic Anhydride Perchloric Acid	2:1:1	∼1ml of perchloric acid added as catalyst
5-AcBF				5:1:1	
8-AcBF				8:1:1	

Fibre Pretreatment

Before any chemical modification, all fibre samples were dried in a vacuum oven at 80°C for 1 hour to remove surface and loosely bound moisture. A 60% w/v fibre to solution concentration was used for all treatments. This ensured consistency across treatment batches.

4.2.1. Alkali Treatment

Alkali treatment was conducted using sodium hydroxide solutions of three different concentrations: 2%, 5%, and 8% (w/v) as seen in Figure 4.2a. Each solution was prepared by mixing the appropriate quantity of NaOH in distilled water. Bamboo fibres were immersed in the solution at room temperature for 2 hours. This method is consistent with standard practices reported in the literature, where NaOH concentrations typically range between 0.5% and 10% and immersion times vary between 20 minutes and 8 hours, depending on the intended modification level (Hu et al., 2018; Kudva et al., 2024; Phuong et al., 2010).

4.2.2. Silane Treatment

A coupling solution of 3-aminopropyltriethoxysilane was prepared in an 80:20 denatured ethanol-to-water ratio for the silane treatment. The pH of the solution was adjusted to 5 by adding acetic acid and acetic anhydride. Three different concentrations of silane—2g/L, 5g/L, and 8g/L—were used in this study. Bamboo fibres were submerged in each solution for 2 hours at room temperature (Figure 4.2b). The hydrolysis and condensation reactions of silane in aqueous conditions allow it to bond with hydroxyl groups on the fibre surface, forming stable covalent bonds (Lu et al., 2013; Vishal et al., 2024; Wagaye et al., 2024).

4.2.3. Acetylation Treatment

The acetylation process began with immersing the fibres in toluene and acetic acid mixture at 2:1:1, 5:1:1, and 8:1:1 (toluene: acetic acid: acetic anhydride). The solution was stirred while being heated to 60°C for 5 minutes (Figure 4.2c). Subsequently, acetic anhydride and a few drops of perchloric acid catalyst were added to initiate the esterification process. The solution was continuously stirred for a total of 2 hours. This approach follows the standardised acetylation technique where fibres are initially soaked in acetic acid, then treated with acetic anhydride at slightly elevated temperatures, often with a catalyst (Bledzki et al., 2008; Zygouris, 2024).

Post-treatment

After undergoing the above treatments, all fibres were rinsed 3 to 4 times using ethanol and distilled water to eliminate residual chemicals. Rinsing was continued until the wash water attained a neutral pH (approximately 7). Finally, the cleaned fibres were dried in a vacuum oven at 80°C for 20 hours to ensure complete moisture removal before further characterisation or composite fabrication.

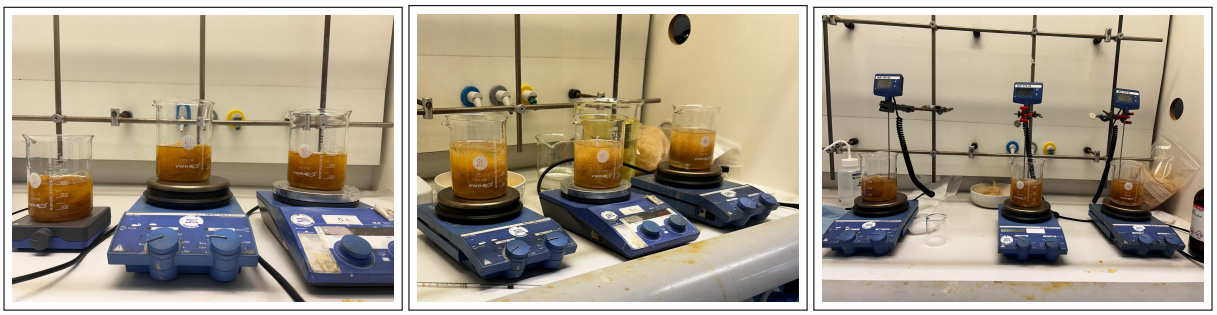

(a) NaOH Treatment **(b)** Silane Treatment **(c)** Acetylation Treatment

Figure 4.2: Treatment of bamboo fibres in the various solutions as the magnetic stirrers ensure a homogenous solution

4.3. Fibre & Matrix Characterisation

This section outlines the procedures to characterise the bamboo fibres' fundamental physical and chemical properties before and after surface treatments. These methods provided insights into the effects

of treatment on morphology, composition, mechanical behaviour, and interfacial performance.

4.3.1. Density

Fibre density was measured using an Anton Paar Ultrapyc 5000 helium pycnometer (Figure 4.3) as per ASTM Standard D8171 (American Society for Testing and Materials, 2018). Helium pycnometry is a technique used to determine a solid material's true (skeletal) density by measuring its volume through helium gas displacement. It operates on Boyle's Law, where helium, an inert gas, is introduced into a chamber containing the sample and allowed to expand into a reference chamber. By observing the pressure changes before and after expansion, the volume occupied by the solid (excluding open pores) can be calculated. With the known mass of the sample, true density is then determined as mass divided by volume. Helium's ability to penetrate fine pores ensures accurate volume measurement, making the method highly precise (Lowell et al., 2012). This approach eliminates the influence of water uptake, which is common in natural fibres, ensuring more reliable density estimation.

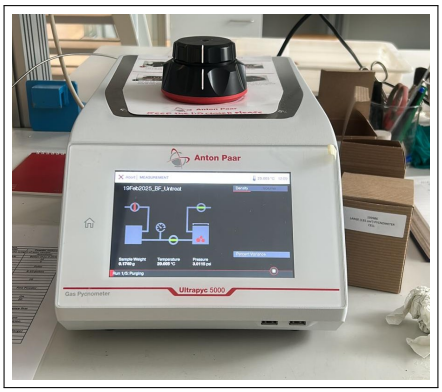

Figure 4.3: Anton Paar Ultrapyc 5000 with the digital display indicating the current status of the experiment. The specimen chamber can be seen here with the black cover on top.

4.3.2. Water Absorption

Water absorption tests assessed hydrophilicity by immersing fibre specimens in distilled water as seen in Figure 4.4. The mass of each specimen was recorded after 3 months. This long-term measurement helped quantify the water uptake behaviour of untreated versus treated fibres, providing insight into the efficacy of hydrophobic surface treatments.

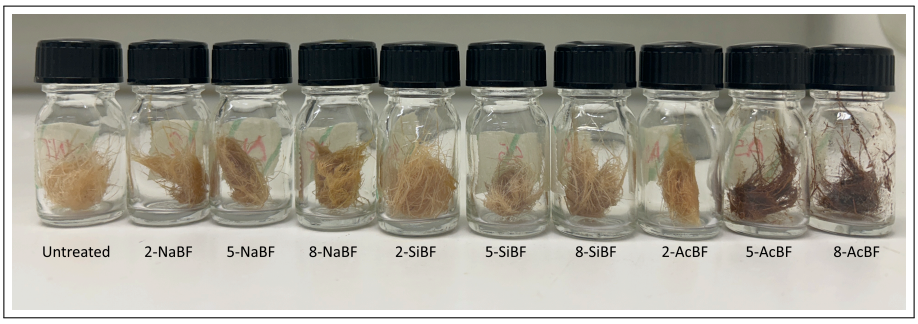

Figure 4.4: Immersion of fibres in water in small glass containers to prevent contamination during the dwell phase

4.3.3. Functional Group Analysis

FTIR spectroscopy was employed using a PerkinElmer Spectrum 100 Optica Spectrometer (Figure 4.5). FTIR is an analytical technique to identify organic, polymeric, and some inorganic materials by measuring how molecules absorb infrared light at different wavelengths. The principle is based on the fact

that molecular bonds vibrate at characteristic frequencies, and when IR radiation passes through a sample, specific wavelengths are absorbed, corresponding to these vibrational modes. FTIR collects all the absorption data simultaneously and applies a mathematical Fourier Transform to convert the raw interferogram signal into an interpretable IR spectrum, which acts as a molecular fingerprint of the material (Griffiths & de Haseth, 2008).

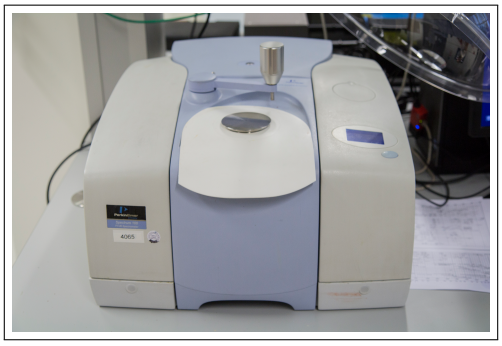

Figure 4.5: PerkinElmer Spectrum 100 Optica Spectrometer

Spectra were acquired across the range of 4000 to 500cm^{-1}, at a resolution of 1cm^{-1}, with 32 scan accumulations per measurement. This technique allowed for identifying characteristic chemical groups and provided qualitative evidence of chemical modification due to treatment.

4.3.4. Thermal Degradation

The thermal stability of the fibres was evaluated using a PerkinElmer TGA 4000 Thermogravimetric Analyzer (Figure 4.6). All tests were performed in an inert nitrogen (N_2) atmosphere at a flow rate of 20mL/min to prevent oxidative degradation.

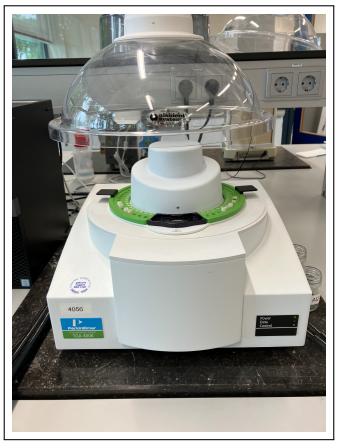

Figure 4.6: PerkinElmer TGA 4000 Thermogravimetric Analyzer

The thermal profile was defined in two stages:

- A ramp from 35°C to 105°C at 5°C/min to acquire sufficient data to accurately capture the degradation behaviour, followed by a 15-minute isothermal hold to minimise moisture.
- A subsequent ramp from 105°C to 995°C at 5°C/min, ending with another 15-minute isothermal hold.

This procedure facilitated accurate determination of onset degradation temperatures, mass loss characteristics and char yield, comparing untreated and treated fibres.

4.3.5. Morphology

Fibre surface morphology was examined using a JSM-7500F SEM. This analysis enabled the observation of structural and surface modifications due to chemical or physical treatments. Before imaging, samples were sputter-coated with a thin layer of gold to establish a conductive surface layer as seen in Figure 4.7. This step was crucial for minimising charging effects and enhancing the signal quality, thereby improving image resolution and reliability for comparative analysis of untreated and treated fibres.

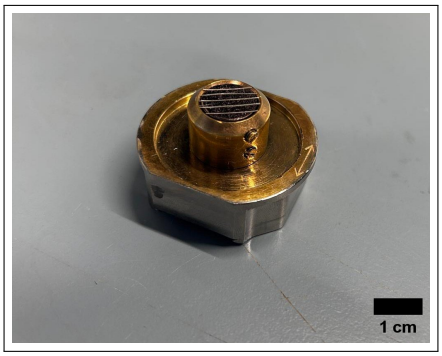

Figure 4.7: Pieces of fibre were cut and then stuck on a metal stub with the help of conductive tape (seen in black); this specimen was then coated with gold and placed in the designated SEM specimen holder.

4.3.6. Single Fibre Tensile Test

Tensile properties of individual fibres were measured following ASTM C1557 (American Society for Testing and Materials, 2020a) standards using a Zwick/Roell 10kN universal testing machine equipped with a 100N load cell.

Specimen preparation involved mounting fibres on paper tabs (Figure 4.8), with an adhesive applied at an 80mm gauge length. Fibres were carefully chosen to ensure that only individual fibres were chosen, with additional verification under the microscope. However, in certain instances, it was unavoidable to ensure a completely smooth, single fibre. The average diameter of the prepared fibres was then measured to enable accurate calculation of strengths after the test. The average value was chosen as using the minimum or maximum values could grossly over or under-estimate the strength, respectively. Just before testing, the fibres were placed along with the tab in the oven at 50°C for 30 mins to dry the fibres. Tabs were carefully slit in the middle immediately before testing. A low strain rate of 0.25mm/min to accurately capture the fibre behaviour, keeping in mind the potential low maximum load. Due to high diameter variability (as verified via SEM), a larger sample size of 10 specimens was tested to ensure the statistical reliability of the results. From this point forward, for all further analysis, the acetylation treatment was excluded as it severely damaged the fibres, making them non-handleable.

Further, the average tensile modulus of the fibres were calculated using:

$$E_f = \frac{\Delta\sigma}{\Delta\epsilon} \tag{4.1}$$

where the stress and strain were selected from within the slope of the linear region of the force-displacement plot as recommended by the ASTM standard.

4.3.7. Rheometry

Rheological characterisation was carried out using the Haake Mars III Rheometer (Figure 4.9) to evaluate the processability of Durabio and inform the selection of manufacturing parameters. The primary experiment performed was a temperature sweep from 150°C to 240°C under a constant shear stress of 10 Pa. At each temperature increment, the polymer was allowed to reach thermal equilibrium before recording viscosity and the resulting shear rate. Controlled stress mode was selected over controlled strain because, at lower temperatures where the viscosity is high, achieving a fixed shear rate would require substantial mechanical force, potentially damaging the equipment. This test allowed for the

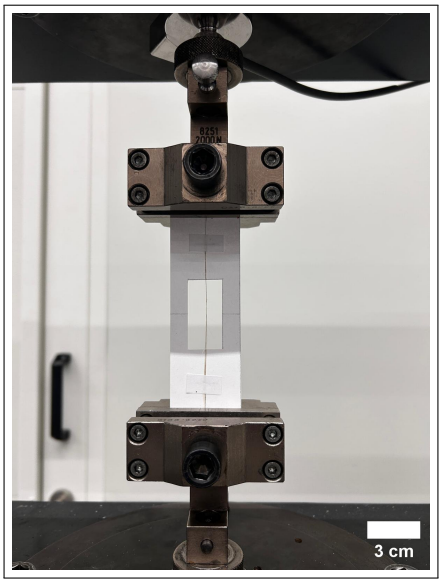

Figure 4.8: The single fibres were stuck on the paper tab using cyanoacrylate glue and a small piece of paper to secure it. The tab was loaded on the UTM, and the paper was cut along the mid-line.

identification of the polymer's thermal softening profile and processing window by capturing the sharp decrease and further stabilisation in viscosity as temperature increased.

In addition to the temperature sweep, two further tests were planned. The first was an incremental stress analysis at a constant temperature of 200°C to observe how viscosity changes with increasing load. The temperature of 200°C was selected as this was both sufficiently lower than the fibre degradation and also the viscosity had already started to stabilise. The second was a time sweep under a constant temperature of 200°C and stress selected from the incremental stress analysis to assess the polymer's rheological stability over prolonged processing durations. Unfortunately, neither of these analyses could be performed due to an unexpected rheometer malfunction. A combined evaluation of these tests would have given us the ideal processing window, pressure required and dwell time while keeping in mind the fibre degradation temperature.

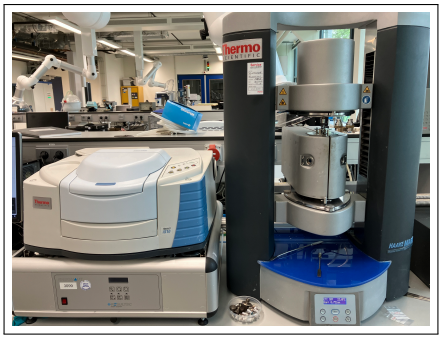

Figure 4.9: Haake Mars III Rheometer

4.3.8. Matrix Solubility

A solvent-based dissolution study was conducted to investigate the solubility characteristics of the PC matrix for potential reuse without compromising fibre integrity.

Initially, acetone was evaluated as a potential solvent due to its common availability and low toxicity. A weighed sample of PC was immersed in acetone under ambient conditions. However, the resulting

solution turned turbid, and the residual polymer exhibited an opaque appearance, deviating from PC's known optical characteristics. This indicated incomplete dissolution.

Subsequently, THF was selected as an alternative solvent due to its higher polycarbonate solubility. The dissolution of PC in THF was performed under continuous stirring. The resulting polymer solution was optically clear, indicating successful dissolution and suggesting the absence of visible degradation or chemical modification.

A saturation study was performed to determine PC's weight-to-weight (w/w) saturation concentration in THF to characterise solubility behaviour further. Increasing weights of THF were incrementally added to a fixed PC mass in a conical flask under constant magnetic stirring until no further dissolution was observed. This procedure allowed the identification of the saturation point, which is crucial for optimising solvent usage in recycling protocols.

These experiments provide a basis for selecting THF as a preferred solvent in future matrix recovery processes where fibre preservation is a priority.

4.4. Composite Manufacturing

4.4.1. Material Preparation

The composite manufacturing process involved the preparation of both matrix films and pre-impregnated fibres, followed by consolidation using compression moulding. The focus was on achieving uniform fibre dispersion and a controlled fibre volume fraction to ensure reproducibility and comparability across composite samples.

Matrix

DuraBio pellets were first converted into films using a custom-fabricated aluminium compression mould as seen in Figure 4.10a. This mould was specifically designed to produce larger films within the constraints of the available compression moulding setup, enabling better film thickness control (Figure 4.10b). The method enabled the quick production of matrix films required for film stacking in composite fabrication.

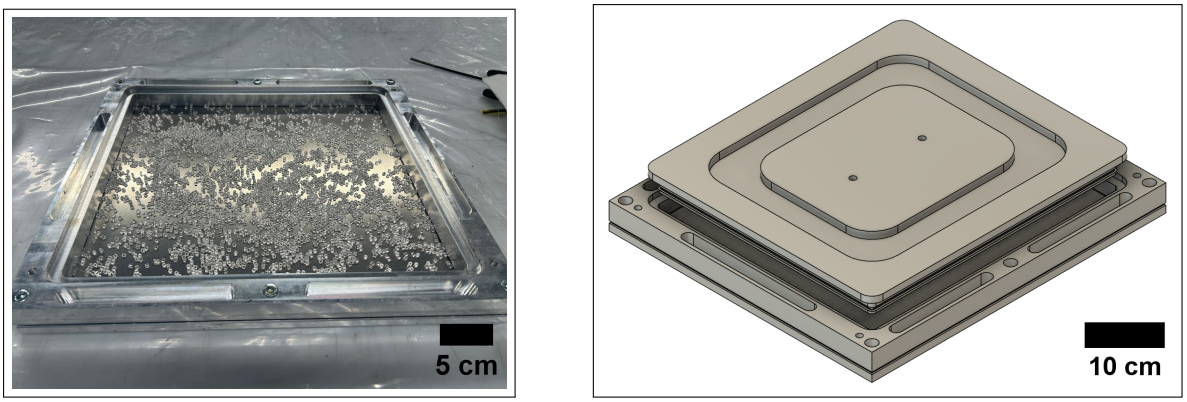

(a) Preparation for film pressing by weighing and uniformly distributing pellets in the mould

(b) CAD schematic of the custom aluminium mould for pressing of larger films

Figure 4.10: Film pressing setup and mould schematic

To initiate the moulding process, PC pellets were pressed at a temperature of 200°C under a pressure of 5 bar. This pressure was chosen based on prior observations where lower pressures yielded a high void content in the films. Prior to this, a preheating dwell at 105°C was implemented to allow complete moisture evaporation, thus minimising the risk of voids and air bubble entrapment during the melt phase. These processing parameters are summarised in Figure 4.11.

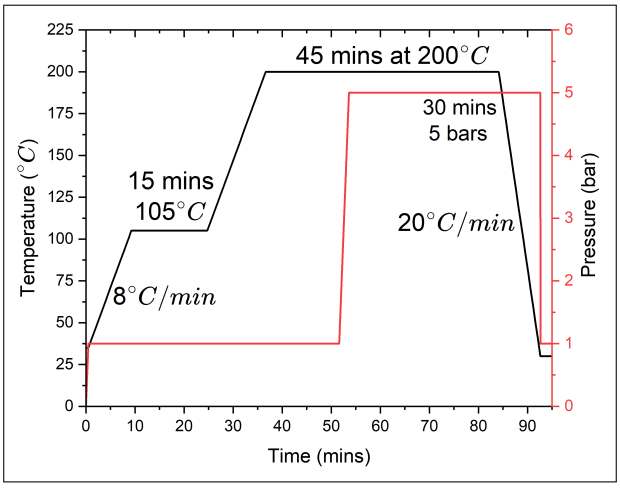

Figure 4.11: Compression Moulding Paramaters

While this processing temperature is slightly lower than the recommended Durabio processing temperature of 230°C, this was done to ensure uniformity during composite manufacturing, which could not be done at 230°C due to the degradation temperature of bamboo fibre.

From an input of 100g of PC pellets, approximately 33g of usable films were obtained, indicating significant material loss due to excessive bleed-out from the mould. Some attempts were made to recycle this bleed-out material and spare film segments by re-pressing them into new films. While these secondary films were of acceptable quality, the issue of non-uniform thickness persisted. Achieving very thin and uniform films remained challenging, affecting reproducibility and matrix consistency in later composite processing steps.

Pre-Impregnated Fibres

Given the challenges of achieving uniform film thickness and its impact on fibre volume fraction and matrix homogeneity, a solution-based prepreg method was justified. This method used PC's previously established solubility characteristics in THF, with a 30% w/w PC-THF solution selected to maximise solubility while avoiding undissolved residues. This also included the usage of waste pieces of Durabio obtained from bleed-out of polymer during film formation as seen in Figure 4.12c.

Before impregnation, fibre bundles were carefully weighed to allow for post-process estimation of matrix mass fractions. The raw fibres included undesirable stem regions used to arrange the fibre in a mat. The fibres were selected to be approximately the same length and arranged into UD mats to improve handling. They were secured with tape across one end as seen in Figure 4.12b. These stems were left unimpregnated and subsequently trimmed off after the drying stage.

The fibre mats were immersed in the PC-THF solution and left to dry at room temperature. Slow solvent evaporation achieved uniform PC deposition across the fibre surfaces, resulting in continuous prepreg sheets. The excess solution was allowed to drip from the mats and collected for reuse, which can be seen in Figure 4.12d.

The mats were left to dry for a full day to ensure thorough THF removal. Due to tape and solution drying, the fibres hardened and remained bundled, which aided handling but introduced challenges in achieving ideal fibre distribution during moulding.

4.4.2. Composite Moulding

The dried prepreg mats were placed flat and straight into the aluminium mould for composite consolidation (Figure 4.13a). Due to the hardening of the fibres in bundles, perfect unidirectional alignment and uniform distribution were difficult to maintain. However, the laminates were assumed to be ideally

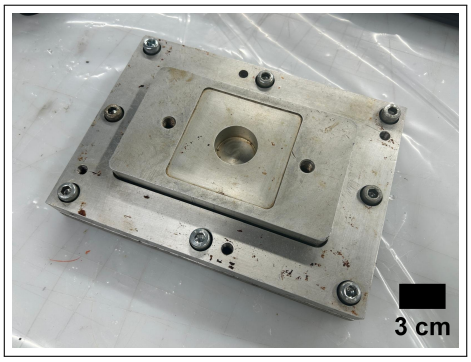

(a) Custom mould made for compression moulding of laminate of smaller size

(b) Arrangement of fibres into a mat using the stem end and securing the mat with tape

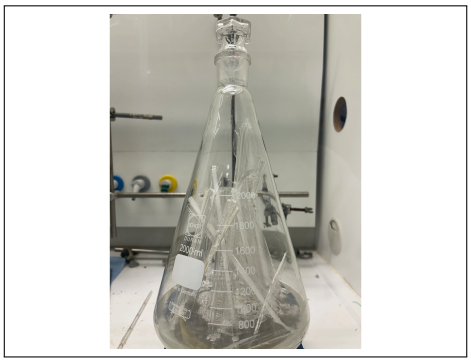

(c) Dissolution of Durabio in THF using a magnetic stirrer with reuse of waste pieces of PC from the film pressing

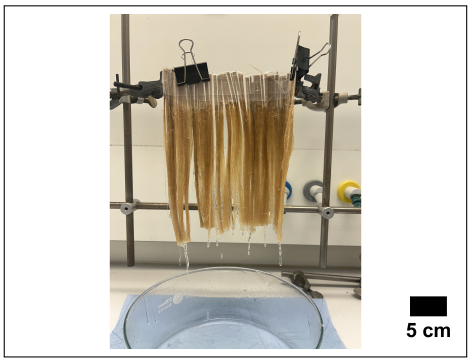

(d) Drying of fibres at room conditions after immersing the fibres in the PC-THF solution

Figure 4.12: Preparation and pre-impregnation of fibres

UD and uniformly distributed for all subsequent calculations.

During stacking, additional PC films were inserted between fibre layers to achieve the targeted 60% matrix mass fraction in the final laminate. The arrangement of fibres and films was guided by their mass, shape, and length, with uniformity achieved by symmetrically placing the films with fibres divided between them based on their mass. Further balance was achieved by alternating the direction of the fibres based on the side from which the dry stem was trimmed. This adjustment enabled greater control over the final composition of the composite.

Before pressing, the stacked laminates were placed in an oven at 130°C, which is approximately the T_g of Durabio (120°C) (Baltscheit et al., 2020), for 30 minutes. This step softened the fibres slightly, allowing attempts to straighten the bundles and improve alignment before final consolidation (Figure 4.13b).

Composite pressing was conducted using the same optimised parameters applied during PC film preparation-5bar pressure at 200°C with an initial dwell at 105°C. This consistent thermal and pressure regime helped ensure comparable quality between the neat films and final composite laminates (Figure 4.13c).

4.4.3. Specimen Preparation

Specimen Cutting

The consolidated laminate was first cut into strips of the desired width using a CompCut ACS 600 precision cutting machine (Figure 4.14a). To ensure uniformity, the final specimen length was then trimmed using a SecoTom 60 machine (Figure 4.14b). Both machines utilised water as a coolant to prevent damage to the specimen and cutting blades. While using water as a coolant is known to negatively affect the mechanical performance of natural fibre composites—due to their poor hygrothermal resistance—it

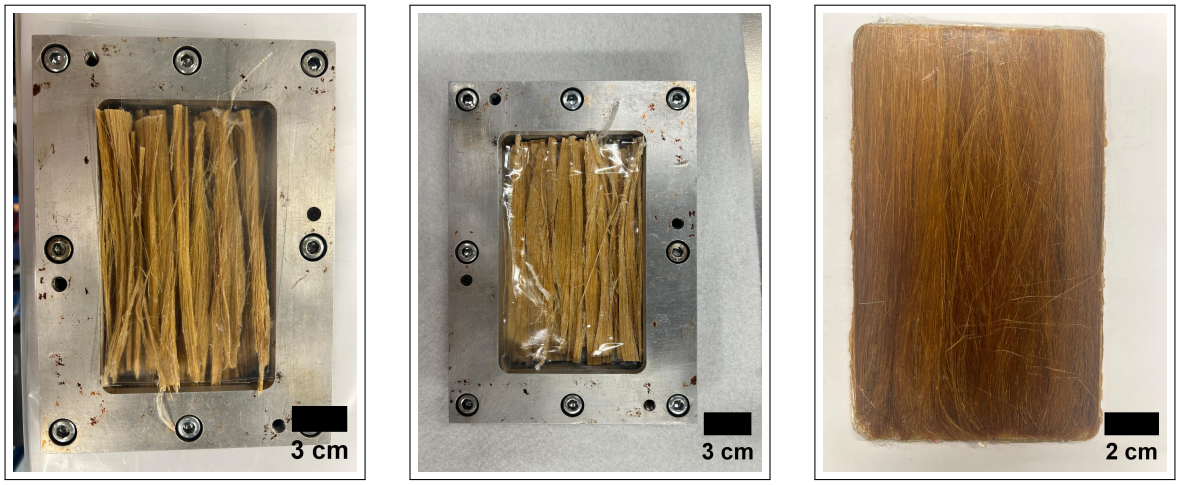

(a) Uniform and unidirectional arrangement of fibres and matrix films in the mould

(b) Softening and straightening of fibres after heating in the oven

(c) Final laminate obtained after compression moulding

Figure 4.13: Preparation and result of compression moulding of bamboo fibre polycarbonate laminates

was necessary to employ water cooling when operating this equipment.

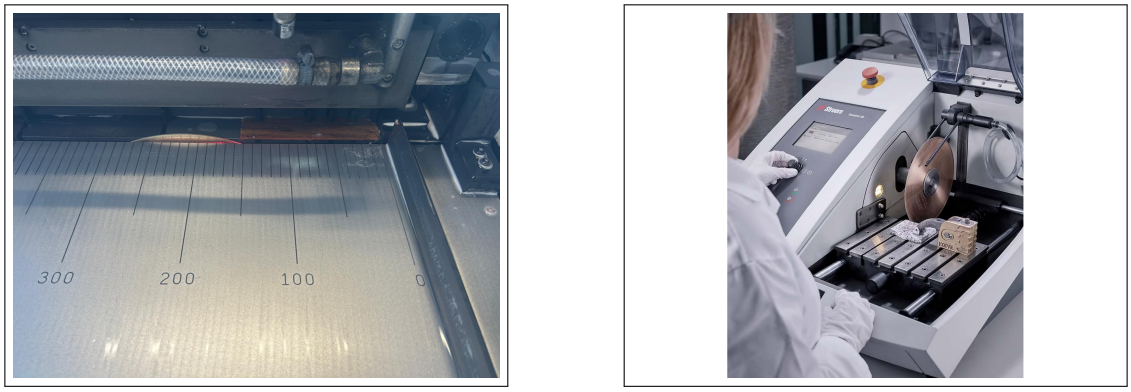

(a) Close-up view of the CompCut ACS 600

(b) Secotom 60 (Beaumann, 2024)

Figure 4.14: Specimen cutting equipment

To mitigate potential moisture-induced degradation, all specimens were subsequently dried overnight in an oven at 40°C. This ensured the removal of absorbed moisture and minimised any adverse effects on mechanical testing performance due to water exposure during cutting.

Specimen Weighing and Measuring

The physical dimensions of each specimen were precisely measured using a digital calliper, and the weight of the specimens was recorded using a Mettler Toledo precision scale (Figure 4.15). These measurements were used to calculate the actual density of the laminates, which was later used to verify the fibre volume fraction in the composite structure.

4.5. Composite Characterisation

4.5.1. Cross-Sectional Microscopy

Cross-sectional microscopy was performed to evaluate the fibre impregnation quality and distribution within the composite. To avoid artefacts associated with moisture uptake in natural fibres, a conscious decision was made not to embed the specimens in resin prior to imaging. The high capillarity of lignocellulosic fibres can lead to rapid water absorption during embedding and polishing, resulting in trapped

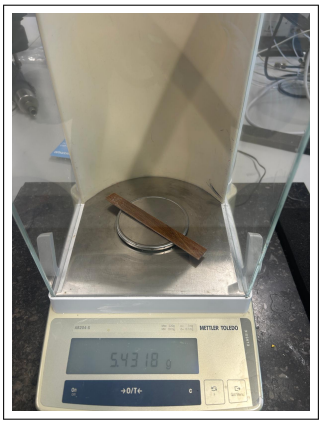

Figure 4.15: Specimen weighing using the Mettler Toledo scale

moisture or air bubbles that compromise image quality.

Instead, imaging was conducted on the transverse cross-sections of fractured tensile and flexural specimens, which had been oven-dried to minimise residual moisture. These samples were sectioned carefully and mounted for optical analysis without additional surface treatment.

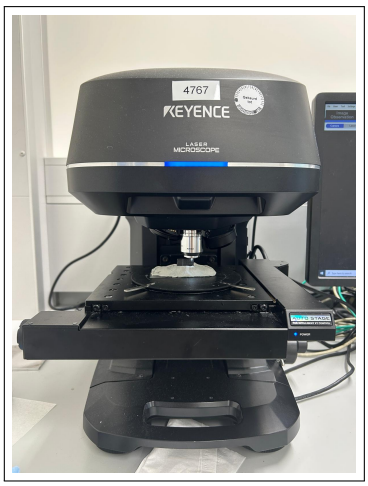

(a) 3D laser scanning confocal microscope VK-X1000

(b) Wide area 3D measurement system VR-5000

Figure 4.16: Optical microscopy equipment

Imaging was carried out using a Keyence Laser Confocal Microscope (VK-X1000) (Figure 4.16a), employing the laser confocal stitching mode to generate high-resolution composite images of the full cross-sectional area. This approach allowed detailed visualisation of fibre wetting, distribution, and interfacial quality across the sample width.

4.5.2. Determination of Laminate Quality

To assess laminate quality, both quantitative and qualitative methods were employed. Quantitatively, the density of each laminate specimen was determined using Archimedes' principle as per ASTM D792 (American Society for Testing and Materials, 2020b). This involved measuring the sample mass in air and while submerged in distilled water using a Mettler Toledo precision scale equipped with a submerged tray support (Figure 4.17). The density was calculated using the following equation:

$$\rho_a = \frac{A}{A-B}(\rho_0 - \rho_L) + \rho_L \tag{4.2}$$

This approach, based on Archimedes' principle, relies on the difference in mass between air and immersion states to calculate the sample's bulk density.

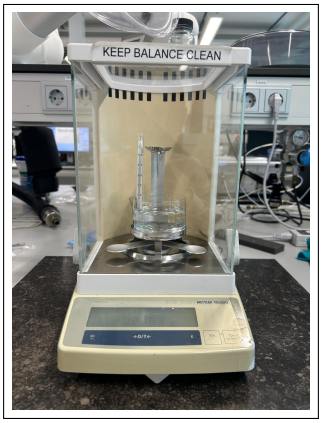

Figure 4.17: Density measurement setup using the Mettler Toledo scale

In addition to density measurements, qualitative observations were performed. Visual inspection identified macroscopic defects such as dry spots, voids, or inconsistent fibre packing. Further, high-resolution optical imaging of the surface was conducted using a Keyence VR-5000 optical microscope (Figure 4.16b).

Combined, these methods provided a holistic evaluation of laminate quality through both physical measurement and surface morphology assessment.

4.5.3. Tensile Testing

Tensile testing was performed according to the ASTM D3039 - Standard Test Method for Tensile Properties of Polymer Matrix Composite Materials (American Society for Testing and Materials, 2014).

The tests were conducted using a 20 kN Universal Testing Machine (Zwick) equipped with a 20 kN load cell at a crosshead speed of 1mm/min as recommended by the standards. An extensometer clamped directly onto the specimens was used to record strain. Using an extensometer provided highly accurate strain data by eliminating compliance effects from the machine as seen in Figure 4.18. Consequently, the extensometer data was used for all strain-related calculations.

Due to limitations in fibre length, the fabricated specimens were shorter than the standard recommends, with a total length of 140mm and width of 15mm, as permitted for unidirectional specimens by the standard. The grip-to-grip gauge length was set to 90 mm to ensure adequate clamping and avoid slippage.

The modulus of elasticity (chord modulus) was calculated according to the following formula between two strain values, 0.001 and 0.003, as the ASTM D3039 standard recommended:

$$E_{1a} = \frac{\Delta\sigma}{\Delta\varepsilon} \tag{4.3}$$

Fibre-Matrix Bonding Efficiency

The experimentally measured properties were compared with predictions calculated using the Rule of Mixtures to evaluate the efficiency of composite properties across the various treatments used in this study. This procedure is a modified version of the calculations performed by Woigk et al. (Woigk et al., 2019). The longitudinal tensile modulus of the composite was estimated using the RoM (Daniel et al., 1994), as shown in:

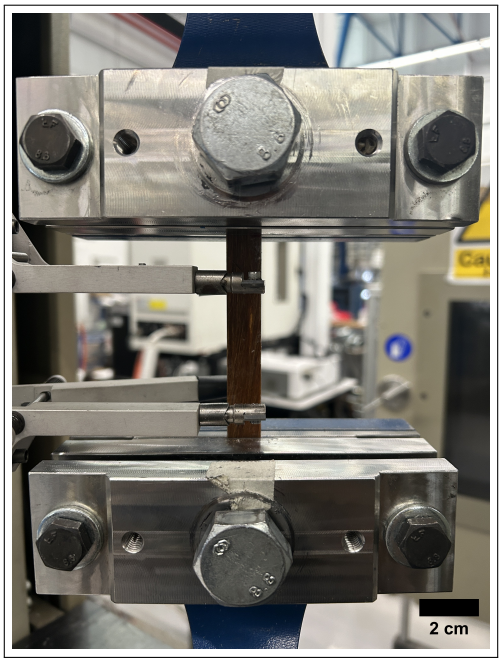

Figure 4.18: Tensile testing setup on the 20kN UTM with extensiometer for accurate measurement of displacement

$$E_{1t} = \frac{\left(\frac{E_f w_f}{\rho_f}\right) + \left(\frac{E_m w_m}{\rho_m}\right)}{\frac{wf}{\rho_f} + \frac{wm}{\rho_m}} \tag{4.4}$$

The following considerations and steps were followed in calculating the bonding efficiency of the laminates:

1. The fibre modulus used in these calculations was obtained from single fibre tensile tests.
2. The matrix modulus was back-calculated from the experimentally determined tensile modulus of the laminate reinforced with untreated fibres using the RoM. This matrix modulus was then used consistently across all laminate calculations.

$$E_m = \left[\left\{E_{1a}\left(\frac{w_f}{\rho_f} + \frac{w_m}{\rho_m}\right)\right\} - \left(\frac{E_f w_f}{\rho_f}\right)\right] \times \frac{\rho_m}{w_m} \tag{4.5}$$

3. Fibre and matrix densities were taken from experimental measurements. Notably, the matrix modulus and density were experimentally derived because datasheet values for Durabio are based on injection moulding, whereas the laminates in this study were manufactured via compression moulding.
4. All calculations assumed a fibre-to-matrix mass fraction of 40:60. Additionally, it was assumed that the fibres or matrix did not undergo any thermal degradation and maintained constant properties.
5. Given the high void content in the laminates, relying solely on tensile modulus could lead to incomplete conclusions. Therefore, both the experimentally measured and theoretically calculated moduli were normalised using the corresponding laminate densities to account for void-induced effects to give us specific moduli.

$$\text{Specific } E_{1a} = \frac{E_{1a}}{\rho_a} \qquad \text{Specific } E_{1t} = \frac{E_{1t}}{\rho_t} \tag{4.6}$$

6. Finally, the bonding efficiency was determined using:

$$k = \frac{\text{Specific } E_{1a}}{\text{Specific } E_{1t}} \times 100 \tag{4.7}$$

which quantifies the effectiveness of fibre impregnation and interfacial bonding. Specifically, it expresses the measured property as a percentage of the theoretical maximum predicted by the model.

4.5.4. Flexural Testing

Flexural testing was conducted following ASTM D7264 - Standard Test Method for Flexural Properties of Polymer Matrix Composite Materials (American Society for Testing and Materials, 2021).

A 20 kN universal testing machine (Zwick), equipped with a 20 kN load cell with a crosshead speed of 1mm/min, was used to perform the flexural tests. As illustrated in Figure 4.19, a four-point bending setup was selected over the three-point bending method. This choice was made as the 4PB eliminates shear forces in the gauge length of the test specimen while maintaining a constant bending moment, thus eliminating failure due to loads other than pure bending.

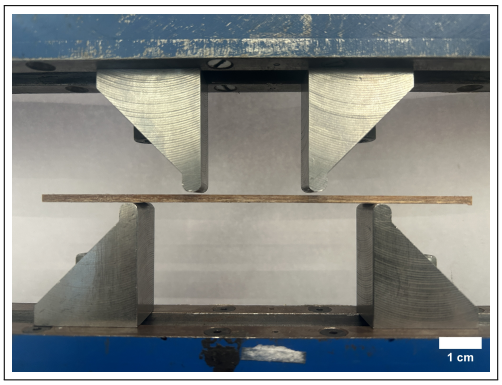

Figure 4.19: 4-point flexural testing setup

The following equations, provided by the ASTM standard, were used for stress and strain calculations:

$$\sigma = \frac{3PL}{4bh^2} \qquad \epsilon = \frac{48\delta h}{11L^2} \tag{4.8}$$

The mid-span deflection δ had to be calculated using beam theory as the displacement obtained from the test is the displacement at the loading pind and is defined as:

$$\delta = \frac{3}{2}\delta_{\text{nominal}} \tag{4.9}$$

Due to the variations in laminate thickness and fibre length, the recommended 130 mm span could not be used. Therefore, based on the 32:1 span-to-thickness ratio, the span length for each laminate was chosen based on the average thickness of the panel.

Close-up images of the failure locations from tensile and flexural testing were captured using the Keyence VR-5000 optical microscope to examine the failure modes closely. These images provided insights into fracture behaviour, including fibre pull-out, matrix cracking, and delamination, helping to identify the dominant failure mechanisms in each laminate.

5

Result Analysis

This chapter presents a detailed analysis of the experimental observations across multiple material and composite evaluation stages. It begins with characterising fibre and matrix, focusing on morphology, density, water absorption, composition, degradation, single fibre tensile behaviour, and rheology. These baseline properties form the foundation for understanding how individual constituents influence composite performance. Observations from the pre-preg manufacturing process are also highlighted. The chapter then transitions to composite manufacturing outcomes, evaluating processing quality, consolidation, and integrity. Finally, mechanical testing and cross-sectional microscopy results are presented to assess the interfacial performance of the developed composites.

5.1. Fibre & Matrix Characterisation

5.1.1. Density

The trends exhibited by the skeletal density of fibres based on the chemical treatment and its concentration can be seen in Figure 5.1a. For alkali-treated fibres, a noticeable reduction in density was observed at lower concentrations (2%), attributed to partial lignin removal, which increased the internal porosity of the fibres. However, at higher concentrations, complete removal of wax and lignin led to pore collapse, resulting in void closure and fibre compaction, thereby increasing skeletal density (Murwamadala et al., 2024).

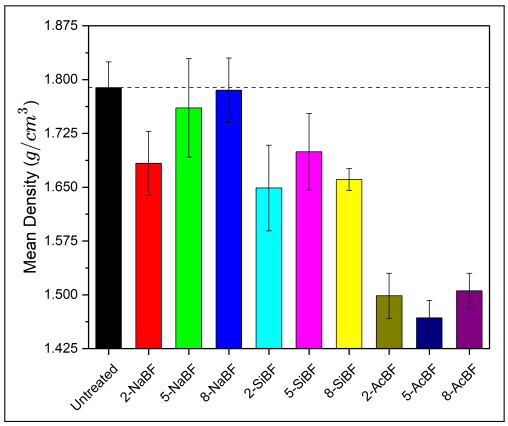

(a) Skeletal density of treated fibres in comparison to the untreated BF

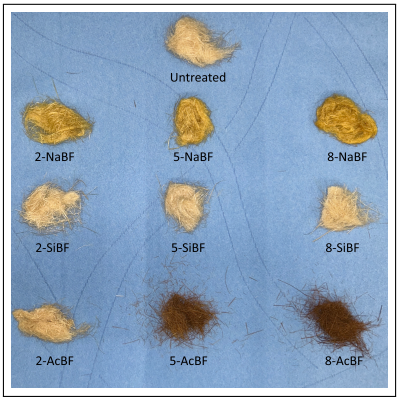

(b) Alkali and silane treated fibres showing changes in colour and acetylated fibres showing deterioration

Figure 5.1: Density and visual analysis of the treated and untreated fibres

In the case of silane treatment, minimal lignin removal at 2% reduced density, however, at 5% silane treatment, a higher density than 2% and 8% was observed. This could indicate optimal removal of lignin and wax, along with effective substitution of silane bonds that filled the pores and coated the fibre surface. At 8% silane concentration, excessive removal of binding material may have caused

pore and void collapse, reducing the effectiveness of silane coverage on the fibre and contributing to a higher density.

In contrast, acetylation treatment caused significant damage to the fibre microstructure, particularly at higher concentrations, leading to a substantial drop in skeletal density. Additionally, a lower substitution efficiency of acetyl groups at 5% suggests limited chemical integration, which failed to counteract the structural degradation induced by the treatment. These variations underscore the importance of treatment concentration in modulating fibre structure and density.

5.1.2. Water Absorption

Chemical treatments type and concentration significantly influence the water absorption behaviour of bamboo fibres, as seen in Figure 5.2. The untreated fibre displayed a high water absorption at approximately 84%, which is expected due to the abundance of hydrophilic hydroxyl groups and open microstructure that readily allows moisture uptake.

Alkali-treated fibres showed a consistent reduction in water absorption with increasing NaOH concentration. Treatment with 2-NaBF removed some hemicellulose and surface impurities, reducing hydrophilicity and decreasing absorption to around 75%. The 5% and 8-NaBF treatments further decreased water uptake to approximately 73% and 70%, respectively. This trend can be attributed to the deeper removal of amorphous, hydrophilic components and the potential collapse of the fibre lumen at higher concentrations, which seals internal pores and limits water ingress.

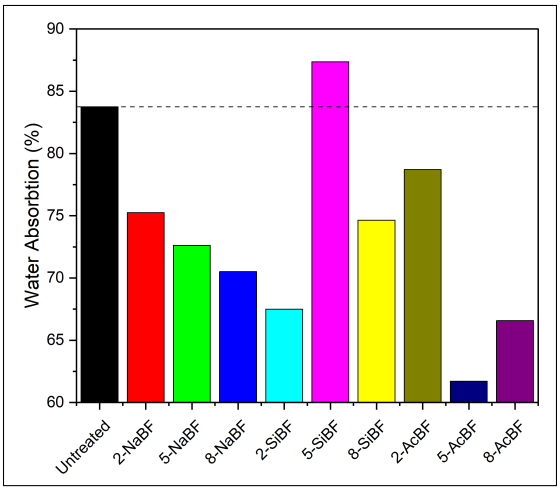

Figure 5.2: Water absorption of treated fibres in comparison to the untreated BF

Silane-treated fibres exhibited more variable behaviour. At 2% concentration, silane treatment could lead to the formation of some hydrophobic Si–O–Si linkages on the fibre surface, reducing absorption to below 68%. However, water absorption sharply increased to nearly 88% at 5%, possibly due to the presence of reversible Si-O-C groups, which are themselves polar and attract water. The self-condensation of silane groups can be controlled by adjusting the pH of the solution and ensuring its mild acidity (Xie et al., 2010). At 8%, the water absorption reduced again to around 74%, suggesting improved network formation and better silane hydrolysis that restored some hydrophobicity.

Acetylated fibres showed the most effective suppression of water absorption. However, the high levels of chemical modification caused fibre degradation as seen in Figure 5.3, rendering the samples structurally unstable, which, being problematic for practical handling, made the values inaccurate.

5.1.3. Morphology

A clear evolution in surface morphology was observed across the untreated and treated fibre conditions, which can be seen in both the SEM images in Figure 4.7 and visually in Figure 5.1b, highlighting the effectiveness and varying intensity of the different chemical treatments applied. The untreated fi-

bres (Figure 5.3a) presented a rough and heterogeneous surface, characterised by surface impurities, waxes, and retained lignin. This morphology characterises the typical state of lignocellulosic fibres.

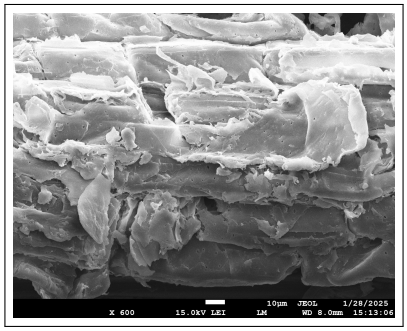

(a) Untreated fibres' rough surface showing the presence of wax and dirt

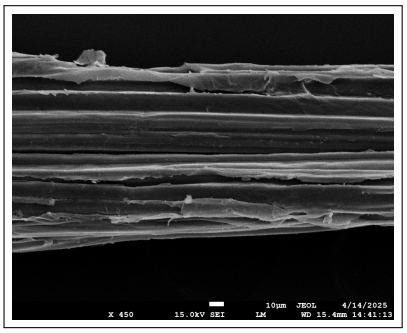

(b) 2-NaBF treated fibre showing removal of wax and smooth fibre surface

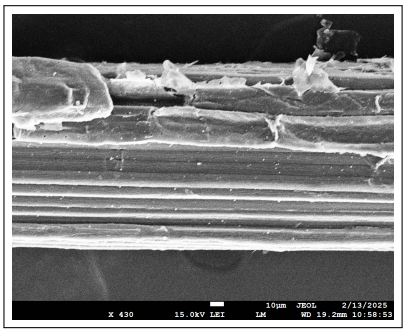

(c) 5-NaBF treated fibre showing increased presence of micro-fibril exposure

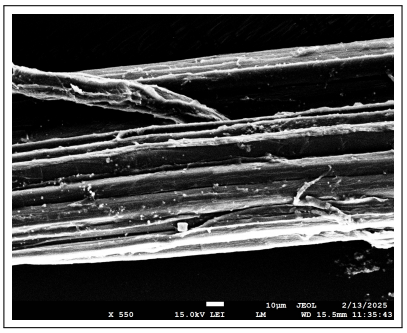

(d) 8-NaBF treated fibre with higher microfibril presence than 2% and 5%

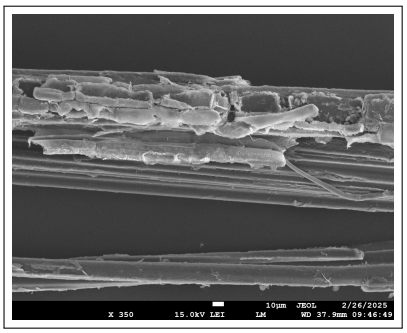

(e) 2SiBF treated fibre showing wax removal and micro-fibril exposure indicating insufficient silane bonding

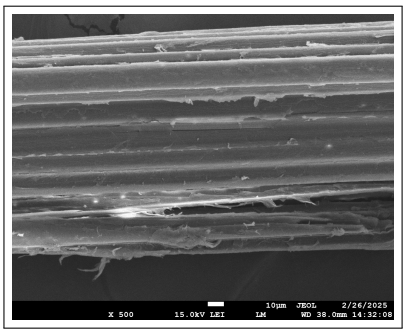

(f) 5-SiBF treated BF showing reduced fibril exposure indicating filling of pores by silane bonds

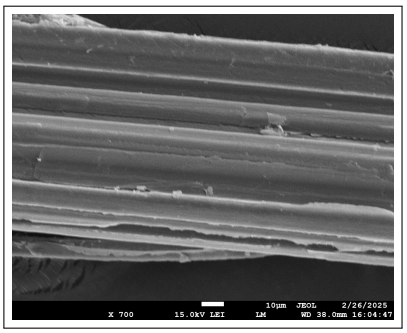

(g) 8-SiBF treated BF with the smoothest surface indicating high silane bond coverage in pores

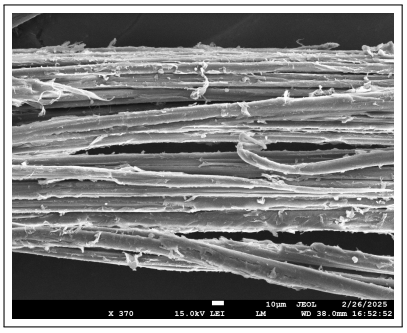

(h) 2-AcBF treated BF with the removal of wax and lignin shown by exposure of fibrils

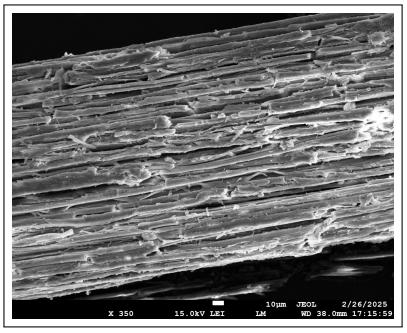

(i) 5-AcBF treated BF indicating damage to fibres due to harsh chemicals

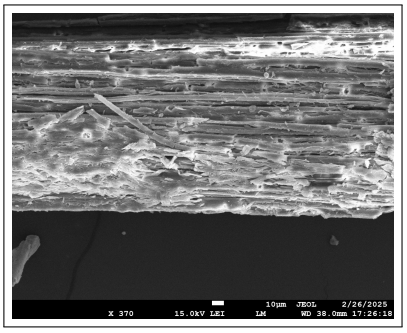

(j) 8-AcBF treatment showing high level of damage with increasing concentration

Figure 5.3: SEM images of treated and untreated bamboo fibres showing the effect of different chemicals and processes on the surface morphology of the fibres

In contrast, alkali-treated fibres progressively improved surface cleanliness and uniformity with increasing NaOH concentration as seen in Figure 5.3b, Figure 5.3c and Figure 5.3d. The removal of superficial dirt and partial delignification at lower concentrations was evident, resulting in a relatively smoother fibre surface. Higher concentrations facilitated deeper removal of binding materials such as wax and residual lignin, exposing finer micro-fibrillar structures. The increased visibility of these fibrils characterises effective fibrillation and a potential increase in available surface area for matrix adhesion.

Silane treatment also led to a noticeable modification of the fibre surface. At a 2% silane concentration (Figure 5.3e), moderate waxes and surface lignin removal were observed, although some heterogeneity remained. However, 5% and 8% silane treatments (Figure 5.3f and Figure 5.3g) resulted in markedly smoother surfaces, with evidence of pore filling and developing a more continuous coating. This suggests successful silane grafting, reducing the presence of protruding fibrils and forming a more consolidated surface interface, which is beneficial for chemical coupling with polymer matrices.

Acetylation had a distinctly different impact. While 2% acetylated fibres (Figure 5.3h) retained their structure and exhibited reduced surface roughness due to partial hemicellulose removal, higher concentrations (Figure 5.3i and Figure 5.3j) demonstrated excessive degradation which is similar to behaviour observed with other natural fibres (Bledzki et al., 2008). SEM images showed damaged fibre walls and collapsed microstructures, suggesting that aggressive acetylation conditions can compromise fibre integrity. Instead of controlled exposure of fibrils, these conditions appeared to degrade structural cellulose, leading to brittle fibres and decreased morphological definition.

5.1.4. Functional Group Analysis

FTIR analysis revealed distinct chemical changes in fibre composition following the different chemical treatments. For alkali-treated fibres (Figure 5.4a), there was clear evidence of removal of O–H and C–H bonds associated with lignin, seen in the broad absorbance reduction between 3500-2750 cm^{-1}. Additionally, a reduction in the C=O and C=C bonds of lignin near 1600 cm^{-1} was observed. No other significant peaks showed alteration, supporting that lignin was the primary target of the alkali treatment.

In the case of silane-treated fibres (Figure 5.4b), a similar removal of O–H and C–H groups attributed to lignin was noted. However, in contrast to alkali treatment, the C=O bands at $\sim$1600 cm^{-1} showed limited changes, indicating no significant impact on hemicellulose. The spectrum also revealed the presence of C–O–C bonds around 1000 cm^{-1} and a range of Si-based functional groups distributed between 1750-1000 cm^{-1}, confirming successful silane grafting onto the fibre surface.

For acetylated fibres (Figure 5.4c), the O–H groups of lignin were similarly reduced, suggesting partial lignin removal. There was an increase in signals corresponding to C=O, C–O–C, and C–H groups between 1750-1250 cm^{-1}, consistent with substituting acetyl groups into the fibre matrix. The presence of out-of-plane C–H bending vibrations further indicated that while acetylation was effective, it caused limited damage to the cellulose backbone. These findings collectively validate the specific chemical interactions expected from each treatment and their selective effects on fibre constituents.

Finally, the FTIR shown in Figure 5.4d shows the chemical functionalities of DuraBio, untreated bamboo fibre, and BF impregnated with DuraBio. The DuraBio spectrum shows characteristic peaks of a polycarbonate backbone. Upon impregnation, the FTIR profile displays combined features from both DuraBio and BF, with the difference between the peak amplitudes between 1200-800 cm^{-1} being smoother, indicating an overlay of the characteristics of BF and DuraBio, suggesting successful impregnation of the matrix on the fibre and polymer.

5.1.5. Thermal Degradation

The thermal degradation (Figure 5.5 & Table 5.1) of lignocellulosic biomass typically occurs in three distinct stages (Mudoi & Sinha, 2024). The first stage, up to around 150°C, corresponds to the evaporation of moisture physically bound within the fibre structure. The second stage, between 200°C and 400°C, involves the active pyrolysis of the biomass, where most of the mass loss takes place. This phase includes the decomposition of hemicellulose, followed by cellulose breakdown. The final stage, occurring above 450°C, is associated with the slower degradation of lignin and the residual char.

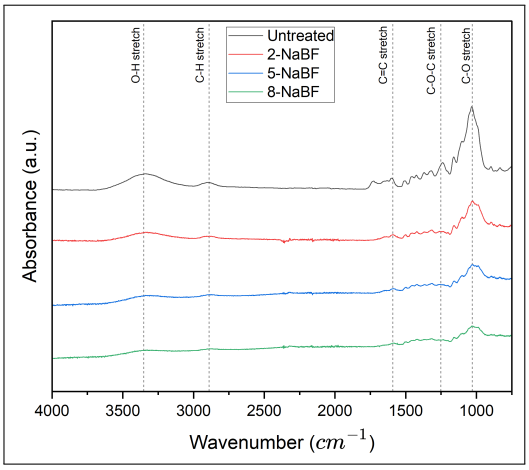

(a) Removal of O-H and C-H bonds of lignin between 3500-2750 cm^{-1} and reduction in C=C bond at ≈1600 cm^{-1}

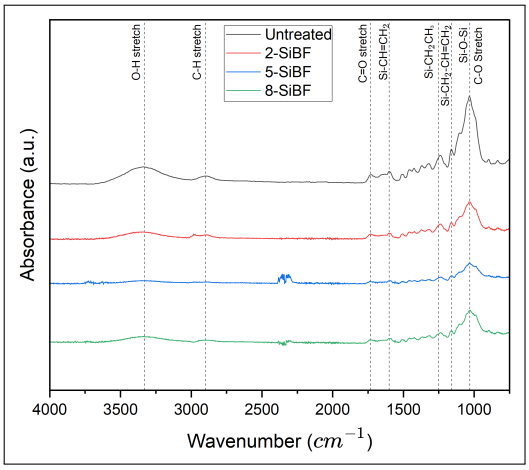

(b) Removal of O-H and C-H groups of lignin and presence of various Si-functional groups between 1750-1000 cm^{-1}

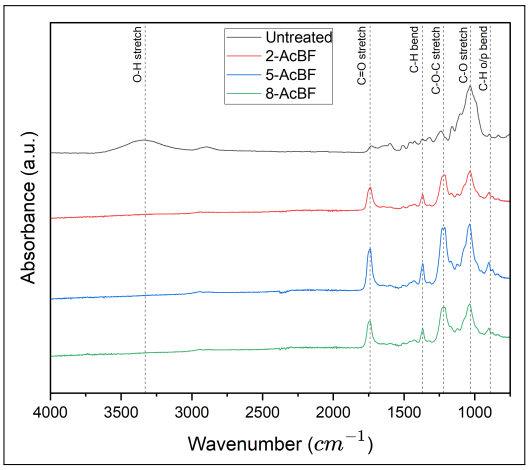

(c) Increased presence of acetyl groups between 1750-1250 cm^{-1} and presence of out-of-plane C-H at ≈900 cm^{-1}

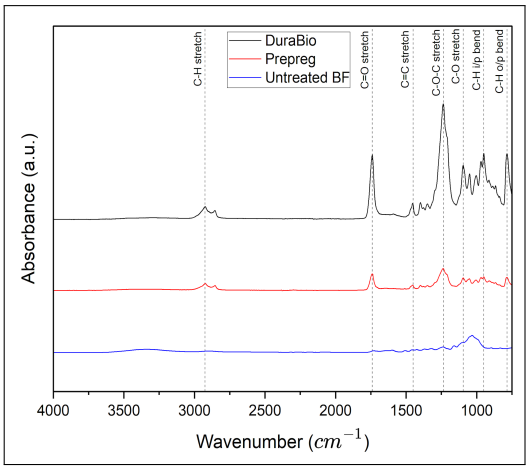

(d) Absorbance plot for the pre-preg shows an overlay of the DuraBio and BF plots with no major chemical changes

Figure 5.4: FTIR plots for all treated fibres along with a comparative FTIR of the untreated BF, DuraBio and pre-preg fibres

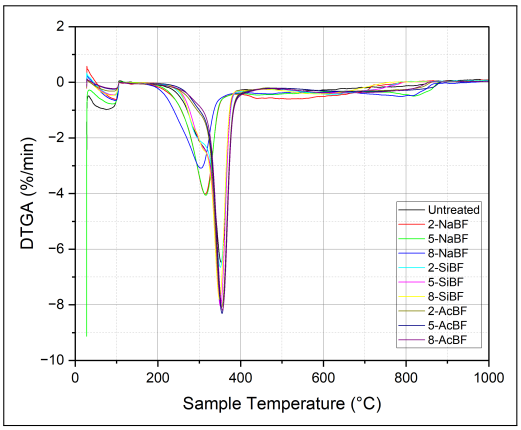

(a) Alkali fibres show a lower maximum rate of degradation and lower peak temperature than other treatments

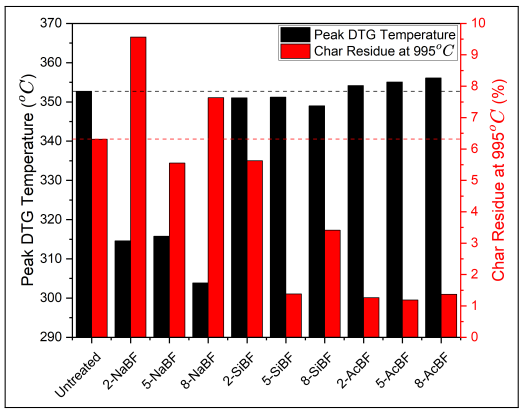

(b) Comparative assessment of DTG peak temperature and char residue across all treatments.

Figure 5.5: DTG results and comparative assessments of thermal degradation behaviour of treated bamboo fibres

Alkali-treated fibres exhibit a maximum degradation rate at a lower temperature than other treatments, indicating reduced thermal stability. This treatment also results in a lower peak degradation

rate, which can be attributed to removing lignin that exposes the more thermally labile hemicellulose. In contrast, silane- and acetylation-treated fibres show nearly identical maximum rates of degradation, likely due to the substitution of Si and acetyl functional groups onto the fibre surface, which impart stabilising effects.

Silane and acetyl groups show lower char residue and higher DTG peaks. However, silane does not contribute to the carbon residue, and acetylated fibres exhibited structural degradation, leading to reduced char yield. In contrast, alkali treatments introduce Na^+ ions on the fibre surface, which alter the decomposition mechanism and lead to a higher char yield (Sebestyén et al., 2011).

Table 5.1: Summary of thermal degradation analysis of treated bamboo fibres

	Wt. Loss (%)			Wt. (%)	Peak DTG	
Sample	Stage 1 Upto 150°C	Stage 2 200°C-400°C	Stage 3 450°C-800°C	Final Char Residue At 995°C	Temperature (°C)	Wt. Loss (%)
Untreated	3.94	70.98	16.33	6.31	352.71	44.33
2-NaBF	3.35	55.54	27.49	9.57	314.58	62.64
5-NaBF	3.54	55.19	26.08	5.55	315.76	62.39
8-NaBF	3.58	51.31	27.79	7.64	303.86	64.66
2-SiBF	2.53	70.19	19.98	5.63	351.03	48.93
5-SiBF	2.11	75.44	18.91	1.38	351.20	47.04
8-SiBF	2.25	74.42	17.67	3.41	348.99	47.25
2-AcBF	1.62	72.69	19.34	1.27	354.15	52.14
5-AcBF	1.72	70.32	20.04	1.19	355.08	54.55
8-AcBF	1.79	68.93	22.88	1.37	356.10	55.20

5.1.6. Single Fibre Tensile Test

The specific tensile properties of chemically treated bamboo fibres are presented in Figure 5.6. These values were normalised by the skeletal density of each fibre, allowing for a direct comparison of the specific strength and stiffness. The exact fibre strength and modulus values, along with relevant fibre metrics, have been summarised in Table 5.2. Across all treatments, improvements over untreated fibre performance were evident, both in terms of absolute tensile values and in specific properties normalised by density.

Alkali-treated fibres, particularly 2-NaBF, exhibited the highest improvements in both absolute and specific tensile strength and modulus. The partial removal of surface-bound non-cellulosic constituents such as lignin, hemicellulose, and waxes aligns the cellulose microfibrils, enabling a cleaner load path. Simultaneously, the treatment reduces the overall skeletal density of the fibre by increasing internal porosity and removing heavier hydrophilic components. The combined effect of improved internal alignment and reduced density results in a pronounced increase in specific tensile performance.

In 5-NaBF, improvements in absolute modulus remained high; however, the gain in specific properties was somewhat less pronounced. While deeper delignification and fibrillation were observed via SEM, these also introduced greater microstructural heterogeneity and localised defects, leading to variability in tensile behaviour. Increased fibrillation may improve interfacial adhesion but can compromise the integrity of the primary cellulose backbone. The density also increased slightly compared to 2-NaBF. As a result, the specific modulus plateaued, and strength showed only marginal improvement over the untreated baseline.

At 8-NaBF, a decline in both absolute and specific tensile properties was recorded. Excessive chemical degradation caused by high alkali concentration led to partial degradation of the cellulose phase. The presence of microcracks along the fibre length contributes to early failure and inefficient load-bearing behaviour. Additionally, the skeletal density increased due to the collapse of internal pores and voids, further penalising specific property values.

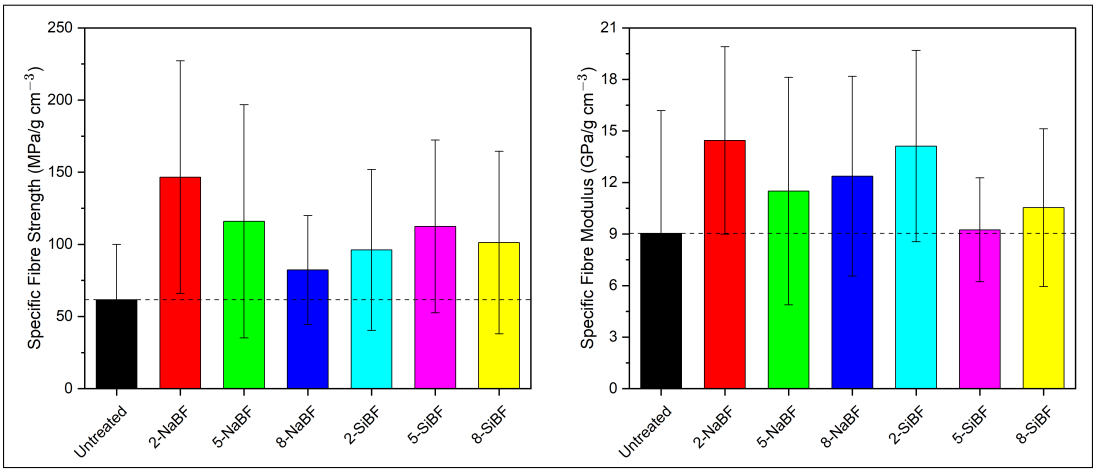

Figure 5.6: Specific single fibre tensile properties of the different treatments showing high standard deviation bars indicative of the heterogeneity of bamboo fibres

Fibres treated with silane also showed improvements in both absolute and specific tensile properties, especially in 5-SiBF. Silane coupling facilitates the formation of Si–O–Si bonds with cellulose. While absolute values were lower than those of 2-NaBF, the reduction in density allowed for gains in specific properties. SEM images showed smoother, more continuous surfaces with fewer defects, supporting more homogeneous load transfer and reduced stress concentrations.

In 8-SiBF, however, a reduction in specific tensile performance was observed. This can be attributed to the formation of brittle surface layers due to excessive silane deposition. In parallel, a slight increase in density was noted, possibly due to the mass of the deposited silane layer, which further lowered specific performance metrics.

5.1.7. Rheology

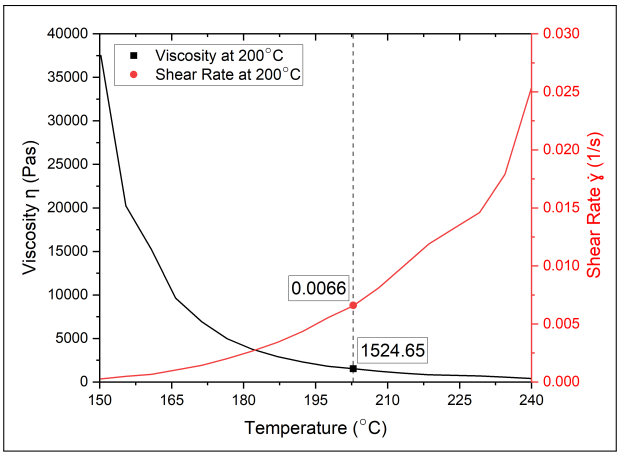

Figure 5.7: Viscosity and shear rate profile of Durabio over temperature

The graph in Figure 5.7 illustrates the temperature-dependent viscosity and shear rate of the polymer under a constant shear stress of 10 Pa. As temperature increases from 150°C to 240°C, viscosity decreases significantly, indicating thermal softening and enhanced flowability. At 200°C, the viscosity is approximately 1525 Pa·s with a corresponding shear rate of 0.0066 s^{-1}. Therefore, the temperature of 200°C was selected for composite processing as stated in Section 4.3.7.

Table 5.2: Fibre property summary

	Untreated	2-NaBF	5-NaBF	8-NaBF
Tensile				
Strength (MPa)	110.64 ± 64.24	249.51 ± 129.28	205.92 ± 136.21	148.47 ± 64.22
Elongation at Max. Strength (mm)	0.71 ± 0.23	0.88 ± 0.28	0.79 ± 0.28	0.69 ± 0.36
Modulus (GPa)	16.21 ± 12.10	24.59 ± 8.76	20.43 ± 11.16	22.34 ± 9.89
Other Metrics				
Fibre Density (g/cm^3)	1.7943	1.7023	1.7767	1.8063
Water Absorption (%)	83.74	75.26	72.62	70.51
Degradation Temperature (°C)*	267	272	271	250

	2-SiBF	5-SiBF	8-SiBF
Tensile			
Strength (MPa)	161.70 ± 87.63	194.24 ± 98.18	168.06 ± 99.72
Elongation at Max. Strength (mm)	0.54 ± 0.19	1.04 ± 0.40	0.85 ± 0.22
Modulus (GPa)	23.74 ± 8.76	15.99 ± 4.96	17.49 ± 7.24
Other Metrics			
Fibre Density (g/cm^3)	1.6819	1.7289	1.6606
Water Absorption (%)	67.49	87.37	74.64
Degradation Temperature (°C)*	269	277	265

	2-AcBF	5-AcBF	8-AcBF
Tensile			
Strength (MPa) Elongation at Max. Strength (mm) Modulus (GPa)	N/A		
Other Metrics			
Fibre Density (g/cm^3)	1.4978	1.4803	1.5153
Water Absorption (%)	78.71	61.72	66.58
Degradation Temperature (°C)*	275	279	273

* Extrapolated degradation onset temperature (Ref. Appendix B).

5.2. Composite Analysis

5.2.1. Prepreg Quality

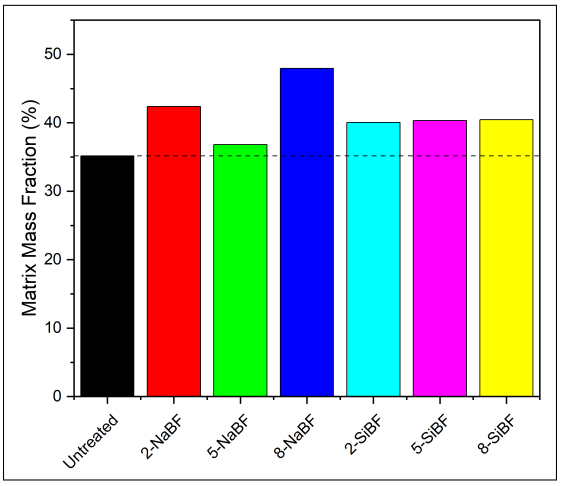

Figure 5.8: Uptake of Durabio after pre-impregnation of bamboo fibre

The matrix uptake behaviour of bamboo fibres varies significantly with surface treatment, as evident from Figure 5.8. Alkali-treated fibres showed the highest matrix mass fraction due to the removal

of surface waxes and lignin, which exposed cellulose fibrils and increased surface roughness and porosity. This enhanced both the surface area available for bonding and the internal pore network for resin infiltration. In contrast, silane-treated fibres exhibited moderate improvement over untreated fibres. Although silane treatment does not significantly alter fibre morphology, it introduces reactive silane groups that form secondary covalent bonds with the matrix, improving interfacial compatibility (Threepopnatkul et al., 2009). Untreated fibres with intact hydrophobic surface layers showed the lowest uptake due to poor wettability and limited resin diffusion. Additional FTIR plots for verification of successful impregnation of fibres have been plotted in Appendix A.

5.2.2. Laminate Quality

Void Content Analysis

The void contents of the different laminates have been shown in Figure 5.9). Alkali-treated fibres exhibit a progressive increase in void content with increasing NaOH concentration, peaking at over 30% for the 8-NaBF treatment. While alkali treatment enhances matrix uptake by removing surface waxes and lignin, higher concentrations significantly disrupt the fibre microstructure. Furthermore, the exposed cellulose lacks functional groups compatible with Durabio, resulting in poor chemical affinity and wetting. This interfacial incompatibility further contributes to void formation, particularly during compression moulding, where the high temperature allows the matrix to flow and interact with other similar matrix molecules and separate from the fibres.

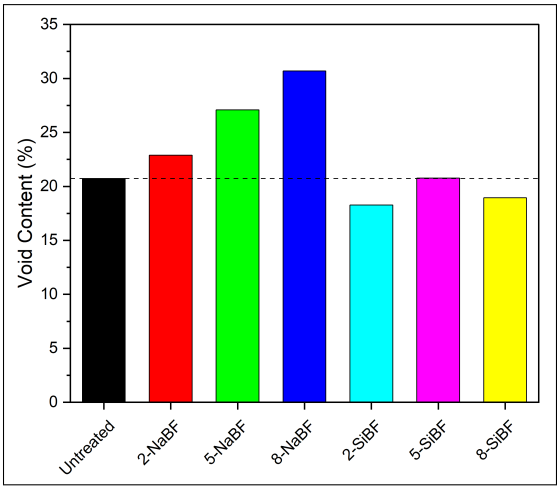

Figure 5.9: Void content of the different laminates

In contrast, silane-treated fibres show a consistent decrease in void content with increasing silane concentration, with the 8-SiBF laminate exhibiting the lowest void fraction among all samples. Silane coupling agents introduce reactive silane groups that form secondary covalent bonds with the polymer matrix, improving fibrematrix adhesion. Enhanced wetting reduces the likelihood of air entrapment, and the modified fibre surfaces provide a nucleation site for the matrix during compression moulding.

It must be noted that all void contents observed are significantly higher than the commonly accepted threshold of below 2% for structural composites. This deviation can be primarily attributed to two factors. Firstly, Durabio has a high melt flow index. Secondly, the inability to optimise processing parameters—especially pressure and dwell time—due to the breakdown of the rheometer further contributed to the sub-optimal consolidation and entrapped air within the laminates.

Cross-Sectional Microscopy

Visual analysis and confocal microscopy of transverse cross-sections revealed clear trends in laminate quality as seen in Figure 5.10. The untreated laminate exhibited moderate void content with some visible defects, as supported by the void content analysis. The 2-SiBF-treated sample displayed the best overall quality with fibre alignment and matrix distribution, all supported by the lowest void content.

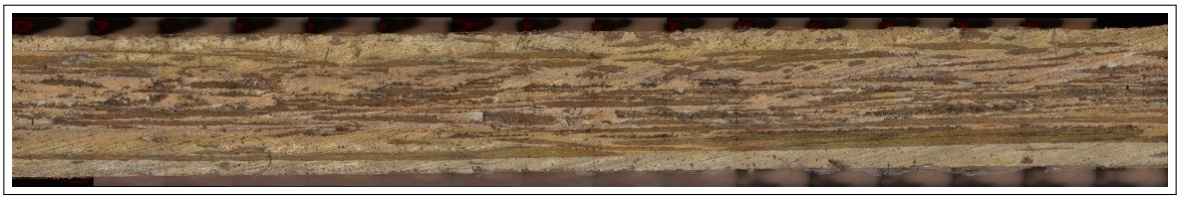

(a) Untreated showing good fibre-matrix distribution, fibre alignment and low void content

(b) 2-NaBF with visible and dispersed voids between fibre bundles indicating low impregnation

(c) 5-NaBF with higher and more regular void regions with fibre misalignment and dry spots

(d) 8-NaBF shows highest void content, dry regions and fibre degradation throughout the specimen

(e) 2-SiBF with much improved laminate quality despite some non-uniformity in fibre-matrix distribution

(f) 5-SiBF showed some small non-concentrated voids with minor fibre misalignment

(g) 8-SiBF shows a single region with high void content, which could be due to fibre misalignment issues

Figure 5.10: Cross-sectional microscopy images of the laminates highlighting voids (in red), misaligned and degraded fibre (in green) and entrapped moisture (in blue)

In contrast, the 2-NaBF-treated laminate showed slightly increased void content and minor inconsistencies in fibre dispersion, indicating that NaBF may not aid consolidation as effectively. The 5-NaBF sample presented more severe issues, with increased voids, less uniform fibre packing, and signs of

partial fibre-matrix separation. At 8-NaBF, the laminate displayed the poorest quality overall — with the highest void content, extensive fibre misalignment and some fibre degradation.

SiBF-treated laminates maintained relatively low void content across all concentrations. Although the 5 and 8-SiBF samples had some local fibre misalignment and minor heterogeneity, their visible void contents remained below untreated and all NaBF-treated laminates.

5.2.3. Tensile Testing

The tensile strength and modulus of the composites varied notably with chemical treatment and concentration as seen in Figure 5.11. Untreated laminates exhibited a tensile strength of 121.3 MPa and a modulus of 18.62 GPa.

NaOH-treated laminates showed mixed trends. A slight improvement in strength was seen at 2-NaBF. However, higher concentrations led to significant degradation, with 5% and 8% NaBF laminates dropping even below the untreated laminate. This decline correlates with increased void content. The specific tensile strength graph reflects this, with the 8-NaBF sample showing the lowest performance overall.

In contrast, silane-treated laminates exhibited superior tensile performance, particularly at 2% and 5% concentrations. The highest tensile strength was recorded for 2-SiBF, which also showed a relatively low void content. Both 5-SiBF and 8-SiBF composites too maintained high strength.

The tensile modulus followed a similar trend with the silane-treated composites, particularly 5 & 8-SiBF, reaching up to 20 GPa, suggesting improved stiffness due to better interface quality and lower porosity.

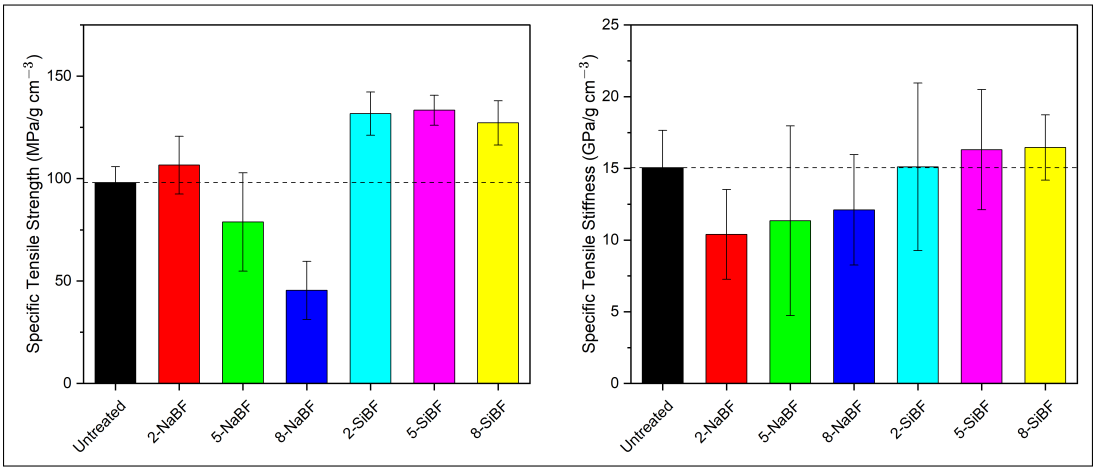

Figure 5.11: Mean specific tensile properties of all laminates

Fibre-Matrix Bonding Efficiency

The bonding efficiency values across the different treatments are illustrated in Figure 5.12. The untreated laminate shows a high BE, which is expected since the matrix modulus was back-calculated using the tensile modulus of this sample. As such, the experimentally measured modulus matches with the theoretical ROM prediction, with the slight shortfall attributable solely to the presence of voids, which lowers the actual laminate density used in the specific modulus calculation. Therefore, this value only serves as a baseline and not an accurate representation of the BE for the untreated laminate.

Among the treated fibres, the NaBF-treated laminates exhibit markedly lower BE values, indicating poor fibre-matrix interfacial bonding. Conversely, the SiBF-treated laminates show a progressive improvement in BE with increasing concentration. Notably, the high BE values of 5- and 8-SiBF also

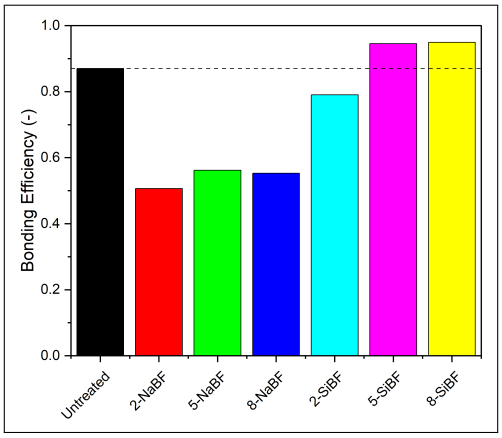

Figure 5.12: Fibre-matrix bonding efficiency

closely match the theoretical maximum, which could indicate near-optimal interfacial bonding.

These results are well in line with the results seen so far in terms of void content and mechanical properties, as seen in Figure 5.11, Figure 5.9 and Table 5.3.

Failure Analysis

All tested specimens exhibited a brittle mode of failure under tensile loading, characterised by a sudden fracture, with the maximum and breaking load being equal in nearly all cases. Most specimens showed fibre fracture accompanied by partial fibre–matrix debonding, indicating a mixed failure mechanism as seen in Figure 5.13. Notably, the 8-NaBF specimens displayed an extreme case of interfacial debonding, where failure predominantly occurred along the fibre–matrix interface rather than within the fibres themselves. This is indicative of poor adhesion between fibre and matrix in these samples, possibly due to high void content. In contrast, silane-treated specimens primarily exhibited fibre-dominated failure, indicating improved interfacial bonding and more effective load transfer from the matrix to the fibres. Additional images of specimen failure analysis have been shown in Appendix D.

(a) 5-NaBF specimen showing signs of poor impregnation and fibre-matrix debonding

(b) 8-NaBF specimen showing debonding-based failure with failure along the fibre

Figure 5.13: Microscopy images of the failure location of tensile testing specimens

5.2.4. Flexural Testing

The flexural strength and modulus results further emphasise the disparity between NaOH and silane treatments as seen in Figure 5.14. The untreated laminate had a flexural strength of 154.2 MPa and a modulus of 12.62 GPa. Upon treatment with 2-NaBF, flexural strength slightly increased but decreased at higher concentrations. The void content trend again aligns with this drop, increasing with concentration and likely impairing matrix-dominated flexural properties.

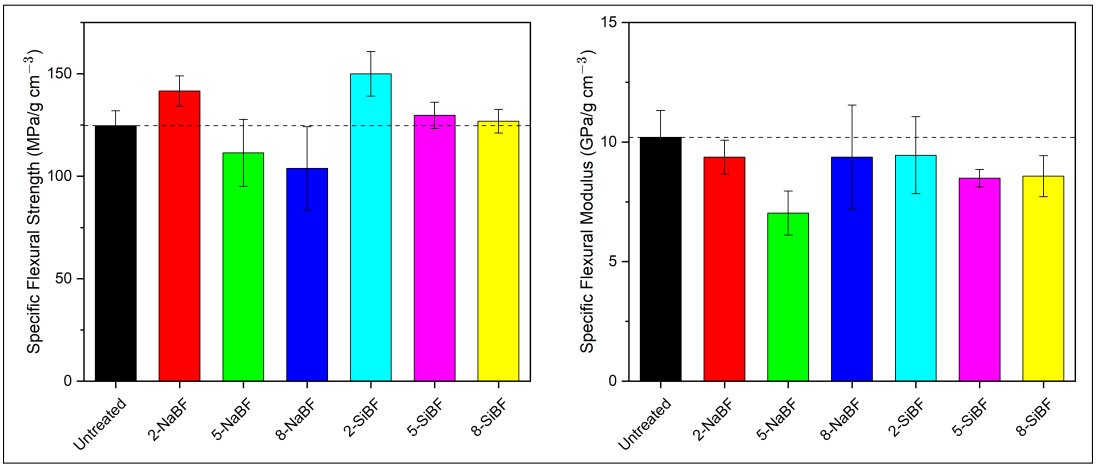

Figure 5.14: Mean specific flexural properties of all laminates

Silane-treated laminates showed improved flexural strength, peaking at 184.89 MPa for 2-SiBF. Despite the modest reduction at higher concentrations, 5-SiBF and 8-SiBF retained strengths above 150 MPa. This can be attributed to better wetting and fibre-matrix compatibility conferred by the silane treatment, along with reduced void content.

Flexural modulus results indicated lower stiffness for the treated specimens. This can be indicative of a more gradual load transfer between fibre and matrix due to the treatments. Additional statistics of all mechanical test results have been documented in Appendix C.

Failure Analysis

During flexural tests, most specimens fractured within the loading span, although a few failed directly under the loading nose, as seen in Figure 5.15. Silane-treated specimens exhibited primarily tensile or combined tensile–compressive failure modes. These breaks were characterised by distinct fibre rupture. A relatively low number of specimens showed evidence of fibre–matrix debonding, suggesting strong interfacial adhesion. In contrast, NaOH-treated specimens showed more variable and severe failure behaviour. While 2-NaBF specimens displayed failure modes similar to the silane group, involving tensile or combined tensile–compressive fracture, the 5-NaBF and 8-NaBF specimens exhibited extensive interfacial debonding and more brittle, fragmented failure surfaces. These observations point to a degradation of the fibre–matrix interface with increasing NaOH concentration. Additional images of specimen failure analysis have been shown in Appendix D.

(a) 2-NaBF specimen showing fibre-matrix debonding in the middle

(b) 8-NaBF specimen showed fibre rupture and debonding

Figure 5.15: Microscopy images of the failure location of flexural testing specimens

Table 5.3: Summary of mechanical and composite quality metrics

	Untreated	2-NaBF	5-NaBF	8-NaBF
Tensile				
Strength (MPa)	121.32 ± 8.59	124.80 ± 14.75	89.24 ± 24.34	49.31 ± 13.77
Elongation at Max. Strength (mm)	0.59 ± 0.09	0.61 ± 0.07	0.48 ± 0.10	0.71 ± 0.09
Modulus (GPa)	18.62 ± 2.88	12.16 ± 3.28	12.85 ± 6.70	13.14 ± 3.74
Flexural				
Strength (MPa)	154.20 ± 8.05	165.71 ± 7.80	126.15 ± 16.52	112.76 ± 19.71
Modulus (GPa)	12.62 ± 1.24	10.97 ± 0.74	7.96 ± 0.93	10.17 ± 2.11
Composite Quality				
Prepreg Matrix Mass Fraction (%)	35.16	42.38	36.80	47.96
Density (g/cm^3)	1.2375	1.1708	1.1325	1.0859
Void Content (%)	20.73	22.88	27.08	30.68
Bonding Efficiency (%)	87.00	50.66	56.15	55.28

	2-SiBF	5-SiBF	8-SiBF
Tensile			
Strength (MPa)	162.37 ± 11.61	161.79 ± 7.92	154.45 ± 11.75
Elongation at Max. Strength (mm)	0.32 ± 0.06	0.50 ± 0.04	0.57 ± 0.08
Modulus (GPa)	18.63 ± 6.44	19.77 ± 4.54	19.99 ± 2.47
Flexural			
Strength (MPa)	184.89 ± 11.95	157.31 ± 7.00	154.00 ± 6.30
Modulus (GPa)	11.65 ± 1.77	10.30 ± 0.39	10.41 ± 0.93
Composite Quality			
Prepreg Matrix Mass Fraction (%)	40.05	40.31	40.46
Density (g/cm^3)	1.2329	1.2130	1.2143
Void Content (%)	18.27	20.76	18.94
Bonding Efficiency(%)	79.02	94.55	94.90

Part III
Conclusions & Recommendations

6

Conclusion

This chapter comprehensively summarises the primary findings of this research, addressing each research sub-question and the overarching research question, and ultimately connecting them to the research objective. The central aim of this study was to investigate the viability of bamboo fibre-reinforced bio-derived polycarbonate composites as a sustainable material solution for secondary aerospace structures. This was motivated by the increasing demand for environmentally friendly alternatives to synthetic fibre and petroleum-derived matrix composites, especially in applications where moderate mechanical properties, moisture resistance, and cost-efficiency are sufficient. The research responds to challenges such as the high moisture absorption of natural fibres, weak fibre-matrix interfacial bonding, and variability in physical properties.

The experimental work followed a structured sequence starting with the selection and preparation of raw materials: untreated bamboo fibre and Durabio, a commercial bio-based polycarbonate. The bamboo fibres were subjected to three categories of chemical treatments—alkali, silane, and acetylation, with concentration factors of 2, 5 and 8 for each treatment. All treatments followed uniform protocols involving immersion, rinsing, and oven drying at fixed temperatures.

Following the fibre treatments, composite laminates were fabricated using a solvent-based prepreg approach. Durabio was dissolved in tetrahydrofuran to achieve a 30 wt% solution, providing optimal viscosity for fibre impregnation at room temperature. The prepregs were hand-laid in a unidirectional configuration and stacked into an aluminium mould designed for relatively short fibre thermoplastic lamination. Additional thin films of Durabio were added in between the prepreg stacks to achieve a target fibre mass fraction of 40%. This ensured reproducible curing and consistent laminate thickness across all test samples. The carefully designed process workflow allowed for accurate comparisons of how different treatments impacted the final composite behaviour.

6.1. Research Question Outcomes

SQ1 - Effect of Chemical Treatments on Bamboo Fibre

The type and concentration of chemical treatment significantly influenced bamboo fibre skeletal density. Alkali-treated fibres showed reduced density at low concentrations due to partial lignin removal and porosity increase. In contrast, higher concentrations caused pore collapse and compaction, raising density. Silane treatment had varied effects: 2% slightly reduced density, 5% peaked due to optimal substitution and pore filling, and 8% increased density from lignin over-removal and poor coating. Acetylation consistently reduced density, especially at higher concentrations, due to microstructural degradation and low substitution efficiency.

Water absorption followed chemical modifications. Untreated fibres absorbed ≈84% water due to their hydrophilicity. Alkali treatment progressively lowered absorption to ≈70% at 8% via removal of hydrophilic elements and pore sealing. Silane-treated fibres showed a non-linear trend: 2% had the lowest (≈68%), 5% peaked (≈88%) due to potential Si-O-C bonds, and 8% dropped due to better

silane hydrolysis. Acetylated fibres had the lowest uptake overall, though high concentrations caused degradation that reduced measurement reliability.

FTIR and SEM confirmed treatment effects. FTIR showed alkali removed lignin (decreased O–H, C–H), retaining hemicellulose. Silane reduced lignin groups, preserved hemicellulose, and introduced Si groups, indicating grafting. Acetylation partially removed lignin and added acetyl groups (C=O, C–O–C) with minimal cellulose disruption. DuraBio impregnation showed combined FTIR features. SEM images showed that untreated fibres were rough and impurity-rich; alkali increased surface area and exposed microfibrils; silane smoothed and coated fibres via pore filling; high acetylation caused fibre wall collapse and degradation.

Thermal analysis showed that alkali-treated fibres had the lowest stability, with early degradation from lignin removal. Silane and acetylation raised peak degradation temperatures and had similar maximum rates due to Si- and acetyl-group stabilisation. Alkali-treated fibres had a higher char yield due to enhanced decomposition aided by Na^{+} substitution effects.

Single fibre tensile testing showed that treatments improved specific properties. 2-NaBF had the best performance due to microfibril alignment and lower density. Higher alkali levels weakened the structure. Silane also improved properties, with 5-SiBF balancing morphology, density, and strength. At 8%, silane reduced performance due to brittle surface layers and higher density. Overall, optimising concentration is key to enhancing fibre performance without compromising integrity.

SQ2 & SQ3 - Fibre Matrix Bonding and Composite Manufacturing

Matrix uptake was highest in alkali-treated fibres due to the removal of surface waxes and lignin, which increased fibre roughness and porosity, enhancing resin infiltration. Silane-treated fibres showed moderate matrix uptake, benefitting from improved interfacial compatibility due to the presence of reactive silane groups despite minimal morphological changes. Untreated fibres absorbed the least resin due to their hydrophobic surfaces and poor wettability.

Microscopy and void content analysis revealed clear differences in laminate quality across treatments. Untreated and 2-SiBF laminates showed the best fibre alignment and relatively low void content. However, all void values exceeded the acceptable 2% threshold. Alkali-treated laminates exhibited a decline in quality with increasing NaOH concentration, marked by higher voids, fibre misalignment, and degradation. The void peak above 30% for 8-NaBF resulted from fibre microstructural disruption and poor compatibility with Durabio. During compression moulding, alkali-treated fibres lacked compatible functional groups, causing the matrix to escape the interface and trap air. In contrast, silane-treated fibres formed covalent bonds with the matrix via reactive silanol groups, acting as nucleation sites, improving wetting, and reducing air entrapment. Despite minor misalignments at higher concentrations, void content consistently declined with silane treatment, affirming its effectiveness in improving laminate quality.

Silane-treated laminates also demonstrated superior tensile strength and modulus, with performance improving with increasing silane concentration. Alkali-treated laminates showed variable outcomes - 2-NaBF gave slight improvements. However, higher concentrations led to performance drops due to fibre degradation and high voids. Failure analysis showed brittle fracture across all samples, with 8-NaBF displaying significant interfacial debonding. In contrast, silane-treated samples primarily showed fibre-based failure, indicating stronger bonding. Bonding efficiency was highest in silane-treated laminates, nearing theoretical maxima at 5- and 8-SiBF due to improved fibre–matrix adhesion. Conversely, alkali-treated laminates had low bonding efficiency due to surface damage and poor compatibility. The untreated laminate's high BE value was an artefact of its use in reference back-calculations and does not reflect actual bonding quality.

Silane-treated composites displayed superior flexural strength and acceptable modulus, with 2-SiBF achieving the highest strength. Alkali-treated laminates declined in flexural performance with increasing concentration, with 2-NaBF showing minor improvements, corresponding to rising void content and structural damage. Failure in silane-treated specimens was primarily fibre-driven with minimal debond-

ing. At the same time, alkali-treated laminates showed mixed and severe failures, especially at high concentrations, indicating compromised interfacial bonding.

6.2. Answering the Main Research Question

The overarching research question—*"How do fibre treatments and manufacturing processes affect the feasibility of Bamboo Fibre Reinforced Bio-Derived Polycarbonate Composites (BFRTPC) in secondary aerospace applications?"*—was fully addressed. Results demonstrate that chemical treatments directly influence the performance of the composites. Specifically, while alkali treatments improved fibre surface roughness and matrix uptake, they sometimes led to over-etching and fibre embrittlement, resulting in lower composite mechanical properties compared to the best-performing silane-treated samples. On the other hand, silane treatments consistently enhanced fibre-matrix bonding through chemical coupling, significantly improving both tensile and flexural properties. These trends show that although alkali treatment can be effective at low (2—5%) concentrations, silane treatment at 2 g/L offers superior and more reliable improvements across all evaluated properties.

6.3. Concluding Remarks

The research successfully demonstrated ways to improve the performance and feasibility of bamboo fibre reinforced bio-based polycarbonate composites (BFRTPCs) for secondary aerospace applications. The tally presented in Table 6.1 provides a comparative snapshot of the different treatments and concentrations based on a set of evaluated indicators. However, it assumes that all parameters have equal significance. In practical applications, this is not the case. Depending on the specific use-case scenario, certain properties may hold greater weight than others.

Table 6.1: Tally of the effect of chemical treatments on fibre and composite properties compared to the untreated fibres

	2-NaBF	5-NaBF	8-NaBF	2-SiBF	5-SiBF	8-SiBF
Fibre Results						
Density	3	1	-1	3	2	3
Water Absorption	2	3	3	3	-1	2
Thermal Stability	-3	-3	-3	0	0	-1
Specific Fibre Strength	3	2	1	2	2	2
Specific Fibre Modulus	3	2	2	3	1	1
Composite Results						
Prepreg Quality	2	1	3	2	2	2
Void Content	-1	-2	-3	2	0	2
Specific Tensile Strength	1	-2	-3	2	3	2
Specific Tensile Modulus	-3	-3	-2	0	1	1
Bonding Efficiency	-3	-3	-3	-1	1	1
Specific Flexural Strength	3	-2	-3	3	1	1
Specific Flexural Modulus	-1	-3	-1	-1	-2	-2
Final Tally	6	-9	-10	**18**	10	14

It is also important to note the contrasting behaviour of NaBF and SiBF with increasing treatment concentration. NaBF exhibited a consistent decline in performance metrics with higher NaOH concentrations. In contrast, SiBF did not follow a strictly monotonic trend. While all 3 concentrations showed an improvement, the 5-SiBF unexpectedly showed higher water absorption and relatively higher void content. These anomalies, discussed in Chapter 5, can be attributed to the presence of Si-O-C groups, which could have interfered with properties.

Equally important to consider is the broader sustainability impact of adopting bamboo fibre-reinforced polycarbonate composites. While the study underscores their potential to replace petroleum-based plastics with bio-derived alternatives, it must be acknowledged that the fibre treatment processes themselves involve chemical usage. These chemicals not only contribute to the overall environmental footprint but may also generate waste streams that require responsible disposal and treatment.

7

Future Recommendations

The development and evaluation of BFRTPC composites in this study revealed multiple promising outcomes yet also highlighted certain limitations that must be addressed for broader industrial applicability. This chapter outlines these key limitations and proposes actionable directions for future research. By targeting improvements in material consistency, manufacturing practices, environmental impact, and performance analysis, these recommendations aim to enhance both the scientific rigour and practical potential of bio-based composites for aerospace and other applications.

7.1. Limitations of Present Work

While the present study successfully demonstrated the feasibility of bamboo fibre-reinforced bio-derived polycarbonate composites for secondary aerospace applications, certain limitations were observed that should be addressed in future work to improve scientific robustness and industrial applicability.

1. **High Material Scatter:** The natural variability in bamboo fibre properties led to a considerable scatter in mechanical test results. This scatter poses challenges in drawing high-confidence conclusions, especially in industrial settings where consistency is crucial.
2. **Laminate Quality and Fibre Orientation:** Manual prepreg layup led to variability in fibre alignment and local fibre density, affecting uniformity in mechanical performance across composite samples.
3. **Non-Optimised Compression Moulding Parameters:** The applied temperature, pressure, and dwell times were not optimised for peak laminate quality or interfacial bonding due to the failure of the rheometer.
4. **Non-Uniformity of Durabio Film Processing:** The film pressing of Durabio introduced variation in the distribution and thickness across the laminate, which likely influenced void content and bonding quality.

7.2. Recommendations for Future Work

Future endeavours based on limitations and results of present work could include:

1. **Optimisation of Chemical Usage for Fibre Treatments:** The chemical treatment process used substantial volumes of reagents, generating notable waste. A quantitative assessment of chemical waste and mass balance is recommended as it can reduce environmental impact and operational costs.
2. **Environmental Exposure Studies for Composites:** While fibre water absorption was examined, full hydrothermal ageing and environmental durability studies must be conducted on the composites. These should include immersion, cyclic humidity, UV exposure, and elevated temperature testing. Expansion into impact, fatigue, and long-term creep performance will provide a more comprehensive understanding of their practical aerospace application.

3. **Thermal Modelling and Ageing Simulations:** Future work should simulate the manufacturing environment by exposing treated fibres to prolonged thermal cycles (e.g., isothermal dwell or ramp-hold tests) and studying their effect on fibre mass loss, degradation kinetics and the downstream impact on composite properties.
4. **In-Situ Monitoring for Single Fibre Tensile Characterisation:** Current single fibre testing methods can be enhanced using 3D optical measurement, micro-CT, and nano-CT scans to model fibre dimensions and internal structure pre-and post-treatment. This allows precise evaluation of damage evolution and microstructural changes, enabling better correlation with composite behaviour.
5. **Optimisation of Manufacturing Parameters:** Employing a statistical design of experiments (e.g., Taguchi L9 or full factorial) for moulding temperature, pressure, and dwell time would help identify the most influential parameters and enable their systematic optimisation. This would improve process repeatability and laminate quality.
6. **Composite Recycling Using THF:** This study showed promise in dissolving neat Durabio, both virgin and used, in tetrahydrofuran. A valuable future direction is re-dissolving the composite matrix to isolate fibres, aiming for fibre recovery and resin reuse. Assessment of recycled material quality is necessary to validate the circularity potential of BFRTPC systems.
7. **Use of Bio-Derived THF:** Building on the composite dissolution trials using THF, future efforts should evaluate the feasibility of using bio-derived THF, which has been recently demonstrated as a sustainable solvent alternative produced from renewable feedstocks like biomass-derived furfural (Zhu et al., 2022).
8. **Refinement in Prepreg Processing:** Improvements in the prepreg structure could include using mat stitching instead of single-side taping to create unidirectional mats with better integrity. Implementing a closed-loop drying system can recover evaporated THF, reduce solvent loss, and improve sustainability. Additionally, high-resolution laminate imaging should be introduced to quantify material scatter at the composite level and better control for variability.
9. **Cradle-to-Grave Life Cycle Assessment:** A comprehensive LCA should be conducted for each laminate system to understand environmental trade-offs between treatments. This includes tracking energy use, chemical consumption, emissions, and end-of-life recycling potential.

These investigations can further be expanded to other bio-based matrices such as polylactic acid, polypropylene, and polyamide-11 to develop a broader platform of sustainable composites for various structural applications.

References

Alonso-Montemayor, F. J., Navarro-Rodríguez, D., Delgado-Aguilar, M., Neira-Velázquez, M. G., Aguilar, C. N., Castañeda-Facio, A. O., Reyes-Acosta, Y. K., & Narro-Cespedes, R. I. (2022). Plasma-treated lignocellulosic fibers for polymer reinforcement. A review. *Cellulose*, *29*(2), 659–683. https://link.springer.com/article/10.1007/s10570-021-04361-0

Amada, S., & Untao, S. (2001). Fracture properties of bamboo. *Composites Part B: Engineering*, *32*(5), 451–459. https://www.sciencedirect.com/science/article/abs/pii/S1359836801000221

American Society for Testing and Materials. (2014). ASTM D3039M-08: Standard Test Method for Tensile Properties of Polymer Matrix Composite Materials. https://store-astm-org.tudelft.idm.oclc.org/d3039_d3039m-08.html

American Society for Testing and Materials. (2018). ASTM D8171-18: Standard Test Method for Density Determination of Flax Fiber. https://store-astm-org.tudelft.idm.oclc.org/d8171-18.html

American Society for Testing and Materials. (2020a). ASTM C1557-20: Standard Test Method for Tensile Strength and Young's Modulus of Fibers. https://store-astm-org.tudelft.idm.oclc.org/c1557-20.html

American Society for Testing and Materials. (2020b). ASTM D792-20: Standard Test Method for Density and Specific Gravity (Relative Density) of Plastics by Displacement. https://store-astm-org.tudelft.idm.oclc.org/d0792-20.html

American Society for Testing and Materials. (2021). ASTM D7264M-21: Standard Test Method for Flexural Properties of Polymer Matrix Composite Materials. https://store-astm-org.tudelft.idm.oclc.org/d7264_d7264m-21.html

Andrew, J. J., & Dhakal, H. (2022). Sustainable biobased composites for advanced applications: recent trends and future opportunities–A critical review. *Composites Part C: Open Access*, *7*, 100220. https://doi.org/10.1016/j.jcomc.2021.100220

Apostolidis, D. (2023). *Cultivating Sustainability: Assessing the Viability of Bio-Based Resins in Composite Manufacturing* [Master's Thesis]. Delft University of Technology. https://repository.tudelft.nl/record/uuid:e342029f-cf48-4a74-a595-190f24713982

Awais, H., Nawab, Y., Amjad, A., Anjang, A., Akil, H. M., & Abidin, M. S. Z. (2021). Environmental benign natural fibre reinforced thermoplastic composites: A review. *Composites Part C: Open Access*, *4*, 100082. https://doi.org/10.1016/j.jcomc.2020.100082

Azwa, Z., Yousif, B., Manalo, A., & Karunasena, W. (2013). A review on the degradability of polymeric composites based on natural fibres. *Materials & Design*, *47*, 424–442. https://doi.org/10.1016/j.matdes.2012.11.025

Babikian, R., Lukachko, S. P., & Waitz, I. A. (2002). The historical fuel efficiency characteristics of regional aircraft from technological, operational, and cost perspectives. *Journal of Air Transport Management*, *8*(6), 389–400. https://doi.org/10.1016/S0969-6997(02)00020-0

Bachmann, J., Yi, X., Gong, H., Martinez, X., Bugeda, G., Oller, S., Tserpes, K., Ramon, E., Paris, C., Moreira, P., et al. (2018). Outlook on ecologically improved composites for aviation interior and secondary structures. *CEAS Aeronautical Journal*, *9*, 533–543. https://link.springer.com/article/10.1007/s13272-018-0298-z

Bachmann, J., Yi, X., Tserpes, K., Sguazzo, C., Barbu, L. G., Tse, B., Soutis, C., Ramón, E., Linuesa, H., & Bechtel, S. (2021). Towards a circular economy in the aviation sector using eco-composites for interior and secondary structures. Results and recommendations from the EU/China project ECO-COMPASS. *Aerospace*, *8*(5), 131. https://doi.org/10.3390/aerospace8050131

Baltscheit, J., Schmidt, N., Schröder, F., & Meyer, J. (2020). Investigations on the aging behavior of transparent bioplastics for optical applications. *InfoMat*, *2*(2), 424–433. https://doi-org.tudelft.idm.oclc.org/10.1002/inf2.12065

Beaumann, D. (2024). *Material Characterisation of Mechanically Extracted Continuous Bamboo Fibre Reinforced Polymers* [Master's thesis, Delft University of Technology]. https://repository.tudelft.nl/islandora/object/uuid:5Z92Ms7ggcgdNNCa3UjZpK

Beumann, D. (2024). *Material Characterisation of Mechanically Extracted Continuous Bamboo Fibre Reinforced Polymers* [Master's Thesis]. Delft University of Technology. https://repository.tudelft.nl/record/uuid:03ad1d9e-fed4-460a-8b1c-8f92220d2e0a

Biron, M. (2018). *Thermoplastics and thermoplastic composites*. William Andrew. https://books.google.nl/books?hl=en&lr=&id=XRNfDwAAQBAJ&oi=fnd&pg=PP1&dq=thermoplastics&ots=cocypQXaQD&sig=SZhVVDM2r6VdNRdcUwUrx-SCnXM&redir_esc=y#v=onepage&q=thermoplastics&f=false

Bledzki, A. K., Mamun, A. A., Lucka-Gabor, M., & Gutowski, V. S. (2008). The effects of acetylation on properties of flax fibre and its polypropylene composites. *eXPRESS Polymer Letters*, *2*(6), 413–422. https://doi.org/10.3144/expresspolymlett.2008.50

Bonnin, I., Mereau, R., Tassaing, T., & Vigier, K. D. O. (2020). One-pot synthesis of isosorbide from cellulose or lignocellulosic biomass: a challenge? *Beilstein Journal of Organic Chemistry*, *16*(1), 1713–1721. https://doi.org/10.3762%2Fbjoc.16.143

Bosworth, L. A., & Downes, S. (2012). Acetone, a sustainable solvent for electrospinning poly (ε-caprolactone) fibres: effect of varying parameters and solution concentrations on fibre diameter. *Journal of Polymers and the Environment*, *20*, 879–886. https://link.springer.com/article/10.1007/s10924-012-0436-3

Buson, R., Melo, L., Oliveira, M., Rangel, G., & Deus, E. (2018). Physical and mechanical characterization of surface treated bamboo fibers. *Science and Technology of Materials*, *30*(2), 67–73. https://www.sciencedirect.com/science/article/abs/pii/S2603636318300162

Choi, Y. H., & Lyu, M.-Y. (2020). Comparison of Rheological Characteristics and Mechanical Properties of Fossil-Based and Bio-Based Polycarbonate. *Macromolecular Research*, *28*(4), 299–309. https://doi.org/10.1007/s13233-020-8093-1

Costa, M. M., Melo, S. L., Santos, J. V. M., Araújo, E. A., Cunha, G. P., Deus, E. P., & Schmitt, N. (2017). Influence of physical and chemical treatments on the mechanical properties of bamboo fibers. *Procedia Engineering*, *200*, 457–464. https://doi.org/10.1016/j.proeng.2017.07.064

Daniel, I. M., Ishai, O., Daniel, I. M., & Daniel, I. (1994). *Engineering mechanics of composite materials* (Vol. 3). Oxford university press New York. http://tailieudientu.lrc.tnu.edu.vn/Upload/Collection/brief/brief_52287_56208_9620161734KNV.15002218.pdf

Das, S. C., La Rosa, A. D., & Grammatikos, S. A. (2022). Life cycle assessment of plant fibers and their composites. In *Plant fibers, their composites, and applications* (pp. 457–484). Elsevier. https://doi.org/10.1016/B978-0-12-824528-6.00015-1

Department of Defense, U. (2002). Composite Materials Handbook, Volume 1–Polymer Matrix Composites Guidelines for Characterization of Structural Materials. https://indico.fnal.gov/event/13241/contributions/18146/attachments/12002/15271/MIL_Handbook_17.pdf#page=465.13

Dong, S., Xian, G., & Yi, X.-S. (2018). Life cycle assessment of ramie fiber used for FRPs. *Aerospace*, *5*(3), 81. https://doi.org/10.3390/aerospace5030081

Dyer, W. E., & Kumru, B. (2023). Polymers as aerospace structural components: how to reach sustainability? *Macromolecular Chemistry and Physics*, *224*(24), 2300186. https://doi-org.tudelft.idm.oclc.org/10.1002/macp.202300186

Faruk, O., Bledzki, A. K., Fink, H.-P., & Sain, M. (2012). Biocomposites reinforced with natural fibers: 2000–2010. *Progress in polymer science*, *37*(11), 1552–1596. https://doi.org/10.1016/j.progpolymsci.2012.04.003

Griffiths, P. R., & de Haseth, J. A. (2008). Fourier transform infrared spectrometry (2nd edn.) *Analytical and Bioanalytical Chemistry*, *391*(7), 2379–2380. https://onlinelibrary-wiley-com.tudelft.idm.oclc.org/doi/book/10.1002/047010631X

Grosser, D., & Liese, W. (1971). On the anatomy of Asian bamboos, with special reference to their vascular bundles. *Wood Science and technology*, *5*(4), 290–312. https://link.springer.com/article/10.1007/BF00365061

Hottle, T. A., Bilec, M. M., & Landis, A. E. (2017). Biopolymer production and end of life comparisons using life cycle assessment. *Resources, Conservation and Recycling*, *122*, 295–306. https://doi.org/10.1016/j.resconrec.2017.03.002

Hu, G., Cai, S., Zhou, Y., Zhang, N., & Ren, J. (2018). Enhanced mechanical and thermal properties of poly (lactic acid)/bamboo fiber composites via surface modification. *Journal of Reinforced Plastics and Composites*, *37*(12), 841–852. https://doi.org/10.1177/0731684418765085

Huang, S., Fu, Q., Yan, L., & Kasal, B. (2021). Characterization of interfacial properties between fibre and polymer matrix in composite materials–A critical review. *Journal of Materials Research and Technology*, *13*, 1441–1484. https://doi.org/10.1016/j.jmrt.2021.05.076

Hussain, S. A., Yadav, M. P., Sharma, B. K., Qi, P. X., & Jin, T. Z. (2024). Biodegradable Food Packaging Films Using a Combination of Hemicellulose and Cellulose Derivatives. *Polymers*, *16*(22), 3171. https://doi.org/10.3390/polym16223171

Internation Energy Agency. (2023). Aviation [Accessed: 2025-01-09]. https://www.iea.org/energy-system/transport/aviation

Islam, S., Hasan, M. B., Karim, F.-E., Kodrić, M., Islam, M. R., Khatun, M. M., & Motaleb, K. A. (2025). Thermoset and thermoplastic polymer composites reinforced with flax fiber: Properties and application—A review. *SPE Polymers*, *6*(1), e10172. https://doi.org/10.1002/pls2.10172

Jayaraman, P., Pai, A., Rodriguez-Millan, M., Shenoy, S., KN, C., & Hegde, S. (2024). Exploring acoustic properties of banana fiber composites with elastomeric filler through a computational approach. *Materials Research Express*, *11*(1), 015508. https://iopscience.iop.org/article/10.1088/2053-1591/ad1e0b/meta

Kabir, M., Wang, H., Lau, K., & Cardona, F. (2012). Chemical treatments on plant-based natural fibre reinforced polymer composites: An overview. *Composites Part B: Engineering*, *43*(7), 2883–2892. https://doi.org/10.1016/j.compositesb.2012.04.053

Kaushik, B. (2024). *Investigation of Vanillin-Derived Bio-Based Epoxy as a High-Performance Composite Matrix Material* [Master's Thesis]. Delft University of Technology. https://repository.tudelft.nl/record/uuid:16209943-f50e-4be4-9f61-343932d5af26

Kesarwani, S. (2017). Polymer Composites in Aviation Sector. A Brief Review Article. *International Journal of Engineering Research & Technology (IJERT)*, *6*(6), 518. https://www.ijert.org/research/polymer-composites-in-aviation-sector-IJERTV6IS060291.pdf

Khalil, H. A., Bhat, I., Jawaid, M., Zaidon, A., Hermawan, D., & Hadi, Y. (2012). Bamboo fibre reinforced biocomposites: A review. *Materials & Design*, *42*, 353–368. https://doi.org/10.1016/j.matdes.2012.06.015

Kudva, A., Mahesha, G. T., & Pai, D. (2024). Influence of Chemical Treatment on the Physical and Mechanical Properties of Bamboo Fibers as Potential Reinforcement for Polymer Composites. *Journal of Natural Fibers*, *21*(1), 2332698. https://doi.org/10.1080/15440478.2024.2332698

Kushwaha, P. K., & Kumar, R. (2011). Influence of chemical treatments on the mechanical and water absorption properties of bamboo fiber composites. *Journal of Reinforced Plastics and Composites*, *30*(1), 73–85. https://doi.org/10.1177/0731684410383064

Lee, C.-H., Takagi, H., Okamoto, H., & Kato, M. (2015). Preparation and mechanical properties of a copolycarbonate composed of bio-based isosorbide and bisphenol A. *Polymer Journal*, *47*(9), 639–643. https://www.nature.com/articles/pj201539

Li, H., Xu, S., Wang, B., Tian, Z., Xu, Z., & Qian, F. (2025). A new insight into the effects of DMF solvent activation on the polyamide layers of nanofiltration membranes by molecular simulation. *Journal of Membrane Science*, *718*, 123667. https://doi.org/10.1016/j.memsci.2024.123667

Liese, W., & Weiner, G. (1996). Ageing of bamboo culms. A review. *Wood Science and Technology*, *30*(2), 77–89. https://link.springer.com/article/10.1007/BF00224958

Liu, D., Song, J., Anderson, D. P., Chang, P. R., & Hua, Y. (2012). Bamboo fiber and its reinforced composites: structure and properties. *Cellulose*, *19*, 1449–1480. https://link.springer.com/article/10.1007/s10570-012-9741-1

Lowell, S., Shields, J. E., Thomas, M. A., & Thommes, M. (2012). *Characterization of porous solids and powders: surface area, pore size and density* (Vol. 16). Springer Science & Business Media. https://link-springer-com.tudelft.idm.oclc.org/book/10.1007/978-1-4020-2303-3

Lu, T., Jiang, M., Jiang, Z., Hui, D., Wang, Z., & Zhou, Z. (2013). Effect of surface modification of bamboo cellulose fibers on mechanical properties of cellulose/epoxy composites. *Composites Part B: Engineering*, *51*, 28–34. https://doi.org/10.1016/j.compositesb.2013.02.031

Maheswari, C. U., Reddy, K. O., Muzenda, E., & Rajulu, A. V. (2012). Tensile and Thermal Properties of Polycarbonate-Coated Tamarind Fruit Fibers. *International Journal of Polymer Analysis and Characterization*, *17*(8), 578–589. https://doi.org/10.1080/1023666X.2012.718527

Mallick, P. (2007). *Fiber-Reinforced Composites: Materials, Manufacturing, and Design*. CRC Press. https://doi.org/10.1201/9781420005981

Mallick, P. (2017). *Processing of polymer matrix composites*. CRC Press. https://doi.org/10.1201/9781315157252

Miller, A., & Gibson, A. (1996). Impregnation techniques for thermoplastic matrix composites. *Polymers and Polymer Composites*, *4*(7), 459–481. https://doi.org/10.1177/096739119600400701

Mitsubishi Chemical Group. (2024). New Bio-based Engineering Plastic - Durabio [Accessed: 2025-06-06]. https://www.m-chemical.co.jp/en/products/departments/mcc/pc/product/1201026_9368.html

Mohit, H., & Arul Mozhi Selvan, V. (2018). A comprehensive review on surface modification, structure interface and bonding mechanism of plant cellulose fiber reinforced polymer based composites. *Composite Interfaces*, *25*(5-7), 629–667. https://doi.org/10.1080/09276440.2018.1444832

Mudoi, M. P., & Sinha, S. (2024). Thermal degradation study of natural fibre through thermogravimetric analysis. *Materials Today: Proceedings*, *99*, 92–97. https://doi.org/10.1016/j.matpr.2023.05.362

Murwamadala, R., Mathebela, L., & Mubiayi, M. (2024). Impact of Alkali Treatment on the Internal Microstructure, Surface Topography and the Resulting Mechanical Properties of Single Sisal Fibers. *Journal of Natural Fibers*, *21*(1), 2370028. https://doi-org.tudelft.idm.oclc.org/10.1080/15440478.2024.2370028

Mustafa, A., & Talha, M. (2025). Extending Bio-Based and Biodegradable Thermoplastics in Food Packaging: A Focus on Multiphase Systems. *Food Frontiers*. https://onlinelibrary.wiley.com/doi/10.1002/fft2.70008

Ozturk, F., Cobanoglu, M., & Ece, R. E. (2024). Recent advancements in thermoplastic composite materials in aerospace industry. *Journal of Thermoplastic Composite Materials*, *37*(9), 3084–3116. https://doi-org.tudelft.idm.oclc.org/10.1177/08927057231222820

Phuong, N. T., Sollogoub, C., & Guinault, A. (2010). Relationship between fiber chemical treatment and properties of recycled pp/bamboo fiber composites. *Journal of Reinforced Plastics and Composites*, *29*(21), 3244–3256. https://doi.org/10.1177/0731684410370905

Ramachandran, A., Mavinkere Rangappa, S., Kushvaha, V., Khan, A., Seingchin, S., & Dhakal, H. N. (2022). Modification of fibers and matrices in natural fiber reinforced polymer composites: a comprehensive review. *Macromolecular rapid communications*, *43*(17), 2100862. https://doi.org/10.1002/marc.202100862

Sabarinathan, P., Rajkumar, K., Annamalai, V., & Vishal, K. (2020). Characterization on chemical and mechanical properties of silane treated fish tail palm fibres. *International Journal of Biological Macromolecules*, *163*, 2457–2464. https://doi.org/10.1016/j.ijbiomac.2020.09.159

Salit, M. S., Jawaid, M., Yusoff, N. B., & Hoque, M. E. (2014). *Manufacturing of natural fibre reinforced polymer composites*. Springer. https://link.springer.com/book/10.1007/978-3-319-07944-8

Sampathkumar, D., Punyamurth, R., Venkateshappa, S. C., & Bennehalli, B. (2012). Effect of chemical treatment on water absorption of areca fiber. *Journal of Applied Sciences Research*, *8*(11), 5298–5305. https://www.researchgate.net/publication/286332888_Effect_of_chemical_treatment_on_water_absorption_of_areca_fiber

Sebestyén, Z., May, Z., Réczey, K., & Jakab, E. (2011). The effect of alkaline pretreatment on the thermal decomposition of hemp. *Journal of thermal analysis and calorimetry*, *105*(3), 1061–1069. https://doi-org.tudelft.idm.oclc.org/10.1007/s10973-010-1056-6

Senthil Muthu Kumar, T., Chandrasekar, M., Senthilkumar, K., Ayrilmis, N., Siengchin, S., & Rajini, N. (2021). Utilization of bamboo fibres and their influence on the mechanical and thermal properties of polymer composites. *Bamboo Fiber Composites: Processing, Properties and Applications*, 81–96. https://link.springer.com/chapter/10.1007/978-981-15-8489-3_5

Shawon, J., & Sung, C. (2004). Electrospinning of polycarbonate nanofibers with solvent mixtures THF and DMF. *Journal of materials science*, *39*, 4605–4613. https://link.springer.com/article/10.1023/B:JMSC.0000034155.93428.ea

Syduzzaman, M., Faruque, M. A. A., Bilisik, K., & Naebe, M. (2020). Plant-Based Natural Fibre Reinforced Composites: A Review on Fabrication, Properties and Applications. *Coatings*, *10*(10), 973. https://doi.org/10.3390/coatings10100973

Takeuchi, T., Luengrojanaku, P., Ito, H., Rimdusit, S., & Shibata, S. (2024). Effect of Processing Temperature and Polymer Types on Mechanical Properties of Bamboo Fiber Composites. *BioResources*, *19*(1), 41–52. https://doi.org/10.15376/biores.19.1.41-52

Threepopnatkul, P., Kaerkitcha, N., & Athipongarporn, N. (2009). Effect of surface treatment on performance of pineapple leaf fiber–polycarbonate composites. *Composites Part B: Engineering*, *40*(7), 628–632. https://doi.org/10.1016/j.compositesb.2009.04.008

Tsai, W.-H., Chang, Y.-C., Lin, S.-J., Chen, H.-C., & Chu, P.-Y. (2014). A green approach to the weight reduction of aircraft cabins. *Journal of Air Transport Management*, *40*, 65–77. http://dx.doi.org/10.1016/j.jairtraman.2014.06.004

Vaidya, U. K., & Chawla, K. (2008). Processing of fibre reinforced thermoplastic composites. *International Materials Reviews*, *53*(4), 185–218. https://doi-org.tudelft.idm.oclc.org/10.1179/174328008X325223

Verma, D., Goh, K. L., & Vimal, V. (2022). Interfacial studies of natural fiber-reinforced particulate thermoplastic composites and their mechanical properties. *Journal of Natural Fibers*, *19*(6), 2299–2326. https://doi.org/10.1080/15440478.2020.1808147

Vishal, K., Arun, A., & Rajkumar, K. (2024). Extraction and characterization of steam-exploded silane-treated cellulosic natural Vernonia elaeagnifolia long fibre. *Industrial Crops and Products*, *214*, 118576. https://doi.org/10.1016/j.indcrop.2024.118576

Wagaye, B. T., Guo, J., Zhou, B., Gao, C., & Nguyen, L. T. (2024). Surface Modification of Plain-Woven Ramie Fabrics Using Bridged Bis (3-Trimethoxysilylpropyl) Amine Silane for Improved Hydrophobicity. *Fibers and Polymers*, *25*(10), 4307–4320. https://doi.org/10.1007/s12221-024-00737-8

Woigk, W., Fuentes, C., Rion, J., Hegemann, D., Van Vuure, A. W., Dransfeld, C., & Masania, K. (2019). Interface properties and their effect on the mechanical performance of flax fibre thermoplastic composites. *Composites Part A: Applied Science and Manufacturing*, *122*, 8–17. https://doi.org/10.1016/j.compositesa.2019.04.015

Xie, Y., Hill, C. A., Xiao, Z., Militz, H., & Mai, C. (2010). Silane coupling agents used for natural fiber/polymer composites: A review. *Composites Part A: Applied Science and Manufacturing*, *41*(7), 806–819. http://dx.doi.org/10.1016/j.compositesa.2010.03.005

Yaghoubi, V., & Kumru, B. (2024). Retrosynthetic life cycle assessment: a short perspective on the sustainability of integrating thermoplastics and artificial intelligence into composite systems. *Advanced Sustainable Systems*, *8*(5), 2300543. https://doi-org.tudelft.idm.oclc.org/10.1002/adsu.202300543

Zhang, J., Koubâa, A., Xing, D., et al. (2020). High-performance lignocellulose/polycarbonate biocomposites fabricated by in situ reaction: Structure and properties. *Composites Part A: Applied Science and Manufacturing*, *138*, 106068. https://doi.org/10.1016/j.compositesa.2020.106068

Zhu, Y., Yang, J., Mei, F., Li, X., & Zhao, C. (2022). Bio-based 1, 4-butanediol and tetrahydrofuran synthesis: perspective. *Green Chemistry*, *24*(17), 6450–6466. https://doi-org.tudelft.idm.oclc.org/10.1039/D2GC02271K

Zygouris, I. (2024). *Optically Transparent Flax Fiber Reinforced Composite Materials* [Master's Thesis]. Delft University of Technology. https://repository.tudelft.nl/record/uuid:2bc00d93-e64b-4af7-8ae5-d19576f8017c

Part IV
Appendices

A

Verification of Pre-Impregnated Fibres

This chapter presents the FTIR spectra for all the prepregs fabricated using treated fibres. The FTIR spectra of the treated fibres themselves and Durabio are also included. These plots serve as verification for successful impregnation of the fibres.

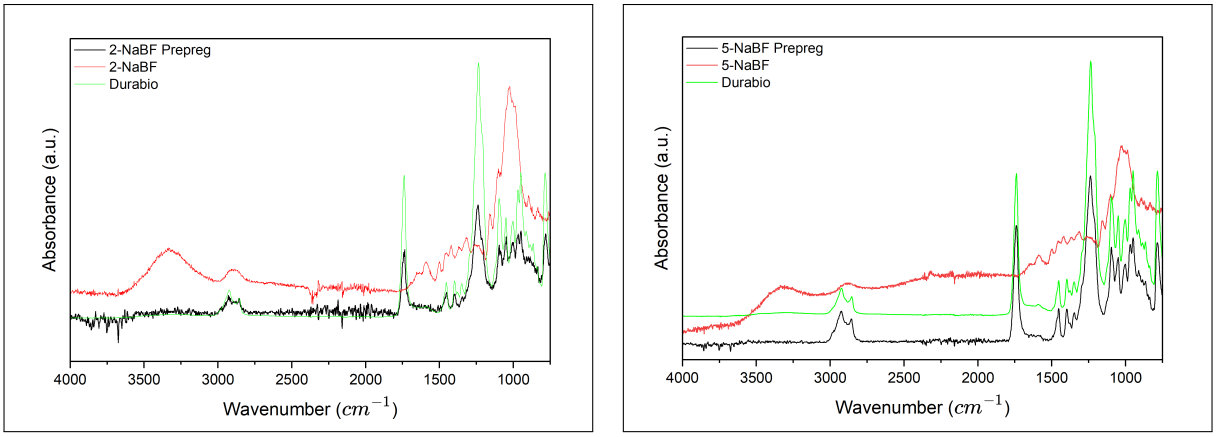

(a) 2-NaBF

(b) 5-NaBF

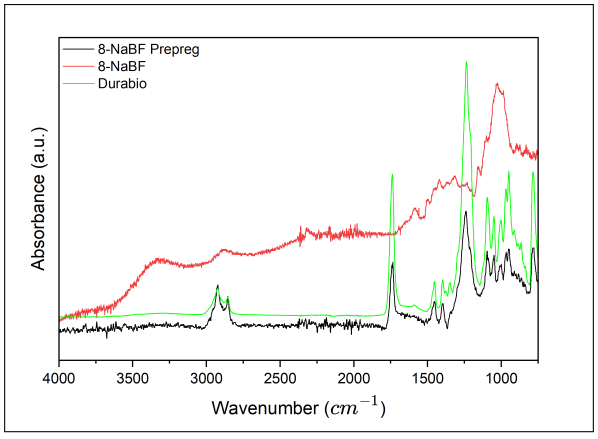

(c) 8-NaBF

Figure A.1: FTIR of alkali-treated prepreg fibres

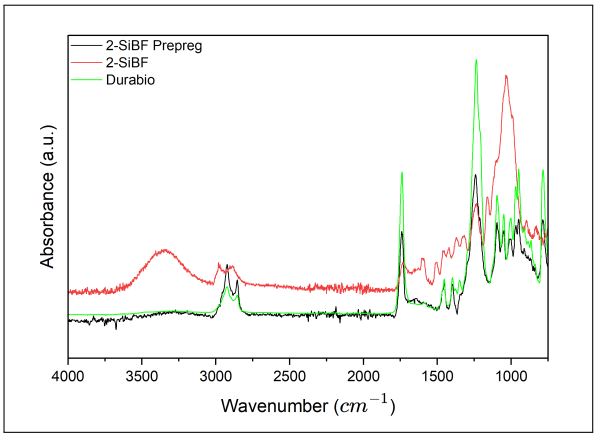

(a) 2-SiBF

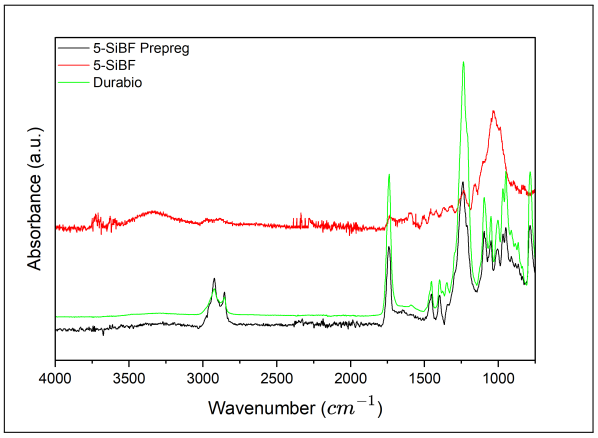

(b) 5-SiBF

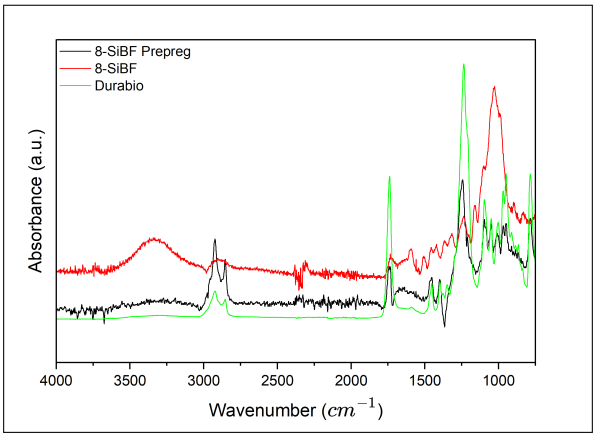

(c) 8-SiBF

Figure A.2: FTIR of silane-treated prepreg fibres

B

Onset of Thermal Degradation

This chapter presents the analysis of the degradation onset temperature. The degradation onset temperature was determined by identifying the point of intersection between the slopes of the thermally stable region and the degradation region in the TGA plots.

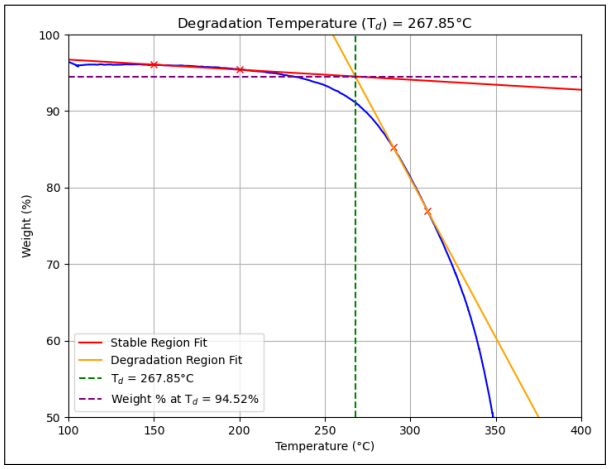

(a) Untreated

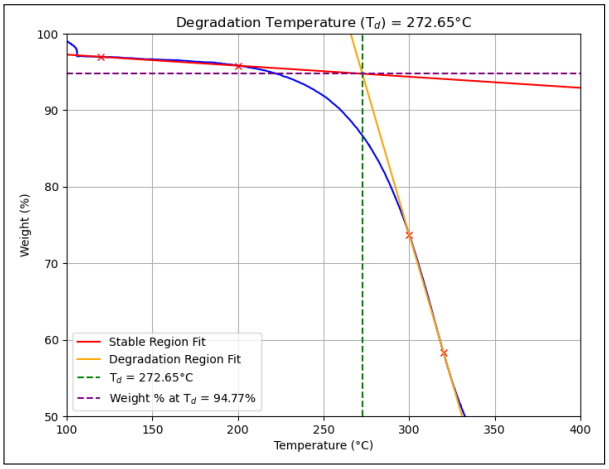

(b) 2-NaBF

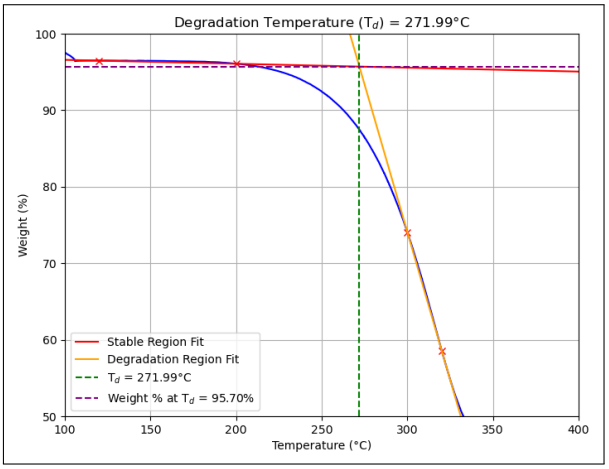

(c) 5-NaBF

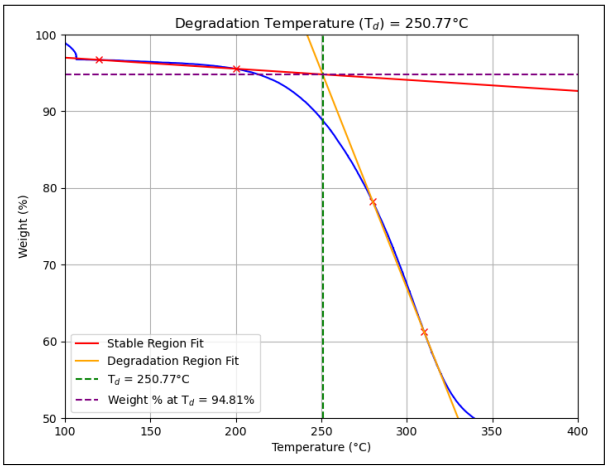

(d) 8-NaBF

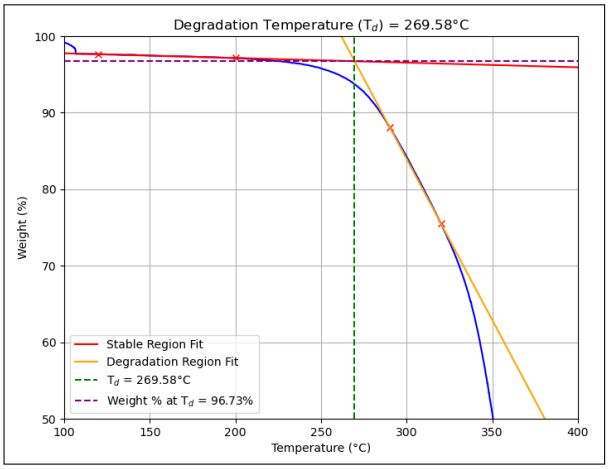

(e) 2-SiBF

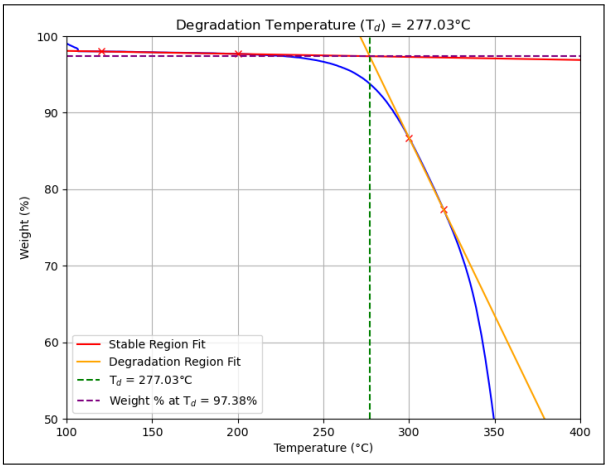

(f) 5-SiBF

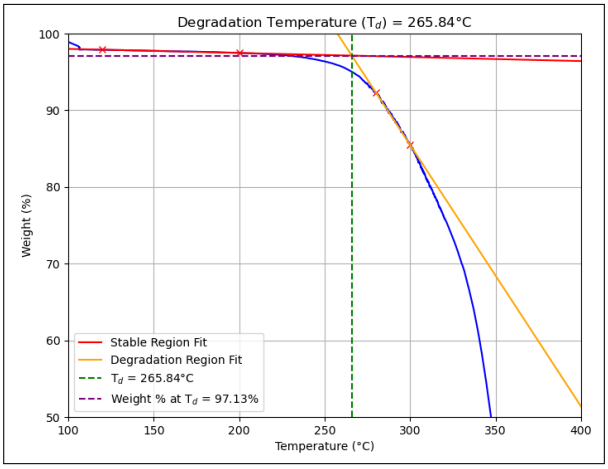

(g) 8-SiBF

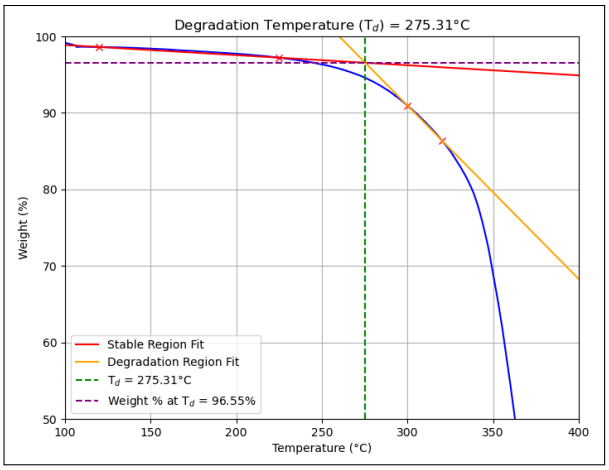

(h) 2-AcBF

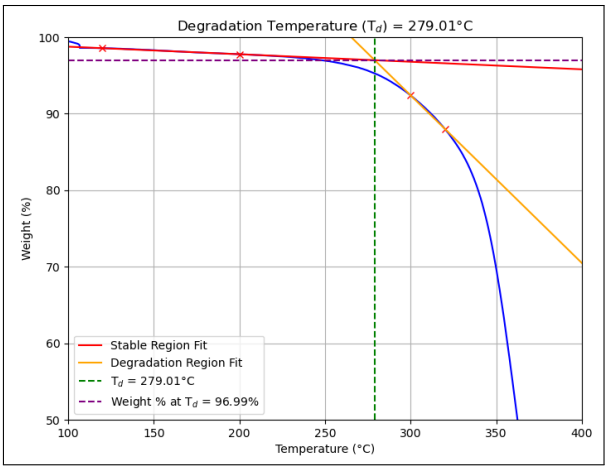

(i) 5-AcBF

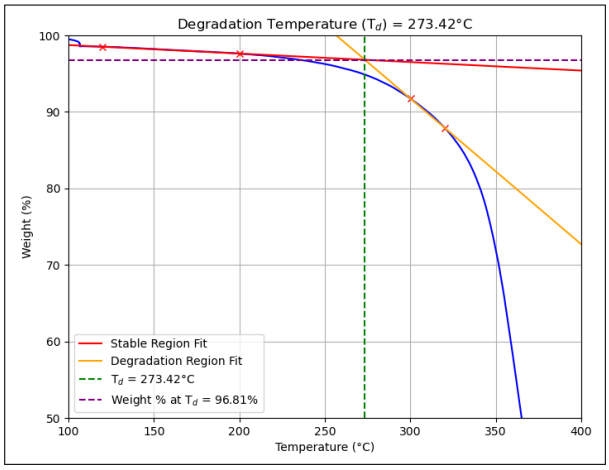

(j) 8-AcBF

Figure B.1: Onset of Degradation calculated by extrapolating the slope of the stable region and degradation region to find the intersection point

C

Mechanical Testing Statistics

Composite materials inherently exhibit variability in their mechanical properties due to variations in fibre, matrix, processing conditions, and test methods. As such, statistical analysis is essential to characterise their behaviour reliably. Statistical data enables the design of structures with appropriate confidence levels, accounting for material uncertainty. Statistical analysis for the testing data was conducted using the MIL-Handbook 17 and the STAT17 excel sheet that automates the calculations (Department of Defense, 2002).

To determine which statistical distribution best represents the dataset for material property characterisation, the following procedure, based on OSL, is used:

1. If the OSL for the Weibull distribution is greater than 0.05, this indicates an adequate fit; therefore, a Weibull basis value is recommended.
2. If the OSL for the Weibull distribution is less than 0.05 and the OSL for the normal distribution is greater than 0.05, then the normal basis value should be used.
3. If both the Weibull and normal distributions have OSL values less than 0.05, and the lognormal distribution OSL is greater than 0.05. A lognormal basis value is recommended.

C.1. Single Fibre Tensile Testing

Table C.1: Statistical Properties for Single Fibre Tensile Test

Strength							
	Untreated	**2-NaBF**	**5-NaBF**	**8-NaBF**	**2-SiBF**	**5-SiBF**	**8-SiBF**
Observed Significance Level (OSL)	0.848	0.386	0.522	0.120	0.259	0.461	0.480
Scale Parameter	124	281	232	165	181	221	190
Shape Parameter	1.76	1.98	1.63	2.30	1.85	2.13	1.81
B-Basis Value	8.49	25.7	15.8	21.0	11.5	28.4	17.1
A-Basis Value	0.667	2.68	1.19	2.98	0.865	3.96	1.68

Modulus						
	Untreated	**2-NaBF**	**5-NaBF**	**2-SiBF**	**5-SiBF**	**8-SiBF**
Observed Significance Level (OSL)	0.0805	0.796	0.555	0.452	0.349	0.206
Scale Parameter	18.1	27.5	23.2	26.7	17.8	19.8
Shape Parameter	1.47	3.14	1.96	3.06	3.74	2.54
B-Basis Value	0.726	6.08	2.48	5.03	5.52	3.53
A-Basis Value	0.0345	1.46	0.290	1.05	1.80	0.674

8-NaBF Modulus	
Observed Significance Level (OSL)	0.125
Mean	22.3
Standard Deviation	10.5
Coefficient of Variation (%)	47.0
B-Basis Value	Negative
A-Basis Value	Negative

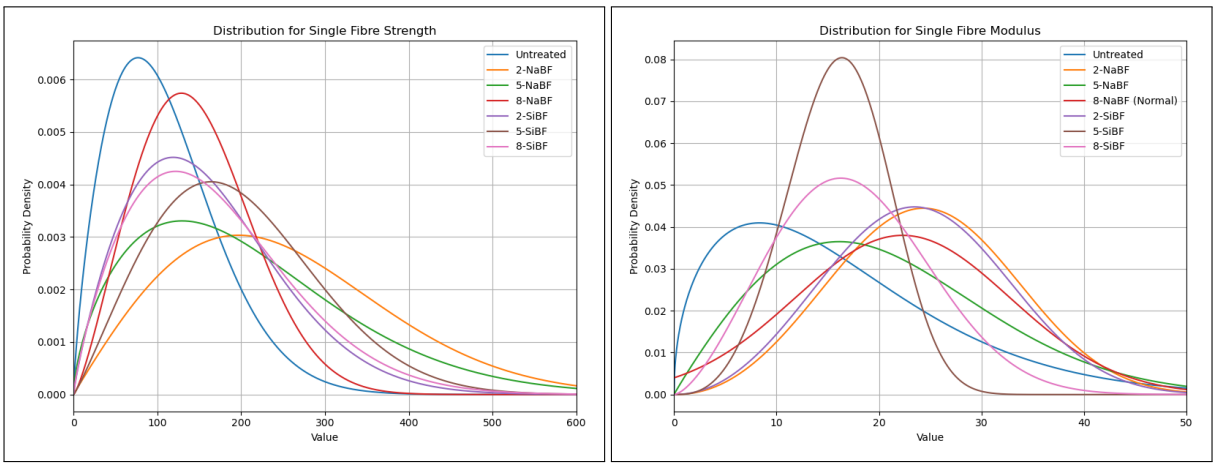

Figure C.1: The distributions indicate moderate to high scatter for untreated and NaOH-treated fibres, with 2-SiBF and 5-SiBF showing relatively consistent moduli.

C.2. Tensile Testing

Table C.2: Statistical Properties for Composite Tensile Test

Strength							
	Untreated	2-NaBF	5-NaBF	8-NaBF	2-SiBF	5-SiBF	8-SiBF
Observed Significance Level (OSL)	0.331	0.510	0.158	0.675	0.218	0.0746	0.363
Scale Parameter	125	131	98.7	54.5	168	166	160
Shape Parameter	15.5	9.71	3.73	4.14	15.1	21.9	14.2
B-Basis Value	74.3	56.9	11.2	7.64	98.2	114	90.2
A-Basis Value	46.1	26.5	1.53	1.28	60.2	81.4	53.6

Modulus							
	Untreated	2-NaBF	5-NaBF	8-NaBF	2-SiBF	5-SiBF	8-SiBF
Observed Significance Level (OSL)	0.136	0.0742	0.453	0.434	0.294	0.341	0.201
Scale Parameter	19.9	13.4	14.6	14.6	20.9	21.6	21.1
Shape Parameter	6.27	3.74	2.06	4.01	3.03	4.92	7.88
B-Basis Value	5.45	1.53	0.284	1.91	1.42	4.14	7.53
A-Basis Value	1.67	0.211	0.007856	0.302	0.123	0.920	2.94

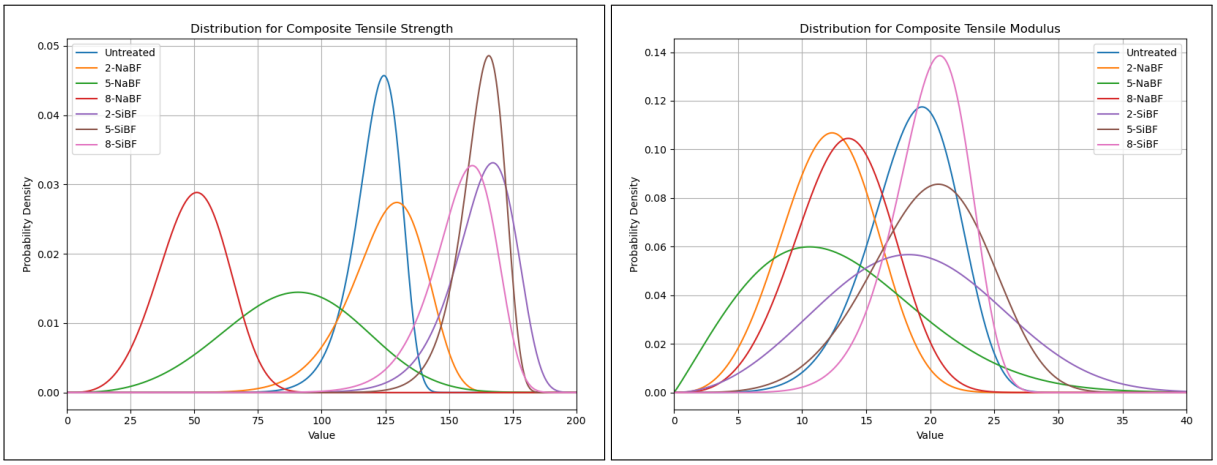

Figure C.2: Silane-treated specimens demonstrate tight and consistent distributions for both strength and modulus. In contrast, higher NaOH treatments result in broader curves.

C.3. Flexural Testing

Table C.3: Statistical Properties for Composite Flexural Test

Strength							
	Untreated	**2-NaBF**	**5-NaBF**	**8-NaBF**	**2-SiBF**	**5-SiBF**	**8-SiBF**
Observed Significance Level (OSL)	0.457	0.257	0.0869	0.162	0.410	0.104	0.478
Scale Parameter	158	170	134	121	191	160	157
Shape Parameter	25.6	20.5	7.26	6.71	15.3	37.4	27.3
B-Basis Value	115	114	43.7	36.1	112	129	117
A-Basis Value	86.1	79.6	15.8	12.0	69.2	106	88.8

Modulus							
	Untreated	**2-NaBF**	**5-NaBF**	**8-NaBF**	**2-SiBF**	**5-SiBF**	**8-SiBF**
Observed Significance Level (OSL)	0.539	0.593	0.728	0.575	0.647	0.518	0.287
Scale Parameter	13.2	11.3	8.36	11.0	12.4	10.5	10.8
Shape Parameter	10.6	16.0	11.0	5.61	7.08	32.5	14.7
B-Basis Value	6.12	6.82	3.98	2.59	3.94	8.16	6.22
A-Basis Value	3.04	4.30	2.03	0.694	1.39	6.50	3.77

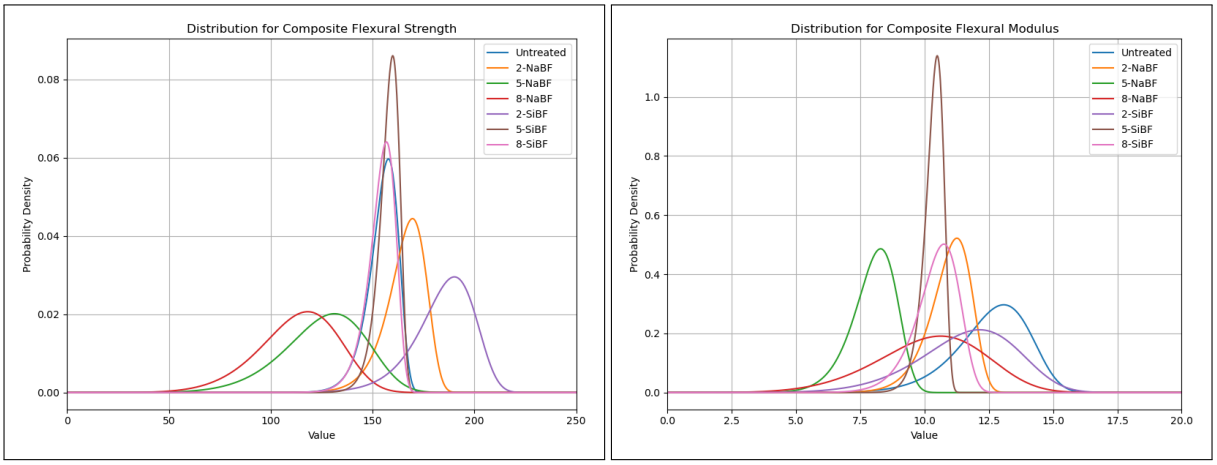

Figure C.3: Flexural strength and modulus distributions are show low scatter for silane-treated specimens. Conversely, alkali-samples exhibit high scatter and reduced reliability

D

Failure Analysis

This chapter presents the failure images of all tested specimens, captured using the VR-5000 optical microscope. These images provide detailed insight into the failure modes and surface characteristics of the specimens after mechanical testing.

D.1. Tensile Failure

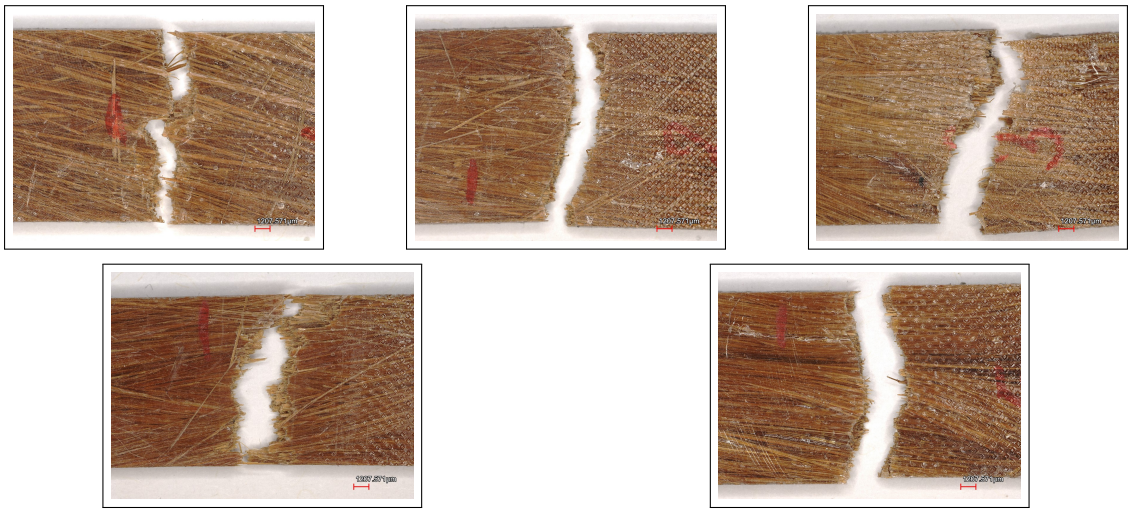

Figure D.1: Untreated laminate consistently showed failure in the grip region

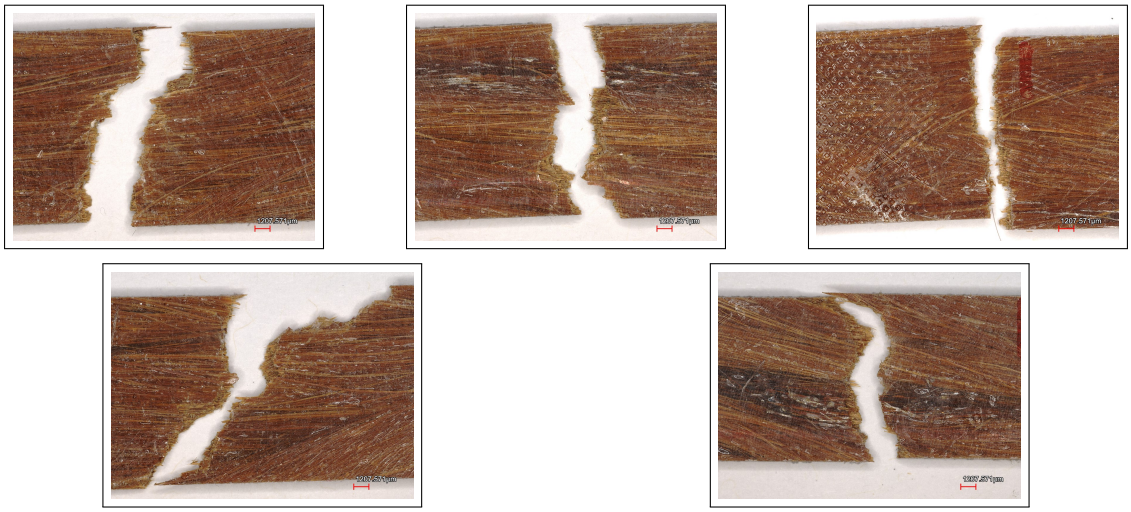

Figure D.2: 2-NaBF laminate showing mainly fibre failure with void present

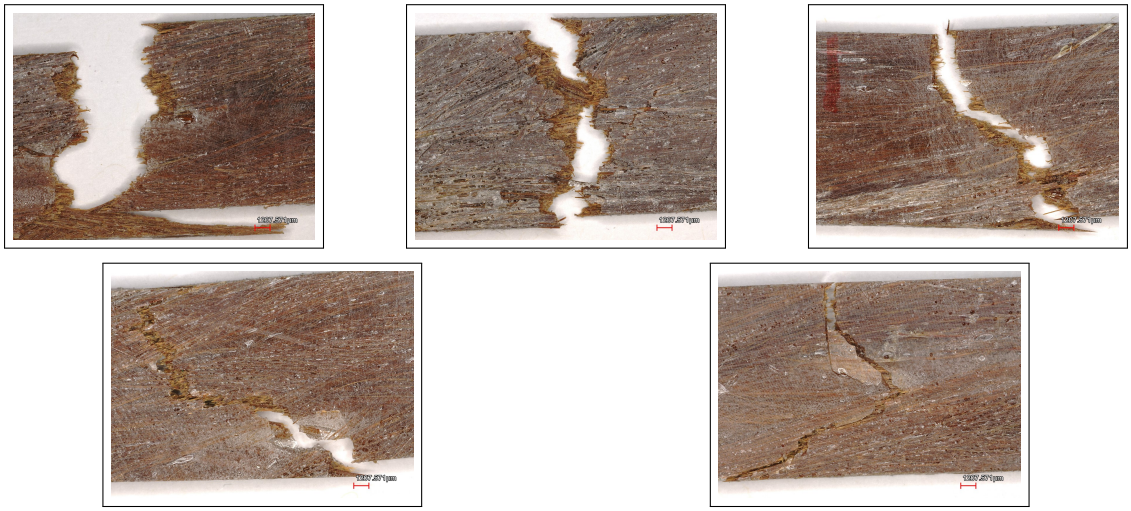

Figure D.3: 5-NaBF laminate showing varied failure modes and high void content

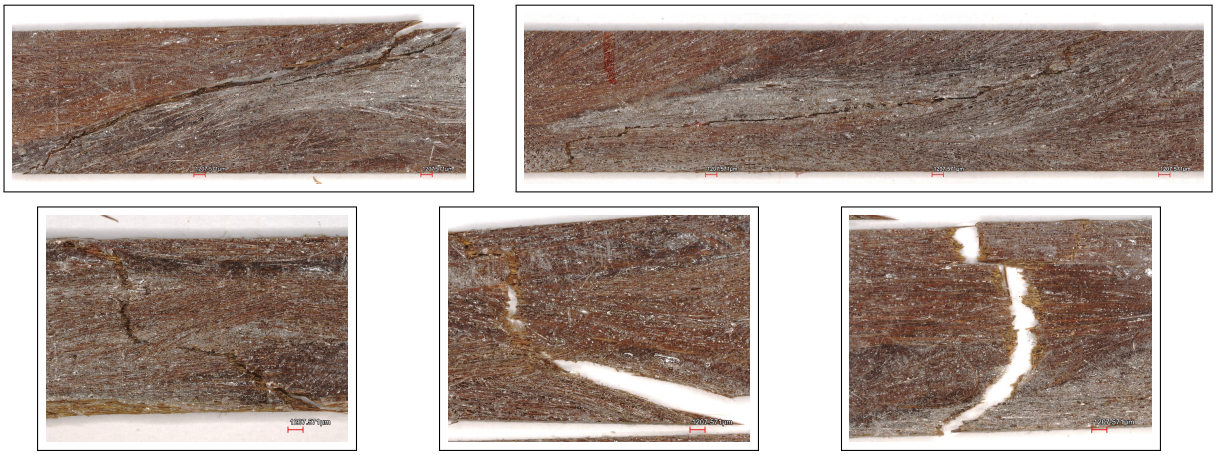

Figure D.4: 8-NaBF laminate showing mainly debonding with a much higher void content

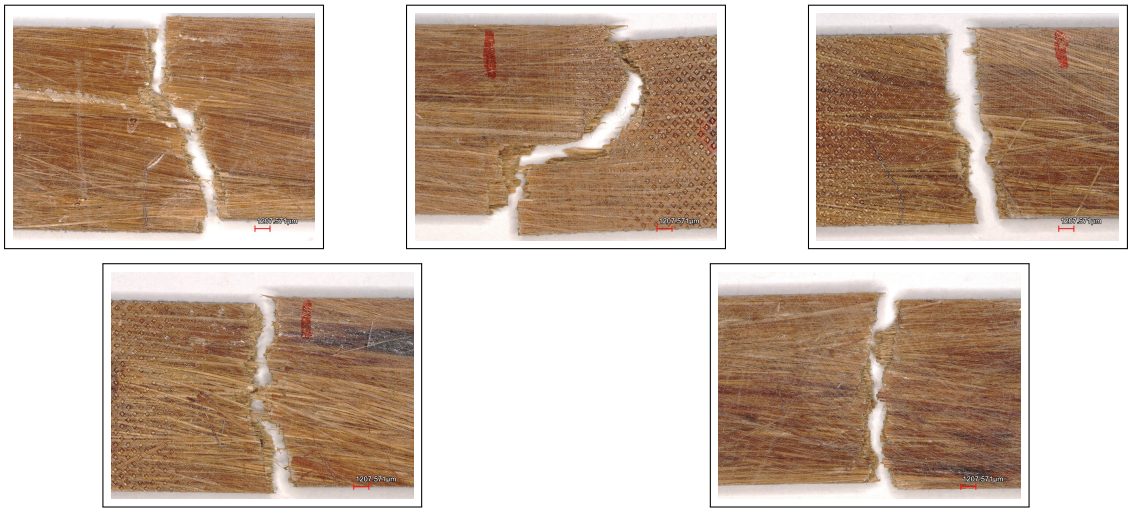

Figure D.5: 2-SiBF laminate mainly showed fibre failure with some debonding visible

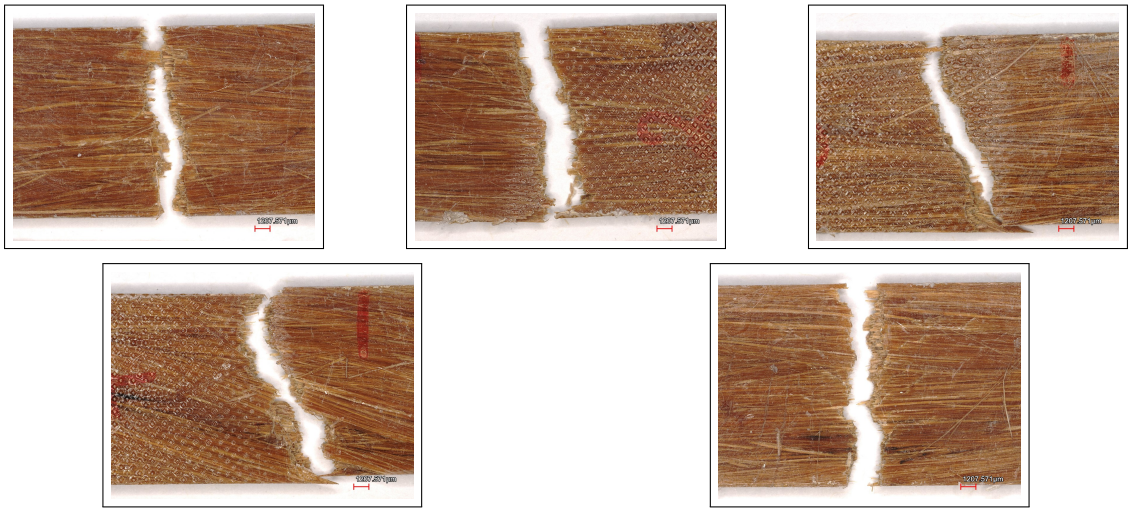

Figure D.6: 5-SiBF laminate primarily failed due to fibre breakage

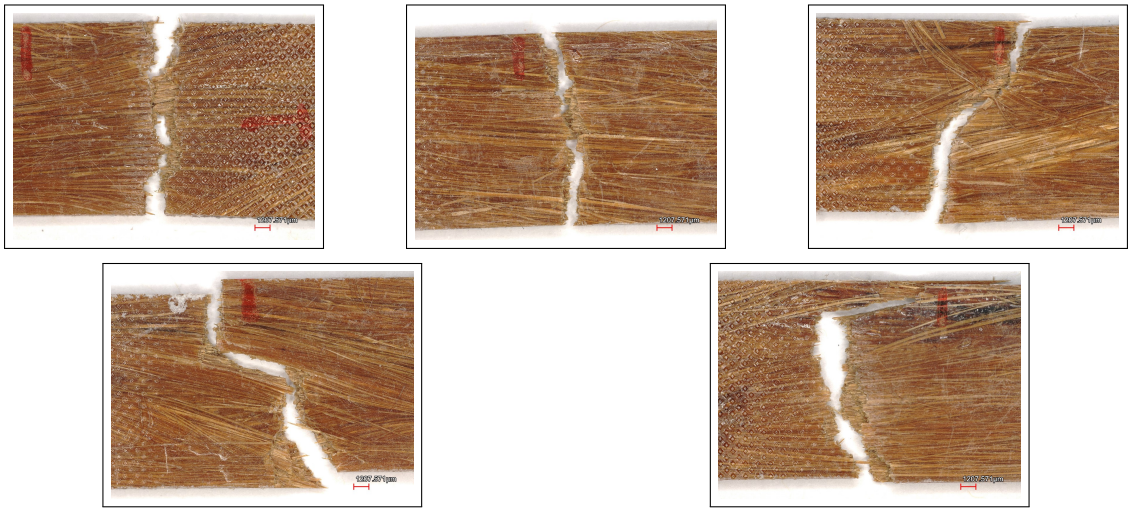

Figure D.7: 8-SiBF laminate showing varying modes of failure

D.2. Flexural Failure

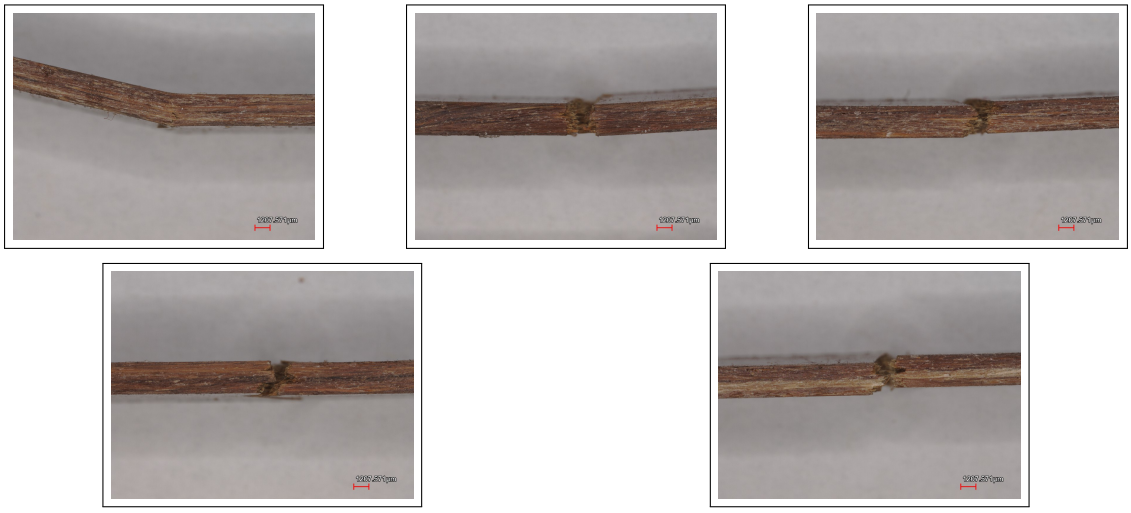

Figure D.8: Untreated shows mixed mode failure in tension or tension-compression

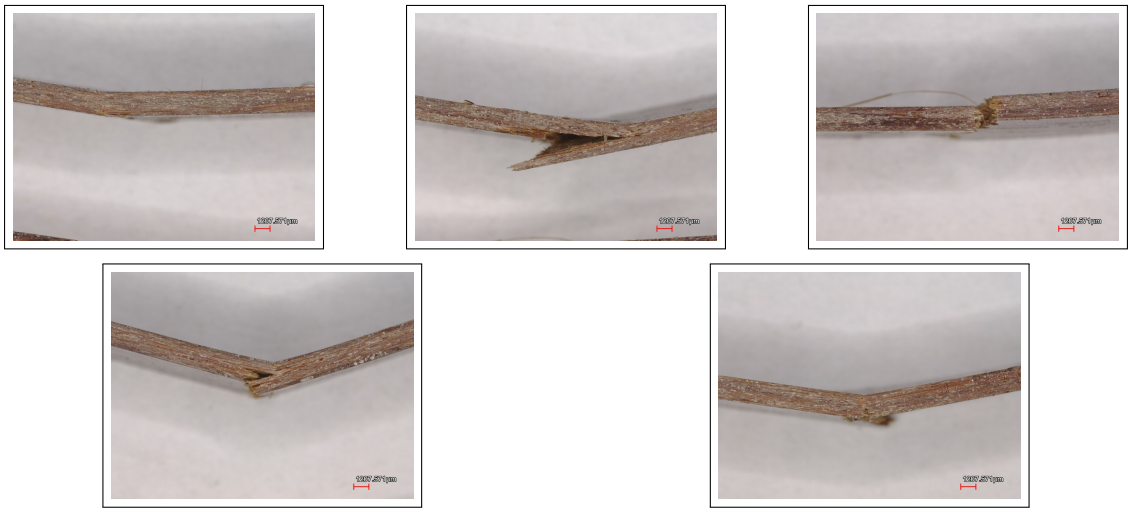

Figure D.9: 2-NaBF showing minimal debonding with mainly tensile failure of outer fibres

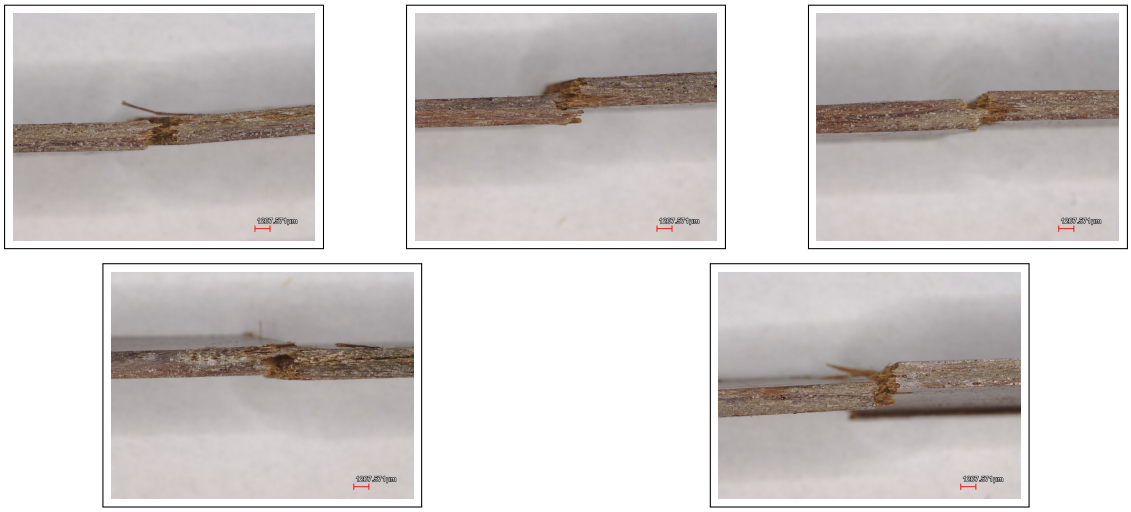

Figure D.10: 5-NaBF with abrupt brittle failure in all specimens with tensile-compressive mode

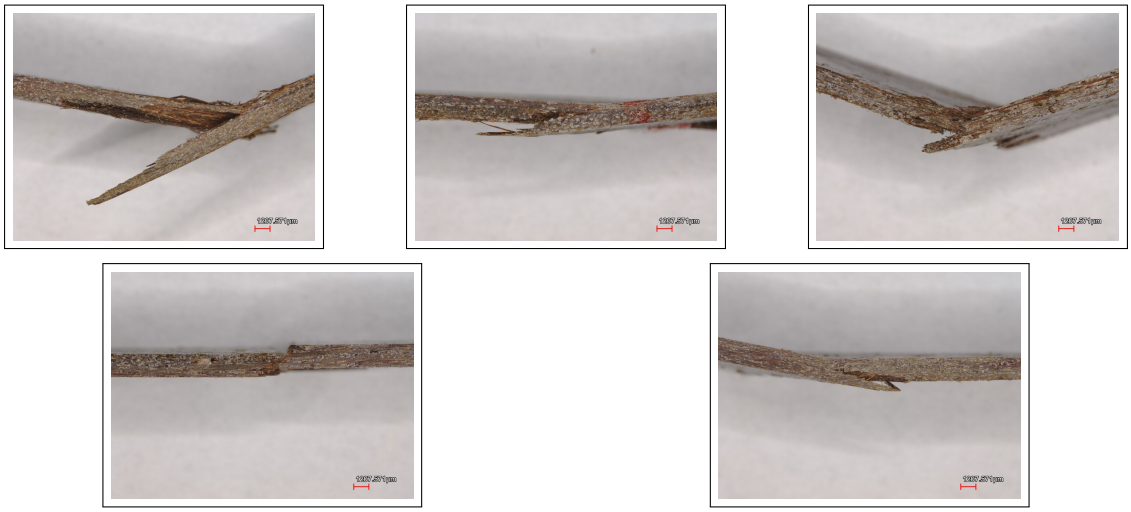

Figure D.11: 8-NaBF showed high debonding-based failure modes accompanied by tensile failure

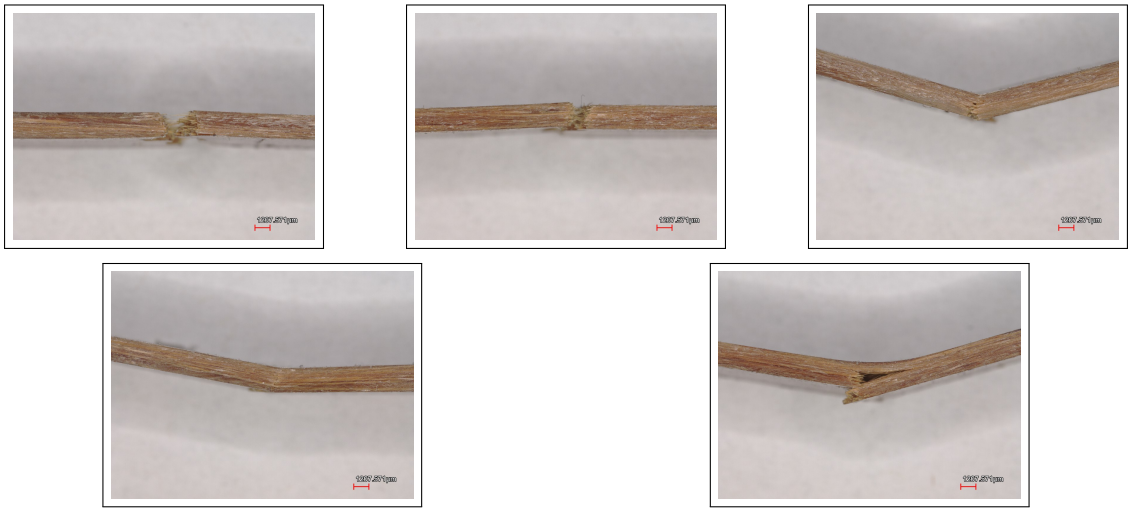

Figure D.12: 2-SiBF shows either brittle failure or incomplete tensile failure on the outer surface

Figure D.13: 5-SiBF showing primarily brittle failures with minimal fibre-matrix debonding

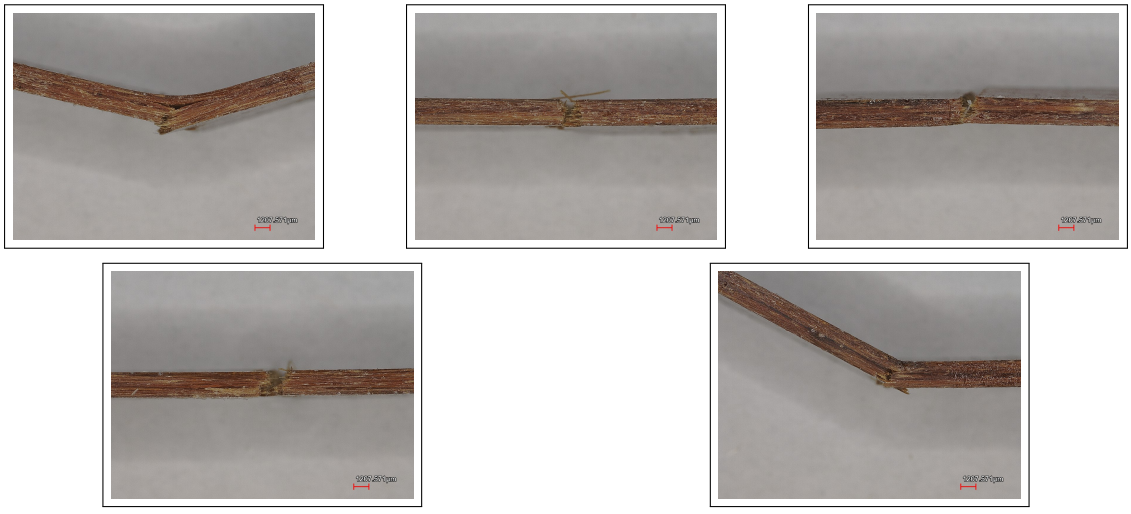

Figure D.14: 8-SiBF shows mixed mode failure with some debonding visible with tensile failure

A day at a time towards a sustainable tomorrow

TU Delft